PATHOPHYSIOLOGY AND PHARMACOLOGY OF NITRIC OXIDE – CYCLIC GUANOSINE MONOPHOSPHATE SIGNALING IN DIABETIC CARDIOMYOPATHY

PhD thesis

Csaba Mátyás, M.D.

Doctoral School of Basic Medicine

Semmelweis University

Supervisor: Tamás Radovits, M.D., Ph.D.

Official reviewers: Zsuzsanna Miklós, M.D., Ph.D.
Attila Borbély, M.D., Ph.D.

Head of the Final Examination Committee: Péter Ferdinandy, M.D., D.Sc.

Members of the Final Examination Committee: Beatrix Sármán, M.D., Ph.D.
Béla Juhász, Pharm.D., Ph.D.

Budapest
2017

Table of contents

1. THE LIST OF ABBREVIATIONS 6

2. INTRODUCTION 10

2.1. TYPE ONE DIABETES MELLITUS 11

2.2. TYPE TWO DIABETES MELLITUS 11

2.3. DIABETIC CARDIOMYOPATHY 12

2.3.1. Diastolic dysfunction in diabetes mellitus 13

2.3.2. Systolic dysfunction in diabetes mellitus 14

2.3.3. Metabolic alterations in diabetes mellitus contribute to the development of diabetic cardiomyopathy 15

2.3.4. Mitochondrial dysfunction in diabetic cardiomyopathy 16

2.3.5. The role of oxidative stress in the diabetic myocardium 16

2.3.6. Apoptosis and cell death in diabetic cardiomyopathy 19

2.3.7. Myocardial hypertrophy in diabetic cardiomyopathy 19

2.3.8. Fibrotic remodeling of the diabetic heart 20

2.4. THE ROLE OF CYCLIC GUANOSINE MONOPHOSPHATE (CGMP) SIGNALING IN DIABETIC CARDIOMYOPATHY 21

2.4.1. Generation, degradation and effects of cGMP 21

2.4.2. Deterioration of cGMP-signaling in oxidative stress and in diabetic cardiomyopathy 23

2.4.3. Pharmacological modulation of the NO-sGC-cGMP-PKG pathway 24

2.4.4. Pharmacology and cardioprotective effects of the sGC activator cinaciguat. 26

2.4.5. Pharmacology and cardioprotective effects of the PDE5A inhibitor vardenafil 27

3. OBJECTIVES 29

4. METHODS 30

4.1. ANIMAL MODELS 30

4.1.1. Rat model of type 1 diabetes mellitus 30

4.1.2. Rat model of type 2 diabetes mellitus 30

4.2. STUDY PROTOCOL 31

4.2.1. Comparative investigation of T1DM or T2DM related diabetic cardiomyopathy 31
4.2.2. Experiments on the effect of sGC activation in T1DM related diabetic cardiomyopathy 31
4.2.3. Experiments on the effect of PDE5A inhibition in T2DM related diabetic cardiomyopathy 32
4.3. BIOCHEMICAL MEASUREMENTS 33
4.4. ECHOCARDIOGRAPHY 34
4.5. HEMODYNAMIC INVESTIGATION 34
4.6. FORCE MEASUREMENT IN PERMEABILIZED LV CARDIOMYOCYTES 35
4.7. QUANTITATIVE REVERSE TRANSCRIPTION POLYMERASE CHAIN REACTION (QRT-PCR) MEASUREMENTS 36
4.8. WESTERN BLOT ANALYSIS 39
4.9. HISTOPATHOLOGY 42
4.10. IMMUNOHISTOCHEMISTRY 43
4.11. DETECTION OF APOPTOSIS BY TERMINAL DEOXYNUCLEOTIDYL TRANSFERASE DUTP NICK END LABELING (TUNEL) ASSAY 44
4.12. STATISTICAL ANALYSIS 44
4.12.1. Comparative investigation of T1DM and T2DM-related diabetic cardiomyopathy 45
4.12.2. Experiments on the effect of sGC activation in T1DM-related diabetic cardiomyopathy 45
4.12.3. Experiments on the effect of PDE5A inhibition in T2DM-related diabetic cardiomyopathy 45
4.13. DRUGS 46
5. RESULTS 47
5.1. COMPARATIVE INVESTIGATION OF T1DM- AND T2DM-RELATED DIABETIC CARDIOMYOPATHY 47
5.1.1. Heart weight (HW), body weight and glucose levels 47
5.1.2. Cardiac contractility and ventricular stiffness 48
5.1.3. Histopathology 49
5.1.4. DNA strand breaks and nitro-oxidative stress 50

5.1.5. Myocardial fibrosis 51
5.1.6. Myocardial expression of genes involved in the development of diabetic cardiomyopathy 52
5.1.7. Western blot analysis of TGF-β1 54
5.2. EXPERIMENTS ON THE EFFECT OF SGC ACTIVATION IN T1DM-RELATED DIABETIC CARDIOMYOPATHY 54
5.2.1. Body weight, heart weight and glucose levels 54
5.2.2. Effects of cinaciguat on plasma and myocardial cGMP levels in DM 56
5.2.3. Effects of diabetes mellitus and cinaciguat treatment on myocardial oxidative stress 58
5.2.4. Cinaciguat protects against DM related alteration of the NO-sGC-cGMP-PKG signaling 60
5.2.5. Cinaciguat treatment protects against DM related fibrotic remodeling of the myocardium 61
5.2.6. DM-related myocardium hypertrophy and apoptosis is alleviated by cinaciguat 64
5.2.7. In vivo cardiac function is improved by cinaciguat in DM 66
5.3. EXPERIMENTS ON THE EFFECT OF PDE5A INHIBITION IN T2DM-RELATED DIABETIC CARDIOMYOPATHY 71
5.3.1. The effect of vardenafil on basic characteristics in T2DM 71
5.3.2. Vardenafil prevented T2DM-associated LV dysfunction in vivo 73
5.3.3. Vardenafil prevented T2DM-associated stiffening of LV cardiomyocytes 76
5.3.4. Vardenafil decreased myocardial hypertrophy in T2DM rats 76
5.3.5. Vardenafil reduced alterations associated with nitro-oxidative stress in T2DM 80
5.3.6. Vardenafil suppressed myocardial fibrotic remodeling 82
5.3.7. Phosphodiesterase-5A inhibiton prevented cardiomyocyte apoptosis in ZDF rats 84
5.3.8. Vardenafil protected against the disturbances of myocardial cGMP-PKG signaling in ZDF rats 85
6. DISCUSSION 90

6.1. STRUCTURAL AND MOLECULAR HALLMARKS OF TYPE 1 AND TYPE 2 DM-ASSOCIATED DIABETIC CARDIOMYOPATHY 90
6.1.1. Nitro-oxidative stress 90
6.1.2. DNA damage and apoptosis 91
6.1.3. Myocardial hypertrophy 92
6.1.4. Fibrotic remodeling 93
6.1.5. Deterioration of the NO-sGC-cGMP-PKG signaling pathway 94
6.1.6. Characteristics of cardiac dysfunction T1DM and T2DM 95
6.1.7. Effects of sGC activation by cinaciguat on diabetic cardiomyopathy in T1DM 96
6.1.8. Effects of PDE5A inhibition by vardenafil on T2DM-associated heart failure 98
7. CONCLUSIONS 100
8. SUMMARY 101
9. ÖSSZEFOGLALÁS 102
10. BIBLIOGRAPHY 103
11. BIBLIOGRAPHY OF THE CANDIDATE'S PUBLICATIONS 126
11.1. PUBLICATIONS RELATED TO THE DISSERTATION 126
11.2. PUBLICATIONS NOT RELATED TO THE DISSERTATION 127
12. ACKNOWLEDGEMENTS 131

1. The list of Abbreviations

3-NT	3-nitrotyrosine
A wave	atrial filling
ADP	adenosine diphosphate
AGE	advanced glycation end-product
ANF	atrial natriuretic factor
ANOVA	analysis of variance
ANP	atrial natriuretic peptide
ATP	adenosine triphosphate
AW	left ventricular anterior wall thickness
BAX	Bcl2-associated X protein
Bcl-2	B-cell CLL/lymphoma 2
BG	blood glucose
BNP	B-type natriuretic peptide
BW	body weight
cGMP	cyclic guanosine monophosphate
CO	cardiac output
Co	vehicle-treated control
CoCin	cinaciguat-treated control
Col1a1	Collagen 1a1
Col3a1	Collagen 3a1
CTGF	connective tissue growth factor
d	end-diastole
DiabCin	cinaciguat-treated diabetic
DiabCo	vehicle-treated diabetic
DM	diabetes mellitus
dP/dt_{max}	maximal slope of systolic pressure increment
dP/dt_{min}	maximal slope of diastolic pressure decrement
DT	deceleration time
E wave	early diastolic filling
EDPVR	left ventricular end-diastolic P-V relationship

EF	ejection fraction
EIA	enzyme immunoassay
eNOS	endothelial nitric oxide synthase
ET-1	endothelin-1
F	forward
FFA	free fatty acids
GAPDH	glyceraldehyde-3-phosphate dehydrogenase
GSR	glutathione reductase
H_2O_2	hydrogen peroxide
HE	hematoxylin and eosin
HF	heart failure
HFmrEF	heart failure with mid-range ejection fraction
HFpEF	heart failure with preserved ejection fraction
HFrEF	heart failure with reduced ejection fraction
HgbA1c	haemoglobin A1C
HR	heart rate
HRP	horseradish peroxidase
HSP70a1	heat shock 70kDa protein 1A
HW	heart weight
ID	left ventricular internal diameter
ISO	isolating solution
IVRT	isovolumic relaxation time
LV	left ventricular
LVEDP	left ventricular end-diastolic pressure
LVSP	maximal left ventricular systolic pressure
MAP	mean arterial blood pressure
MMP-2	matrix metallopeptidase 2
MMP-9	matrix metallopeptidase 9
MT	Masson’s trichrome
NOX	nicotinamide adenine dinucleotide phosphate-oxidases
PARP	poly adenosine diphosphate ribose polymerase enzyme
PDE	phosphodiesterase

PKC	protein kinase C
PKG	protein kinase G
PLB	phospholamban
PPAR-α	peroxisome proliferator-activated receptor α
p-PLB	phospho-phospholamban
PRSW	preload recruitable stroke work
P-V	pressure-volume
p-VASP	phosphorylated vasodilator-stimulated phosphoprotein
PW	left ventricular posterior wall thickness
qRT-PCR	quantitative reverse transcription polymerase chain reaction
R	reverse
RGB	red green blue
RIPA	radioimmunoprecipitation assay lysis buffer
RNS	reactive nitrogen species
ROS	reactive oxygen species
RT	room temperature
rTdT	recombinant Terminal Deoxynucleotidyl Transferase
s	end-systole
SD	Sprague-Dawley rat
SEM	standard errors of the mean
sGC	soluble guanylate cyclase
sGC β1	soluble guanylate cyclase β1
SOD1	superoxide dismutase 1
SOD2	superoxide dismutase 2
STZ	streptozotocin
SW	stroke work
T1DM	type 1 diabetes mellitus
T2DM	type 2 diabetes mellitus
Tau_W	time constant of LV pressure decay
TGF-β	transforming growth factor β
TIMP	tissue inhibitor of matrix metallopeptidase
TIMP-1	tissue inhibitor of matrix metallopeptidase 1

TIMP-2	tissue inhibitor of matrix metallopeptidase 2
TL	tibia length
TUNEL	terminal deoxynucleotidyl transferase dUTP nick end labeling
UPL	Universal Probe Library
VASP	vasodilator-stimulated phosphoprotein
WHO	World Health Organization
ZDF	vehicle-treated diabetic
ZDF	Zucker Diabetic Fatty
ZDF+Vard	vardenafil-treated diabetic
ZDFLean	vehicle-treated controls
ZDFLean+Vard	vardenafil-treated controls
α-MHC	myosin heavy chain alpha
β-MHC	myosin heavy chain beta

2. Introduction

Diabetes mellitus (DM) is a chronic metabolic disease, characterized by elevated blood glucose level which leads to a serious damage of different organ systems including the heart, liver, kidneys, vessels and eyes. According to the World Health Organization (WHO) diabetes mellitus is one of the most common chronic diseases globally and the number of people living with diabetes has nearly quadrupled since 1980. According to the Global Diabetes Report in 2016, 442 million adults have diabetes mellitus and 1.5 million deaths are directly attributed to diabetes mellitus each year (World Health Organization 2016b). Moreover, higher-than-optimal blood glucose level caused an additional 2.2 million deaths by increasing the risk of cardiovascular and other diseases. One in three adults aged over 18 years is overweight and one of 10 adults is obese globally. In Hungary, the prevalence of diabetes is 10 %, while 63.3 % is overweight and 26 % is obese of the adult population (World Health Organization 2016a).

The diabetes epidemic is becoming the biggest one in the twenty-first century due to the constant growth in the number of diabetic patients (Tabish 2007). There are several contributing factors that play a key role in the development of diabetes mellitus including low physical activity, unhealthy western-type diet and the ageing population. The constantly growing incidence of diabetes is not only a great epidemiological, but also an economical burden for the health care system (Tabish 2007). For example, the total cost of diabetes was 245 billion USD including the direct medical costs and the reduced productivity in the United States in 2012 (American Diabetes Association 2013). Therefore, novel therapies that aim at decreasing the incidence and prevalence of diabetes and its complications are urgently needed.

Diabetes mellitus, due to the elevated blood glucose level and the disturbance in insulin signaling leads to the development of different complications and co-morbidities including stroke, heart attack, hypertension, dyslipidaemia, blindness and eye problems, kidney failure and heart failure. Diabetic cardiomyopathy is a special form of heart failure that develops in diabetes independently of coronary artery disease or hypertension (Huynh et al. 2014).

According to the American Diabetes Association, diabetes can be classified into four major types that include type 1, type 2, gestational and specific types of diabetes (due to

other causes) (American Diabetes Association 2016). In the diagnosis of diabetes mellitus the value of plasma/blood glucose is a reliable measure. A patient is considered diabetic if fasting blood glucose is over 7.0 mmol/l or blood glucose is above 11.0 mmol/l at 2 hours in oral glucose tolerance test. In addition to the measurement of blood glucose, measurement of the glycated haemoglobin A1C (HgbA1c) is a reliable test in patients follow-up. A patient is considered to be prediabetic if the HgbA1c is between 5.7 – 6.4 % and should be counseled about strategies to lower their risks. Several forms of diabetes are known, in the current work I will focus on the two major types of the disease.

2.1. Type one diabetes mellitus

Type 1 diabetes, which accounts approximately for 5-10 % of all diabetes cases, is a cellular-mediated autoimmune disease leading to the destruction of the pancreatic β–cells and the lack of insulin (American Diabetes Association 2016). Type 1 diabetes usually occurs in childhood or adolescence but patients can develop it at any age. Patients are often presented with acute symptoms of diabetes including high blood glucose level and ketoacidosis (American Diabetes Association 2016). In the development of immune-mediated diabetes several factors play a key role. The disease is strongly associated with HLA DQA and DQB genes (American Diabetes Association 2016). On the other hand, the autoimmune process in type 1 diabetes is also related to different environmental factors (such as viral infections) (American Diabetes Association 2016). Patients with type 1 diabetes mellitus are not obese but are prone to develop other autoimmune diseases such as Addison disease, vitiligo, Hashimoto thyroiditis or autoimmune hepatitis (American Diabetes Association 2016).

2.2. Type two diabetes mellitus

Type 2 diabetes mellitus is responsible for 90 % of all diabetes cases (American Diabetes Association 2016). In type 2 diabetes patients have insulin resistance and usually relative insulin deficiency (American Diabetes Association 2016). In spite of type 1 diabetes mellitus, autoimmune destruction of the pancreatic β–cells does not

occur. However, there are different causes that lead to the development of type 2 diabetes such as overweight or obesity, lack of physical activity and frequent consumption of westernized-diet (Zimmet et al. 2001). It is often associated with strong genetic predisposition, more often than type 1 diabetes (American Diabetes Association 2016). Family history and ethnic background are also important in the development of the disease (Huynh et al. 2014). The risk for developing the disease is increasing with age and obesity. As opposite to the insulinopenia in type 1 diabetes, patients usually have hyperinsulinemia with hyperglycemia in type 2 diabetes. Despite the higher level of insulin the blood glucose level remains elevated due to developed insulin resistance of different organs (American Diabetes Association 2016).

2.3. Diabetic cardiomyopathy

Diabetes mellitus (independently of the type of diabetes) is associated with cardiovascular complications, such as myocardial infarction, chronic heart failure (HF), micro- and macrovascular diseases. Literature data indicate that there is a casual relationship between hyperinsulinemia and the development of hypertension or coronary artery disease (Fontbonne et al. 1991, Lender et al. 1997). Diabetes acts as an independent risk factor for coronary atherosclerosis and ischemic heart disease, however, the altered metabolic state – mainly due to elevated glucose levels – has a direct effect on cardiac structure and function independently of coronary artery disease. The special cardiac disease entity which develops due to the direct effects of diabetes on the myocardium called diabetic cardiomyopathy (Huynh et al. 2014). Several key morphological (described below in detail) and functional (diastolic and systolic dysfunction) (Joffe et al. 1999, Poirier et al. 2001, Radovits et al. 2009a, Radovits et al. 2009b) features have been described in the development and progression of diabetic cardiomyopathy, however, the exact pathomechanism is still under debate (Cai 2006, Sharma et al. 2006, Mourmoura et al. 2013, Pearson et al. 2013, Huynh et al. 2014). Nevertheless, depending on the severity of diabetic cardiomyopathy it leads to the development of HF. HF is a complex clinical syndrome characterized by specific clinical signs and symptoms. It has a great epidemiological burden, as its prevalence is approximately 1-2 % in the adult population of the Western countries and it is one of

the most common causes leading to hospitalization (Mosterd et al. 2007). The latest „ESC Guidelines for the diagnosis and treatment of acute and chronic HF" determines 3 main forms of HF by the value of left ventricular (LV) ejection fraction (EF): 1) HF with reduced EF (HFrEF; LVEF < 40 %), 2) HF with mid-range EF (HFmrEF; LVEF 40-49 %) and 3) HF with preserved EF (HFpEF; LVEF ≥ 50 %) (Ponikowski et al. 2016).

2.3.1. Diastolic dysfunction in diabetes mellitus

Diastolic dysfunction is an early sign of diabetic cardiomyopathy that develops before systolic function deteriorates (Huynh et al. 2014). The prevalence of diastolic heart failure is constantly growing and it is one of the most important features of HFpEF (Ponikowski et al. 2016). HFpEF is associated with diastolic dysfunction characterized by prolonged LV isovolumic relaxation, increased LV stiffness, increased LV end-diastolic pressure and slow LV filling (Zouein et al. 2013). Despite the lack of systolic dysfunction, diastolic heart disease has a similar prognosis as systolic HF (Huynh et al. 2014). Several measures are used in the everyday clinical setting in order to evaluate the severity of diastolic dysfunction including Doppler and tissue Doppler echocardiography and cardiac magnetic resonance imaging. However, on the experimental level diastolic dysfunction can be characterized by invasive hemodynamic measurements and pressure-volume (P-V) loop analysis. P-V loop analysis provides a reliable assessment of cardiac diastolic dysfunction whereas cardiac stiffness and active relaxation can be investigated in detail (Pacher et al. 2008). Doppler echocardiography is a useful application to detect early deterioration and to perform follow-up studies on diabetic cardiomyopathy. Doppler echocardiography measures the peak blood flow across the mitral valve during the cardiac cycles, whereas a characteristic pattern of early diastolic filling (E wave) and the atrial filling (A wave) is seen and isovolumic relaxation time (IVRT) and deceleration time (DT) can be measured (Huynh et al. 2014). Diabetes is associated with a reduced E/A ratio and with prolonged IVRT (Schannwell et al. 2002). Tissue Doppler echocardiography is another useful tool in the assessment of diastolic function as it measures the movement (velocity) of a particular myocardial segment and provides similar indices as above (including E', A').

Additionally, by cardiac magnetic resonance imaging similar alterations in diastolic function are detectable (increased left ventricular filling pressures, reduced E/A ratio, prolonged IVRT) (Rijzewijk et al. 2009). Similarly to the human conditions diastolic cardiac dysfunction is a common phenomenon among experimental animal models of type 1 and type 2 diabetes mellitus. For example, in streptozotocin (STZ)-induced diabetes mellitus and in type 2 diabetic *db/db* mice an early deterioration of diastolic function is seen (as evidenced by E/A ratio, deceleration time, prolonged IVRT) (Joffe et al. 1999, Semeniuk et al. 2002). Additionally, invasive hemodynamic investigation and P-V loop analysis revealed the severe deterioration of diastolic dysfunction in STZ-induced type 1 and in the Zucker Diabetic Fatty (ZDF) rat model of type 2 diabetes mellitus (as represented by increased relaxation time, increased filling pressures and increased cardiac stiffness) (Radovits et al. 2009b). Not only the in vivo measurement of cardiac function, but isolated cardiomyocytes from diabetic animals and humans showed impaired relaxation and increased stiffness in vitro (Fulop et al. 2007, van Heerebeek et al. 2008).

2.3.2. Systolic dysfunction in diabetes mellitus

In spite of the early manifestation of diastolic dysfunction, systolic abnormalities become more evident at later stages in the disease (Boudina et al. 2010). In addition to that, subclinical alterations of the contractile function are difficult to detect with conventional 2-dimensonal echocardiography due to its load- and frequency dependence (Pacher et al. 2008). However, tissue Doppler or speckle tracking strain analysis is able to reveal early signs of contractile dysfunction in diabetes (Fang et al. 2005, Shepherd et al. 2016). In vivo animal studies using magnetic resonance imaging or an invasive hemodynamic approach have shown the impairment of contractile function in different types of animal models (Van den Bergh et al. 2006, Yue et al. 2007). However, it is believed that the development of systolic dysfunction in an experimental setting is dependent on the experimental model used given that contractility is preserved when multiple low-dose STZ is applied in an animal model (Huynh et al. 2013). In spite of that, STZ-induced diabetic C57Bl/6 mice develop severe contractile dysfunction (Westermann et al. 2007). Recently, a study by our research group showed that there is

significant difference regarding the cardiac dysfunction in STZ-induced type 1 diabetic and the ZDF type 2 diabetic animal models whereas type 1 diabetes was associated with decreased cardiac contractility, impaired systolic function coupled with prolonged relaxation and diastolic dysfunction, while type 2 diabetes showed preserved systolic performance and markedly increased cardiac stiffness (Radovits et al. 2009b).

2.3.3. Metabolic alterations in diabetes mellitus contribute to the development of diabetic cardiomyopathy

Impaired glucose homeostasis due to the lack of insulin or insulin resistance with hyperinsulinemia are the hallmarks of diabetes associated metabolic alterations in the heart. In addition to these effects, disturbances in insulin signaling and the downregulation and diminished activity of the glucose transporter type 4 directly contribute to the substrate switching that characterize the diabetic heart (Bugger et al. 2014). Thus, diabetes mellitus is associated with reduced glucose and lactate metabolism (Stanley et al. 1997) which makes it more vulnerable to different harmful stimuli including ischemia/reperfusion in myocardial infarction (Huynh et al. 2014). The levels of free fatty acids (FFA) in the plasma and their rate of metabolism in the heart are increased in diabetes mellitus (Boudina et al. 2007). Furthermore, diabetes can cause a significant increase in myocardial triacylglycerol content (Murthy et al. 1977). Taken together, as FFA uptake exceeds the rate of its oxidation in the heart, lipid accumulation occurs in the diabetic myocardium which may promote lipotoxicity and greatly contributes to apoptosis and tissue injury (McGavock et al. 2006). On the other hand, Oakes et al. pointed out that diabetic hearts are less able to adapt their metabolic substrate use when the concentration of the metabolic substrates were altered (Oakes et al. 2006). In conclusion, the diabetic heart has lost its metabolic flexibility in vivo which phenomenon is an important contributor to the inability of the diabetic myocardium to adapt itself to different stress situations. FFAs can directly inhibit glucose oxidation by activating the peroxisome proliferator-activated receptor (PPAR)-α. In response, PPAR-α increases the expression of pyruvate dehydrogenase kinase-4 thereby mediates the increased mitochondrial FFA uptake and β-oxidation (Hopkins et al. 2003). Additionally, in the diabetic myocardium the acetyl-CoA carboxylase is

inhibited, the level of malonyl-CoA is increased which processes contribute to the enhanced FFA oxidation in the mitochondria resulting in increased level of acetyl-CoA that enters the Szent-Györgyi – Krebs - cycle (Stanley et al. 1997). The above findings further deteriorate the flexibility of metabolism in diabetes mellitus.

2.3.4. Mitochondrial dysfunction in diabetic cardiomyopathy

Proteomic analysis by Turko et al. revealed that myocardial mitochondria in diabetic cardiomyopathy have decreased expression of proteins of the electron transport chain, creatine kinase, the voltage-dependent anion channel 1, however, the level of β-oxidation proteins was increased (Turko et al. 2003b). As described above, the rate of β-oxidation is greatly elevated in the heart of diabetics that delivers more reducing equivalents to the electron transport chain (Boudina et al. 2007). However, due to the decreased expression of electron transport chain proteins the oxidative phosphorylation is significantly limited thus leading to increased production of superoxide anions and reactive oxygen species (ROS) from the mitochondria and to the decreased production of high energy phosphates (Boudina et al. 2007). As a result of the above process the mitochondrial electron transport chain becomes uncoupled and begins to produce large amounts of ROS and promotes oxidative stress (Boudina et al. 2005). Furthermore, ROS in oxidative stress and reactive nitrogen species (RNS) in nitrosative stress directly deteriorates the mitochondrial proteins thus a vicious cycle of oxidative mitochondrial injury develops (Turko et al. 2003a). However, blunted antioxidant protection in the failing myocardium (e.g. in diabetes mellitus) further enhances mitochondrial injury and leads to mitochondrial dysfunction in diabetes (Shen et al. 2006).

2.3.5. The role of oxidative stress in the diabetic myocardium

The presence of increased oxidative stress has been widely described in diabetic cardiomyopathy (Pacher et al. 2007, Bugger et al. 2014, Huynh et al. 2014, Varga et al. 2015), however, the exact mechanism in its development is still unknown (Boudina et al. 2010). Most probably an interplay of several processes leads to the enhanced production of ROS and RNS in diabetes (Varga et al. 2015): 1) lipid overload with

excessive FFA generation (described above in detail) (Boudina et al. 2010); 2) hyperglycemia-induced glucotoxicity and inflammatory response; 3) endothelial nitric oxide (NO) synthase (eNOS) uncoupling; 4) formation of the highly reactive molecule peroxynitrite ; 5) overactivation of ROS producing enzymes.

In spite of the available treatment therapies for high blood glucose, to achieve the optimal anti-hyperglycemic treatment is still challenging and high blood sugar level is poorly controlled in patients (Ross et al. 2011). High or fluctuating glucose levels lead to the enhancement of oxidative stress (Giacco et al. 2010). Glucotoxicity, high glucose levels and the non-specific glycosylation of different proteins (as forming advanced glycation end-products [AGEs]) contribute to the dysfunction of enzymes, contractile proteins and they provoke a whole body inflammatory response (Varga et al. 2015). Inflammatory cell response, including neutrophils, is a major drive in the development of diabetes mellitus associated cardiovascular abnormalities. Neutrophils are sources of nicotinamide adenine dinucleotide phosphate-oxidases (NOX) that produce large amounts of superoxide anions as part of their inflammatory response (Varga et al. 2015). Superoxide directly deteriorates proteins or forms highly reactive molecules including peroxynitrite (together with NO) (Pacher et al. 2007) or hydrogen peroxide (Pacher et al. 2007). Overexpression or overactivation of different NOX enzymes have been described in diabetic cardiomyopathy (Rajesh et al. 2010, Roe et al. 2011, Maalouf et al. 2012) and in hypercholesterolemia (Varga et al. 2013) as well. Furthermore, overactivation of the renin-angiotensin-aldosterone system plays decisive role in diabetes-associated cardiovascular oxidative stress, as vascular NOX is a downstream target of angiotensin II (Kajstura et al. 2001, Westermann et al. 2007) thereby it promotes the production of vascular ROS (Varga et al. 2015). The above theory is supported by experimental data whereas angiotensin II type 1 receptor blockade inhibited glucose-derived cardiac dysfunction by the attenuation of angiotensin 1 receptor – NOX signaling (Privratsky et al. 2003). Beside the role of NOX enzymes in diabetes-related oxidative stress, other enzyme systems can also importantly contribute to ROS production. One of these enzymes is xanthine oxidase that has been shown to be overactivated in diabetes in animal models (Desco et al. 2002, Rajesh et al. 2009). This theory has been evidenced by the protective effects of allopurinol on the hearts of diabetic mice and rats (Rajesh et al. 2009, Gao et al. 2012).

Beside the above mentioned enzyme systems, there is another important player in oxidative stress in diabetes mellitus. Namely, the eNOS enzyme which is located in the endothelial system becomes uncoupled in diabetes as it loses its cofactor tetrahydrobiopterin (Zou et al. 2002). As eNOS becomes uncoupled it produces superoxide anions instead of NO thus NO bioavailability markedly decreases and the level of ROS increases in the diabetic heart (Zou et al. 2002). On the other hand, iNOS and eNOS expression has been shown to be induced in diabetic cardiomyopathy that might further contribute to increased generation of NO. However, NO rapidly reacts with the excessive amount of superoxide anions in oxidative stress and peroxynitrite, a highly reactive molecule, is formed (Pacher et al. 2007). Peroxynitrite is able to directly damage (via protein nitration) different cellular elements including DNA, contractile proteins, proteins of calcium handling, elements of the antioxidant defence system and induces apoptosis and necrosis (Pacher et al. 2007). Furthermore, in cooperation with other ROS peroxynitrite activates matrix metallopeptidases (MMPs) in the diabetic myocardium leading to the remodeling of the myocardium and may impair the NO – soluble guanylate cyclase (sGC) axis (Evgenov et al. 2006). The importance of peroxynitrite in cardiovascular complications of diabetes has been shown in patients as well, as the level of 3-nitrotyrosine (a marker of nitrosative stress) correlated with the presence of high blood pressure (Hoeldtke et al. 2003). The presence of constant myocardial oxidative and nitrosative stress may further deteriorate the antioxidant defence system by the inactivation (probably by protein nitration and oxidation) of its key elements like superoxide dismutases and catalase (Pacher et al. 2007). In fact, oxidative and nitrosative stress aggravate the severity of diabetes mellitus as they promote the oxidation and/or nitration of insulin receptors in peripheral tissues that further compromise insulin resistance of the organs (Stadler 2011). Nonetheless, hyperglycemia coupled with oxidative/nitrosative stress causes nonspecific and nonenzymatic glycation (AGEs), oxidation and nitration of the proteins and lipids that significantly contribute to diabetes mellitus-associated cardiac dysfunction (e.g. contractile proteins – systolic dysfunction, calcium transporters – diastolic dysfunction).

2.3.6. Apoptosis and cell death in diabetic cardiomyopathy

Increased rate of cell death and apoptosis is often observed in the heart of diabetic individuals and in the myocardium of experimental animal models (Frustaci et al. 2000, Chowdhry et al. 2007, Rajesh et al. 2010, Rajesh et al. 2012). Apoptosis is a well-known form of programmed cell death and it is essential in the regulation and for the maintenance of tissue homeostasis (Huynh et al. 2014). In the pathogenesis of diabetes-induced cell death many processes have been identified such as the activation of caspases, increased amount of ROS, increased rate of inflammation, increased activation of transforming growth factor β (TGF-β) signaling and activation of the poly adenosine diphosphate (ADP) ribose polymerase (PARP) enzymes (Bugger et al. 2014). The overactivation of PARP-1 is a major drive of apoptosis and necrosis in diabetic cardiomyopathy (Varga et al. 2015). PARP-1, a major regulator of DNA repair and cell death becomes activated when ROS and RNS directly bind to the DNA causing its oxidative injury (Bai et al. 2012). During its repair operation, PARP-1 binds to the damaged DNA, forms homodimers and cleaves its substrate NAD^+ into nicotinamide and ADP-ribose (Bai et al. 2012, Varga et al. 2015). Then long branches of ADP-ribose polymers are formed on target proteins (e.g. histones and PARP-1) and energy (adenosine triphosphate [ATP]) depletion, mitochondrial dysfunction and subsequent necrosis/apoptosis will occur (Varga et al. 2015). This hypothesis is underlain by literature data where PARP inhibition successfully improved diabetes-associated endothelial and cardiac dysfunction (Garcia Soriano et al. 2001, Soriano et al. 2001, Pacher et al. 2002). Moreover, PARP inhibition also prevented the pathological activation of protein kinase C (PKC) pathways, the hexosamine pathways and the AGE formation induced by hyperglycemia in vitro (Pacher et al. 2005).

2.3.7. Myocardial hypertrophy in diabetic cardiomyopathy

Myocardial hypertrophy is a structural hallmark of diabetic cardiomyopathy characterized by the hypertrophy of the individual cardiomyocytes (Huynh et al. 2014). The Strong Heart Study, conducted in Native Americans, found that myocardial hypertrophy (as represented by increased LVmass and increased wall thicknesses)

develops both in men and women with type 2 diabetes mellitus (Devereux et al. 2000). Moreover, a study conducted in a multi-ethnic population described that the likelihood of developing cardiac hypertrophy (increased LVmass) is greater in patients with type 2 diabetes mellitus (Eguchi et al. 2008). Pathological myocardial hypertrophy is a risk factor for the development of myocardial infarction, stroke and death from HF (Bernardo et al. 2010). Myocardial hypertrophy occurs in response to hemodynamic stress and due to oxidative stress-induced apoptosis and as compensatory mechanisms of the remaining functional cardiomyocytes and due to the neurohormonal (renin-angiotensin-aldosterone system) activation (Huynh et al. 2014). However, concentric hypertrophy of the heart is a long-term consequence of diabetes and obesity regardless of the presence of hypertension (Woodiwiss et al. 2008, Boudina et al. 2010). In the development of LV hypertrophy, adipose tissue derived cytokines (e.g. leptin) play a key role. Leptin has been shown to induce cardiomyocyte hypertrophy in vitro probably via an endothelin-1 mediated oxidative stress response (Xu et al. 2004). Furthermore, hyperglycemia directly propagates the overexpression of endothelin-1 thus it maintains and contributes to the already elevated level of ROS (Huynh et al. 2014). Endothelin-1 is a powerful vasoconstrictor (Kiowski et al. 1995) and induces an inflammatory response (Davidson et al. 2010) thereby it might contribute to the hemodynamic stress and ROS production in diabetes mellitus. Furthermore, LV hypertrophy was associated with elevated levels of atrial and B-type natriuretic peptides (NP; ANP/ANF, BNP) and was shown to be associated with hypertrophic gene signaling and with the reactivation of the fetal gene program in diabetes mellitus (Huynh et al. 2014).

2.3.8. Fibrotic remodeling of the diabetic heart

Interstitial and perivascular fibrotic remodeling of the myocardium is frequently observed in diabetes mellitus in humans (Shimizu et al. 1993) and in experimental animal models as well (Mizushige et al. 2000, Korkmaz-Icoz et al. 2016). In the background of increased fibrosis an over-activation of the TGF-β signaling and its downstream effector connective tissue growth factor (CTGF) might play a role (Radovits et al. 2009a, Bugger et al. 2014). Furthermore, due to the enhanced apoptosis the cardiomyocytes are replaced by fibroblasts and extracellular matrix. However, the

dysregulation of MMPs (e.g. MMP-2) and their inhibitors tissue inhibitor of matrix metallopeptidases (TIMPs) could significantly contribute to the accumulation of extracellular matrix in the myocardium (Westermann et al. 2007, Van Linthout et al. 2008). Increase of collagen is often observed in the heart of diabetic patients (Shimizu et al. 1993). Additionally, the elevated levels of extracellular matrix proteins and the elevation of their gene expression have been observed in the heart of diabetic animals (Mizushige et al. 2000, Westermann et al. 2007, Rajesh et al. 2009, Rajesh et al. 2012). Nevertheless, hyperglycemia only is sufficient to induce cardiac fibroblast and vascular smooth muscle cell proliferation and to trigger myocardial pro-growth signaling pathways (Begum et al. 2000, Tokudome et al. 2004, Yeshao et al. 2005).

2.4. The role of cyclic guanosine monophosphate (cGMP) signaling in diabetic cardiomyopathy

The main steps of the signaling pathway and its pharmacology are summarized on Figure 1.

2.4.1. Generation, degradation and effects of cGMP

The NO-sGC-cGMP pathway. NO is a key transmitter molecule synthetized from L-arginine by NO synthases (endothelial (eNOS), neuronal (nNOS) and inducible (iNOS)) and is involved in many regulatory and biological processes in mammals (e.g. inflammatory processes, vascular and cardiac homeostasis and neuronal transmission). As a gaseous transmitter it diffuses into the target cells such as vascular smooth muscle cells or cardiomyocytes. Thereafter, NO binds to the sGC and activates the enzyme to produce massive amounts of intracellular cGMP from GTP (Takimoto 2012).

The NP - particulate GC (pGC) - cGMP pathway. NPs are polypeptide hormones. ANP and BNP are derived from atria and ventricles while C-type NP is originated from endothelial cells (Kuhn 2003). cGMP is generated by the pGC when NPs are bound to the enzyme. The pGC enzyme is widely expressed in different tissues including the myocardium.

Degradation of cGMP by phosphodiesterases (PDEs). The biological effects of the second messenger cGMP are regulated by PDEs. PDEs are responsible for the degradation of cGMP as they convert it into 5'-GMP (Zhao et al. 2016). Altogether 11 types of PDE (1-11) are known to date and the 1, 2, 3, 4, 5, 8 and 9 are expressed in the heart (Takimoto 2012). Among all PDEs, the PDE5A subtype is a cGMP-specific esterase expressed in vascular smooth muscle cells, however, recent evidence suggest that PDE5A is presented in cardiac myocytes (Tsai et al. 2009). Moreover, PDE5A has been shown to be overexpressed in different cardiac diseases associated with oxidative stress (Nagendran et al. 2007, Lu et al. 2010). PDE5A is localized near to the Z-band of cardiomyocytes (Takimoto 2012). According to a recent publication, PDE9A is also upregulated in cardiac disorders and pathological myocardium hypertrophy thus it could significantly contribute to cGMP-depletion in cardiomyocytes. However, PDE9A regulates mainly the NO-independent pool of cGMP (Lee et al. 2015).

cGMP-dependent effects and protein kinase G (PKG). PKG is a serine/threonine kinase that mediates the main effects of cGMP (Moncada et al. 1991, Evgenov et al. 2006). The two subtypes, PKGI and PKGII are encoded by two different genes and they contain three functional domains that determines cGMP-sensitivity of the enzyme (Takimoto 2012). cGMP, through the activation of PKG has several downstream effects including the negative regulation of cardiac contractility by the reduction of myofilament Ca^{2+} responsiveness. NO-derived cGMP has also anti-adrenergic effects that might be attributable to cardiac troponin I phosphorylation by PKG (Lee et al. 2010). Cardiac diastolic function is regulated by both NO and NP-derived cGMP pools as exogenous BNP increases the speed and extent of ventricular relaxation (Lainchbury et al. 2000). Moreover, PKG contributes to diastolic relaxation by PKG-mediated phosphorylation of the giant protein titin (Takimoto 2012) and by exerting inhibitory effects on L-type Ca^{2+} channels and activating phospholamban-mediated calcium reuptake to the sarcoplasmic reticulum (Kovacs et al. 2016). As discussed above, cardiac hypertrophy is an important contributor to myocardial remodeling in different cardiac diseases. However, the cGMP-signaling mediated effects of PKG activate anti-hypertrophic pathways in the heart. These processes include Gq-coupled and calcineurin related pathways. Recent studies showed that calcineurin pathway is deactivated via L-type Ca^{2+} channel inhibition (Fiedler et al. 2002) and by the phosphorylation of TRCP6

(transient receptor potential canonical 6) receptor (Koitabashi et al. 2010). Other studies also implicated the role of regulator of G protein signaling 2 and 4 (RGS2 and 4) in the anti-hypertrophic effects as PDE5A inhibition failed to modulate cardiac hypertrophy in mice lack RGS2 (Takimoto et al. 2009). On the other hand, cGMP signaling mediates anti-apoptotic effects via the regulation of the mitochondrial K_{ATP} channel and the stress responsive survival signaling cascades (Burley et al. 2007, Kukreja et al. 2011). As a result of PKG activation opening of the mitochondrial K_{ATP} channel and subsequent inhibition of the mitochondrial transition pore occur thus the membrane potential of the mitochondria become stabilized. Other features of cGMP-mediated anti-apoptotic effects are phosphorylation of extracellular signal-regulated kinases and the glycogen synthase kinase 3β and upregulation of anti-apoptotic Bcl2 (Takimoto 2012). PKG also inhibits the pro-apoptotic p38 mitogen-activated protein kinase (Fiedler et al. 2006) and exerts anti-oxidative effects through the upregulation of the mitochondrial superoxide dismutase (Kukreja et al. 2011).

2.4.2. Deterioration of cGMP-signaling in oxidative stress and in diabetic cardiomyopathy

Diseases that are associated with excessive production of RNS and ROS (including diabetes mellitus) have been shown to lead to the impairment of NO-sGC-cGMP-PKG signaling (Huynh et al. 2014). Another important contributor to the impaired NO-signaling is microvascular inflammation coupled with the dysfunction of the vascular endothelial layer (Paulus et al. 2013). In pathological cases associated with oxidative stress (including diabetes mellitus), eNOS can become uncoupled as it loses its co-factor tetrahydrobiopterin. Thus, it produces massive amounts of superoxide anions which further propagates oxidative stress (Silva et al. 2012). Moreover, phosphorylation of eNOS might alter the enzyme's activity, e.g. phosphorylation at Thr495 decreases its activation, thus reducing NO bioavailability (Bouloumie et al. 1997). Furthermore, superoxide anions rapidly react with NO in oxidative stress and peroxynitrite is formed which further decreases the bioavailability of NO (Pacher et al. 2007). Not only the decreased bioavailability of NO, but also superoxide and peroxynitrite-mediated damage of sGC (and many other enzymes and structural proteins) coupled with the

upregulation of different PDEs are contributors of the deteriorated cGMP-signaling (Pacher et al. 2007, Pokreisz et al. 2009, Das et al. 2015) in diabetes mellitus, in particular. Oxidative stress directly leads to the oxidative damage of the sGC enzyme which in turn loses its heme prosthetic group and becomes inactivated (Evgenov et al. 2006). As a result, sGC will not be able to produce intracellular cGMP even if NO is available. Moreover, upregulation of PDEs (especially PDE5A) further decreases the amount of intracellular cGMP and this contributes to the insufficiency of PKG-mediated cardioprotective signaling pathways and causes consequent tissue injury.

2.4.3. Pharmacological modulation of the NO-sGC-cGMP-PKG pathway

NO donors and NOS activators. The first class of drugs that has been tested to treat chest pain are the so called nitrovasodilators including glycerine trinitrate. These drugs have been used since 1879. These compounds release NO by spontaneous decomposition or by bioconversion to activate sGC. Although they are widely used drugs to treat different cardiovascular disorders, everyday use of such drugs is limited due to the development of nitrate tolerance, nonspecific interactions of NO with other molecules (e.g. peroxynitrate) and by the lack of response due to insufficient metabolism (Evgenov et al. 2006). Recently, inhaled NO has been approved for the treatment of persistent pulmonary hypertension of the newborn (Stasch et al. 2011). Besides, tetrahydrobiopterin and eNOS activators have been shown to reduce diastolic dysfunction in animal experiments (Kovacs et al. 2016).

sGC activation and stimulation. Recently discovered classes of drugs are the sGC activators and stimulators that modulate sGC activity. sGC activators and stimulators are ideal substitutes of NO in case of endothelial dysfunction (e.g. in oxidative stress) as they directly bind to sGC and increase its ability to produce cGMP (Kovacs et al. 2016). The difference between the two types of these compounds is that sGC activators are able to reactivate even the oxidized, inactive form of the enzyme, while the stimulators bind to the reduced, heme-containing form of sGC by replacing NO. However, sGC stimulators do not reactivate the inactive, heme-free enzyme (Evgenov et al. 2006). The sGC stimulator riociguat has been approved to treat patients with pulmonary

hypertension. Currently, a trial investigating another sGC stimulator, the vericiguat is conducted in heart failure patients.

PDE5A inhibition. PDE5A inhibitors (sildenafil, vardenafil, tadalafil, avanafil) are on-demand treatment for erectile dysfunction (Korkmaz-Icoz et al. 2017). The role of PDE5A in myocardial remodeling has been shown by Takimoto and colleagues on PDE5A knockout mice (Takimoto et al. 2005). The mechanism of action of PDE5A inhibitors include increased tissue and plasma levels of cGMP which results in vasorelaxation and vasodilation (Kukreja et al. 2011). Among the different PDE5A inhibitors vardenafil is a highly selective one and it displays the highest potency compared to its comparators. Sildenafil and tadalafil have also been approved by the US Food and Drug Administration for the treatment of pulmonary hypertension.

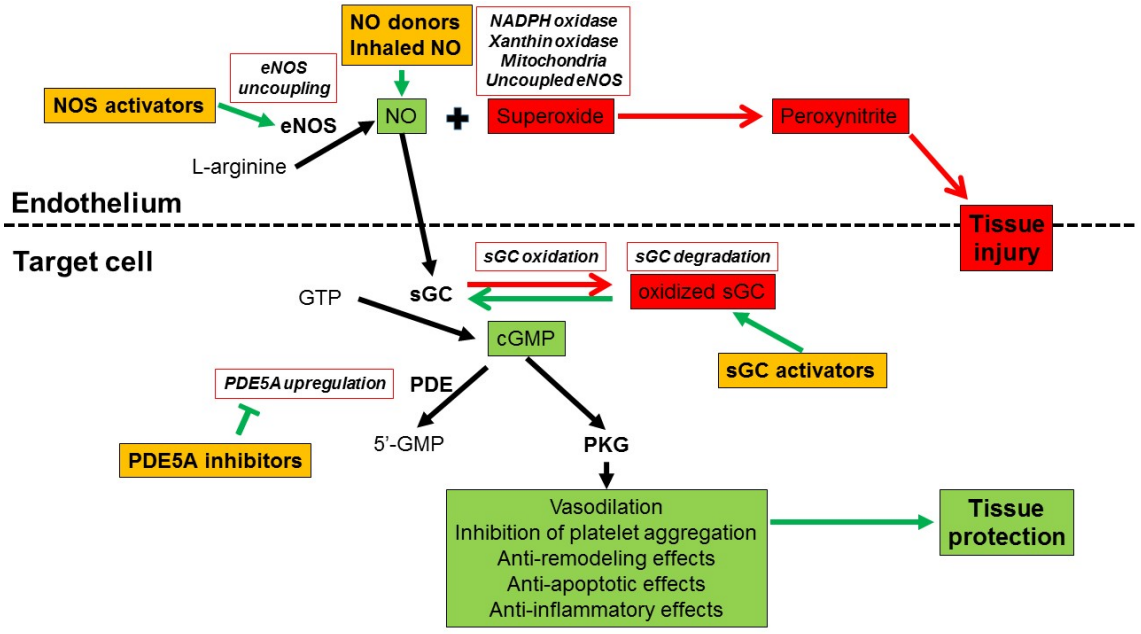

Figure 1. Schematic diagram of physiology, pathophysiology and pharmacology of nitric-oxide (NO) – cyclic guanosine monophosphate (cGMP) pathway
Detailed description of the signaling pathway is available in the text. NO: nitric oxide, NOS: NO synthase, eNOS: endothelial NOS, sGC: soluble guanylate cyclase, GTP: guanosine triphosphate, GMP: guanosine monophosphate, PDE5A: phosphodiesterase-5A, PKG: protein kinase G, NADPH: nicotinamide adenine dinucleotide phosphate, Target cell: cardiomyocytes and/or smooth muscle cells. Physiological effects of the signaling pathway are depicted as green, pathophysiological processes are shown in red and the possible pharmacological interventions are orange-colored.

2.4.4. Pharmacology and cardioprotective effects of the sGC activator cinaciguat

The sGC activator cinaciguat (BAY 58-2667; Figure 2.) has been reported to bind to the heme pocket of NO-insensitive sGC (Stasch et al. 2006) thus stabilizing the enzyme to increase cGMP generation and to augment cGMP-PKG signaling. Cinaciguat produces an additive effect when combined with NO donors (Evgenov et al. 2006). Cinaciguat replaces the oxidized heme prostethic group of the sGC enzyme resulting in the activation of sGC. One of the biggest advantage of the compound is that it is able to discriminate between both redox states of the enzyme (Evgenov et al. 2006). Additionally, cinaciguat increases the maximal catalytic rate of sGC and stabilizes the nitrosyl-heme complex (Evgenov et al. 2006). Interestingly, cinaciguat inhibits the PDE5A enzyme with an IC_{50} of 10 μmol/l (Evgenov et al. 2006). Recent studies described the beneficial cardioprotective effects of cinaciguat in experimental myocardial infarction (Korkmaz et al. 2009), myocardial ischemia/reperfusion injury (Radovits et al. 2011, Salloum et al. 2012), endothelial dysfunction induced by nitro-oxidative stress (Korkmaz et al. 2013), vascular neointima formation (Hirschberg et al. 2013) or in prevention of cardiomyocyte hypertrophy (Irvine et al. 2012, Nemeth et al. 2016). Moreover, the safety and tolerability of the sGC activator cinaciguat have been assessed by phase-I human clinical trials (Frey et al. 2008). Although cinaciguat has demonstrated efficacy in a proof-of-concept study in patients with acute decompensated heart failure (Lapp et al. 2009), the phase-IIb clinical studies for the same indication has been prematurely terminated due to the high number of adverse events (mainly a significant drop of blood pressure) during acute intravenous application (Erdmann et al. 2013, Levy et al. 2014). However, the investigators concluded that rather a chronic, long-term oral administration of the compound could improve endothelial and preserve myocardial function in heart failure patients (Gheorghiade et al. 2012).

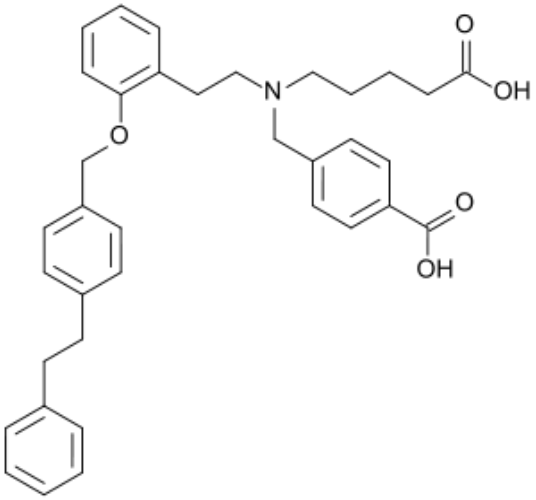

Figure 2. Molecular structure of cinaciguat

2.4.5. Pharmacology and cardioprotective effects of the PDE5A inhibitor vardenafil

As discussed above, inhibitors of PDEs (PDE5A in particular) enhance cGMP-driven effects and increase cardiomyocyte relaxation via PKG-mediated signaling pathways (Kovacs et al. 2016). Vardenafil (Figure 3.) is a highly selective PDE5 inhibitor with a potency about 10-fold higher than that of sildenafil (Saenz de Tejada et al. 2001). The protective effects of enhanced cGMP-signaling via pharmacological inhibition of PDE5A has been demonstrated in several cardiovascular diseases (Kukreja et al. 2012) including ischemia/reperfusion injury related to heart transplantation (Loganathan et al. 2008), cardiopulmonary bypass (Szabo et al. 2009) and myocardial infarction (Kukreja et al. 2004), neointima hyperplasia formation (Hirschberg et al. 2009) and in type 1 diabetes mellitus-associated vascular and cardiac dysfunction in particular (Schafer et al. 2008, Radovits et al. 2009a). Interestingly, vardenafil has been shown to improve blood flow in 70 % of patients with Raynaud's disease and improved clinical signs in 68 % of patients (Kukreja et al. 2011). Moreover, the beneficial cardiac effects of sildenafil on HFpEF patients have been investigated in the RELAX trial. The outcome of the RELAX trial, however, failed to show improvement in exercise capacity and on the clinical outcomes in advanced HFpEF patients treated with sildenafil (Redfield et al. 2013). In spite of these contradictory results, Das et al. proposed that PDE5A inhibition

might be of therapeutic importance in subgroup of patients who have diabetes mellitus (Das et al. 2015). Moreover, sildenafil and tadalafil have been approved for the treatment of pulmonary hypertension (Kukreja et al. 2012).

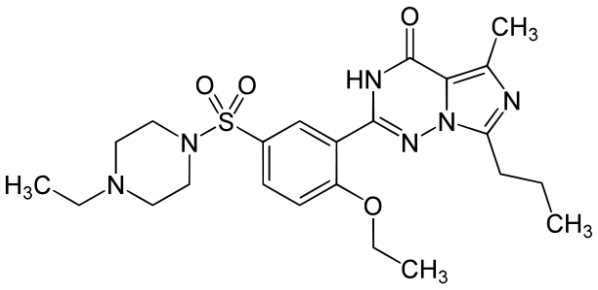

Figure 3. Molecular structure of vardenafil.

3. Objectives

Recent advances of the research on heart failure pointed out that the clinical outcome and the success of drug therapy of heart failure patients depend a lot on the co-morbidities of the patients. Among these co-morbidities, diabetes mellitus is a significant one which leads to the development of a special disease entity, diabetic cardiomyopathy. Diabetic cardiomyopathy is a complex disease characterized by special features including increased oxidative and nitrosative stress, fibrotic and hypertrophic remodeling and the deterioration of cGMP signaling. Therefore, enhancement of cGMP signaling in the myocardium might provide a novel and promising therapeutic option to treat diabetic heart failure.

Based upon that, the aims of the present studies were:

1. Comparison of the functional (systolic and diastolic) and the structural hallmarks (oxidative stress, fibrotic and hypertrophic remodeling and apoptosis) of diabetic cardiomyopathy in animal models of T1DM and T2DM

2. Revelation of the alterations of NO-cGMP signaling in diabetic cardiomyopathy in the two types of DM

3. Explore the possible therapeutic effects of sGC activation by the novel sGC activator cinaciguat in T1DM-associated diabetic cardiomyopathy

4. Study the potential cardioprotective effects of the PDE5A inhibitor vardenafil on the development of T2DM-related diabetic cardiomyopathy

4. Methods

The investigation conformed to the EU Directive 2010/63/EU guidelines and the Guide for the Care and Use of Laboratory Animals used by the US National Institutes of Health (NIH Publication No. 85–23, revised 1996). The experimental protocol was reviewed and approved by the institutional ethical committee (permission number: 22.1/1162/3/2010). Animals received humane care.

4.1. Animal models

4.1.1. Rat model of type 1 diabetes mellitus

Depending on the experimental setting, eight- or twelve-week-old male Sprague-Dawley rats (SD; Charles River, Sulzfeld, Germany) were housed individually in a cage in a room (constant temperature (22±2 ºC), 12/12h light/dark cycles) and received standard laboratory rat diet and water ad libitum. T1DM was induced with a single intraperitoneal injection of STZ (60 mg/kg) (Sigma Aldrich, Saint Louis, MO, USA) in our rats. STZ was freshly dissolved in citrate buffer (pH = 4.5; 0.1 mol/l). Control animals received only the buffer. 72 h after the injection a drop of blood was collected from the tail vein and blood glucose concentration was determined by using a digital blood glucose meter (Accu-Chek® Sensor, Roche, Mannheim, Germany). Animals with a random blood glucose level >15 mmol/l were considered to be diabetic and were included into the study.

4.1.2. Rat model of type 2 diabetes mellitus

The inbred ZDF rat was used as an animal model of T2DM. Rats develop T2DM due to a genetic mutation of the leptin receptor and a special diet (Purina #5008) recommended by the supplier. Homozygous recessive males (fa/fa) develop obesity, fasting hyperglycemia and T2DM. Homozygous dominant (+/+) and heterozygous (fa/+) lean genotypes remain normoglycemic. Six-week old male ZDF diabetic (fa/fa) and ZDF lean (+/?) rats (Charles River) were acclimatized for one week before starting the

experimental protocol. Rats were housed individually in a cage in a room at a constant temperature (22±2 ºC) and humidity, with a 12/12h light/dark cycle and fed Purina #5008 diet and water ad libitum. Experiments on the rats were performed at the age of 30-32 weeks.

4.2. Study protocol

Summary of our study protocol is shown on Figure 4.

4.2.1. Comparative investigation of T1DM or T2DM related diabetic cardiomyopathy

Rat models of T1DM (STZ-induced DM) and T2DM (ZDF) were used to compare the pathophysiology of T1DM and T2DM-related diabetic cardiomyopathy. For T1DM 12-week old SD rats were used and DM was induced by a single i.p. injection of STZ as described above (groups: SD control; n=10 and SD diabetic; n=8). Experiments were performed after eight week of diabetes duration. For T2DM ZDF rats were used (for detailed description of the model see above). Experiments were performed on 32-week old male ZDF Lean (n=9) and ZDF (n=8) rats. The time of sacrifice was chosen based on our pilot and previous studies where cardiac dysfunction is detectable in these models.

4.2.2. Experiments on the effect of sGC activation in T1DM related diabetic cardiomyopathy

Eight-week old SD rats were used. After confirmation of DM induced by STZ injection, rats were randomized into four groups: vehicle-treated control (Co; n=12), cinaciguat-treated control (CoCin; n=12), vehicle-treated diabetic (DiabCo; n=12) and cinaciguat-treated diabetic (DiabCin; n=10) groups. Animals were treated for 8 weeks with 0.5 % methylcellulose (Co, DiabCo) vehicle or with the sGC activator cinaciguat in suspension per os (CoCin, DiabCin; 10 mg/kg/day), starting immediately after DM

confirmation. Water intake was measured every day. Body weight (BW) of the animals were recorded every other day and the dose of cinaciguat was adjusted accordingly.

4.2.3. Experiments on the effect of PDE5A inhibition in T2DM related diabetic cardiomyopathy

6-week old male ZDF diabetic (fa/fa) and ZDF lean (+/?) rats (Charles River) were acclimatized for one week before starting the experimental protocol. 7-week old animals were randomized into four groups: vehicle-treated controls (ZDFLean; n=8), vardenafil-treated controls (ZDFLean+Vard; n=7), vehicle-treated diabetic (ZDF; n=7) and vardenafil-treated diabetic (ZDF+Vard; n=8). Rats were fed Purina #5008 diet and water ad libitum. Per os drug treatment (10 mg/kg BW vardenafil continuously, dissolved in 0.01 mol/l citrate buffer) or vehicle (0.01 mol/l citrate buffer) administration (in water bottle) was initiated at the 7^{th} week of age and continued until the end of the experimental period. Animal cages were handled with care and were not moved after water bottle replacement to prevent spilling of water from the bottles. Functional measurements were performed at the age of 32 weeks. BW of the animals were measured every two days and the dose of vardenafil was adjusted accordingly.

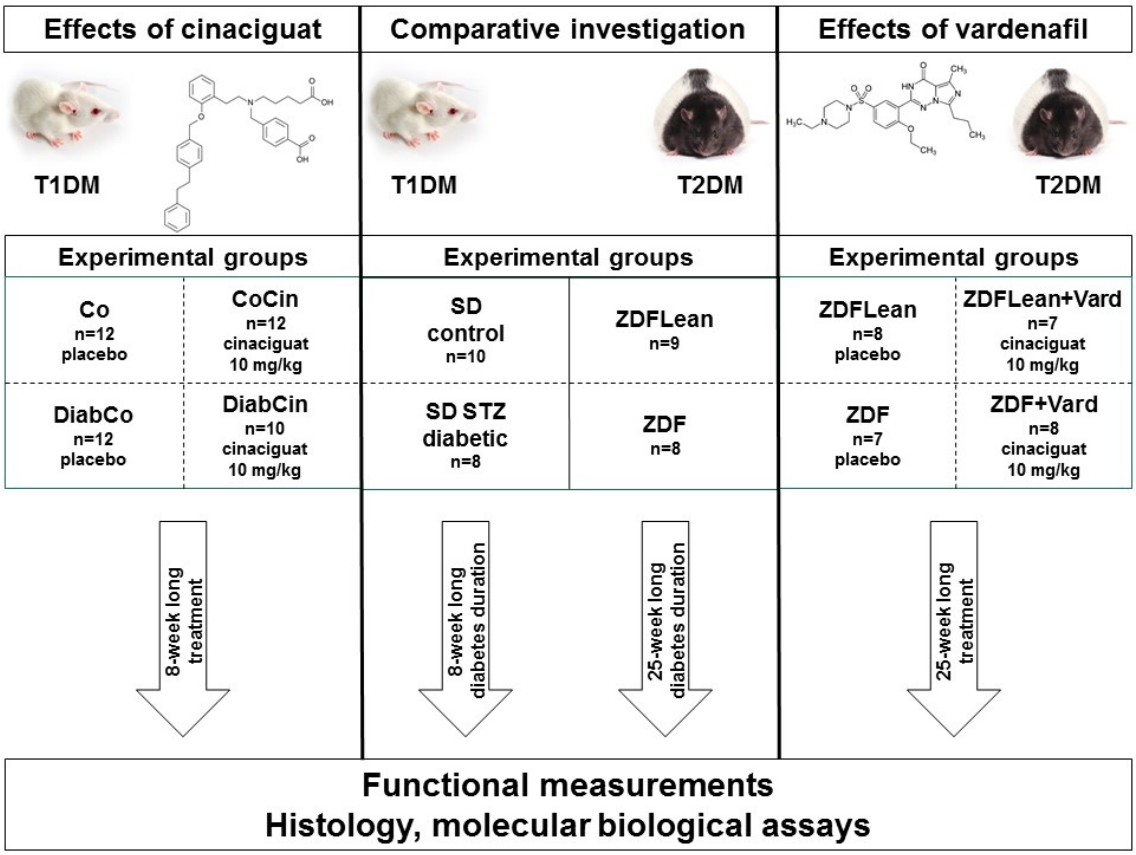

Figure 4. Study protocol
Abbreaviations: Type 1 diabetes mellitus (T1DM), type 2 diabetes mellitus (T2DM). Comparative investigation: Sprague-Dawley (SD), Zucker Diabetic Fatty (ZDF). Cinaciguat effects: vehicle-treated control (Co), cinaciguat-treated controls (CoCin), vehicle-treated diabetic (DiabCo), cinaciguat-treated diabetic (DiabCin). Vardenafil effects: vehicle-treated controls (ZDFLean), vardenafil-treated controls (ZDFLean+Vard), vehicle-treated diabetic (ZDF), vardenafil-treated diabetic (ZDF+Vard).

4.3. Biochemical measurements

Urine samples were collected at the end of the invasive hemodynamic measurements and urine glucose level was determined by a digital blood glucose meter (Accu-Chek® Sensor, Roche).

Blood was collected at the end of the invasive hemodynamic investigation from the inferior caval vein. Blood glucose (BG) level was determined by a digital blood glucose meter (Accu-Chek® Sensor, Roche). Thereafter, plasma was prepared and stored at -80 ºC for long term. Plasma cGMP was measured by a cGMP enzyme immunoassay (EIA)

kit (Amersham cGMP EIA Biotrak System, GE Healthcare, Buckinghamshire, UK) according to the recommendations of the manufacturer. Plasma nitrite/nitrate levels were determined by by Nitric Oxide Colorimetric Assay Kit (#K262-200, Biovision, Milpitas, CA, USA) in order to assess nitric oxide bioavailability.

4.4. Echocardiography

In case of ZDF rats, animals underwent echocardiographic examination at the age of 32 weeks. Animals were anesthetized with 1-2 % isoflurane in 100 % oxygen, placed on a heating pad (body temperature was maintained at 37 °C). Echocardiography was conducted by using a 13-MHz linear transducer (GE 12L-RS, GE Healthcare) coupled with an echocardiography machine (Vivid i, GE Healthcare). Images were analyzed by an independent investigator with an image analysis software (EchoPac, GE Healthcare). B-mode images, acquired in the long-axis and in the short-axis at the mid-papillary level, were used to measure LV anterior, posterior wall thicknesses (LVAW, LVPW) and LV internal diameter (ID) in end-diastole (d) and in end-systole (s). M-mode images were taken on short-axis plane at the mid-papillary level. End-systole was defined at minimal, while end-diastole was defined at maximal LVID. Values of three consecutive cycles were averaged and used for statistical analysis. LV mass was calculated by the following equation: $LVmass=1.04x[(LVAWd+LVIDd+LVPWd)^3-LVIDd^3]$. Relative wall thickness (RWT) was calculated as $RWT=(LVAWd+LVPWd)/LVIDd$. LVmass was normalized to the BW (in kg) (LVmass index) and to the TL (LVmass/TL) to compare cardiac hypertrophy in the animals.

4.5. Hemodynamic investigation

Invasive hemodynamic measurements were carried out. Briefly, at the end of the experimental period, the animals were anesthetized, tracheotomized and intubated to facilitate breathing. Rats were placed on controlled heating pads, core temperature was maintained at 37 ºC. The left external jugular vein was cannulated with a polyethylene catheter for fluid administration. A 2F microtip pressure-conductance microcatheter

(SPR-838, Millar Instruments, Houston, TX, USA) was inserted into the right carotid artery and advanced into the ascending aorta. After 5 min stabilization, mean arterial blood pressure (MAP) and heart rate (HR) were recorded. Afterwards, the catheter was advanced into the LV under pressure control. After 5 min stabilization, signals were continuously recorded at a sampling rate of 1000 samples/s using a P-V conductance system (MPVS-Ultra, Millar Instruments) connected to the PowerLab 16/30 data acquisition system (AD Instruments, Colorado Springs, CO, USA), stored, and displayed on a personal computer by the LabChart7 Software System (AD Instruments). A special P-V analysis programme (PVAN, Millar Instruments) was used to compute and calculate MAP, maximal LV systolic pressure (LVSP), LV end-diastolic pressure (LVEDP), maximal slope of systolic pressure increment (dP/dt_{max}) and diastolic pressure decrement (dP/dt_{min}), time constant of LV pressure decay (Tau_W; according to the Weiss method), ejection fraction (EF), stroke work (SW) and cardiac output (CO). LV P-V relations were determined at different preloads during transient occlusion of the inferior caval vein. The slope of the LV end-systolic P-V relationships (E_{es}; according to the parabolic curvilinear model) and preload recruitable stroke work (PRSW) were calculated as load-independent indexes of LV contractility and the slope of the LV end-diastolic P-V relationship (EDPVR) was calculated as reliable index of LV diastolic stiffness.

After completing the hemodynamic measurements in vivo and in vitro volume calibrations were performed. In vivo volume calibration was performed with hypertonic saline (100 µl) intravenous bolus injection. From the shift of P-V loops parallel conductance (Vp) was calculated and cardiac mass volume was corrected appropriately. Animals were euthanized by exsanguination and in vitro cuvette calibration was carried out as follows: nine cylindrical holes in a block 1 cm deep and with known diameters (ranging from 2 to 11 mm) were filled with fresh heparinized whole blood of the animal. In this calibration, the linear volume-conductance regression of the absolute volume in each cylinder versus the raw signal acquired by the conductance catheter was used as the volume calibration formula.

4.6. Force measurement in permeabilized LV cardiomyocytes

Force measurements were performed as described by Papp and colleagues (Papp et al. 2002). Briefly, frozen LV tissue samples were mechanically disrupted in isolating solution (ISO) (1 mmol/l $MgCl_2$, 100 mmol/l KCl, 2 mmol/l EGTA, 4 mmol/l ATP, 10 mmol/l imidazole, pH 7.0) containing 0.5 mmol/l phenylmethylsulfonyl fluoride, 40 μmol/l leupeptin and 10 μmol/l E-64 protease inhibitors (Sigma-Aldrich). The mechanically isolated cardiomyocytes were incubated in ISO supplemented with 0.5 % (v/v) Triton X-100 (Sigma–Aldrich) for 5 min at 4 °C. Single permeabilized cells were attached with silicone adhesive (DAP 100 % all-purpose silicone sealant; Baltimore, MD, USA) between stainless insect needles, connected to a sensitive force transducer (SensoNor, Horten, Norway) and an electromagnetic high-speed length controller (Aurora Scientific Inc., Aurora, Canada) in ISO at 15 °C. Isometric force measurements were performed by transferring the cardiomyocytes from relaxing to activating solution. The compositions of activating and relaxing solutions were calculated as described previously (Fabiato et al. 1979). All solutions supplemented with protease inhibitors (0.5 mmol/l phenylmethylsulfonyl fluoride, 40 μmol/l leupeptin and 10 μmol/l E-64 (Sigma-Aldrich). Myocyte cross sectional-area was calculated from the widths and heights of cardiomyocytes, and force values were expressed in kN/m^2.

4.7. Quantitative reverse transcription polymerase chain reaction (qRT-PCR) measurements

We performed qRT-PCR experiments from LV samples that were harvested immediately after euthanasia, snap frozen in liquid nitrogen and stored at -80 ºC. After homogenization total RNA was isolated from LV tissue by using RNeasy Fibrous Tissue Kit (Qiagen, Hilden, Germany) according to the manufacturer's instructions. RNA concentration was measured photometrically at 260 nm. RNA purity was ensured by obtaining a 260/280 nm optical density ratio of ~2.0. Reverse transcription was performed with QuantiTect Reverse Transcription Kit (Qiagen) by using 1 μg RNA of each sample and random primers. PCR reactions were performed either on the StepOnePlus™ Real-Time PCR System (Applied Biosystems, Foster City, CA, USA) with TaqMan® Universal PCR MasterMix (Applied Biosystems) and TaqMan® Gene Expression Assay (Applied Biosystems) or on the LightCycler480 system (Roche)

coupled with LightCycler480 Probes Master (Roche) and Universal Probe Library (UPL) probes (Roche). Every sample was quantified in triplicates for the targets specified in Table 1. Gene expression data were normalized to glyceraldehyde-3-phosphate dehydrogenase (GAPDH) and expression levels were calculated using the CT comparative method ($2^{-\Delta\Delta CT}$). All results are expressed as values normalized to a positive calibrator (a pool of cDNAs from all samples of the respective control group).

Table 1. Identification numbers of TaqMan® Gene Expression Assays and sequence for the forward (F) and reverse (R) primers (from 5' to 3') and Universal Probe Library (UPL) probes used in qRT-PCR

Gene target (abbreviation)	Target full name	TaqMan® Gene Expression Assay ID
Catalase		Rn00560930_m1
GAPDH	glyceraldehyde-3-phosphate dehydrogenase	Rn01775763_g1
GSR	glutathione reductase	Rn01482159_m1
SOD2	superoxide dismutase 2	Rn00690587_g1
Thioredoxin-1		Rn00587437_m1
ANF	atrial natriuretic factor	Rn00561661_m1
α-MHC	myosin heavy chain alpha	Rn00568304_m1
β-MHC	myosin heavy chain beta	Rn00568328_m1
Bcl-2	B-cell CLL/lymphoma 2	Rn99999125_m1
BAX	Bcl2-associated	Rn02532082_g1

	X protein		
eNOS	endothelial nitric oxide synthase	Rn02132634_s1	
HSP70a1	heat shock 70kDa protein 1A	Rn04224718_u1	
MMP-2	matrix metallopeptidase 2	Rn01538170_m1	
MMP-9	matrix metallopeptidase 9	Rn00579162_m1	
TIMP-1	tissue inhibitor of matrix metallopeptidase (TIMP) 1	Rn00587558_m1	
TIMP-2	TIMP metallopeptidase inhibitor 2	Rn00573232_m1	
Col1a1	Collagen 1a1	Rn01463848_m1	
Col3a1	Collagen 3a1	Rn01437681_m1	
Fibronectin		Rn00569575_m1	
phospholamban	PLB	Rn01434045_m1	
sarcoplasmic reticulum calcium ATPase 2		Rn00568762_m1	
Gene target (abbreviation)	**Target full name**	**Primer sequence**	**UPL probes**

ANF	atrial natriuretic factor	F:5'-CAACACAGATCTGATGGATTTCA-3' R: 5'-CGCTTCATCGGTCTGCTC-3'	65
α-MHC	myosin heavy chain alpha	F:5'-GGAGGTGGAGAAGCTGGAA-3' R.5'-ATCTTGCCCTCCTCATGCT-3'	65
β-actin		F:5'-CTAAGGCCAACCGTGAAAAG-3' R: 5'-TACATGGCTGGGGTGTTGA-3'	115
β-MHC	myosin heavy chain beta	F:5'-GCTGCAGAAGAAGCTCAAAGA-3' R: 5'-GCAGCTTCTCCACCTTGG-3'	65
Caspase-12		F:5'-TGGATACTCAGTGGTGATAAAGGA-3' R:5'-ACGGCCAGCAAACTTCATTA-3'	94
Collagen-1		F:5'-CTGGCAACCTCAAGAAGTCC-3' R: 5'-CAAGTTCCGGTGTGACTCG-3'	65
Collagen-3		F:5'-CCTGTTGGTCCATCTGGAAA-3' R: 5'-GACCTTGGGGACCAGGAG-3'	82
c-fos		F:5'-CCTGCAAGATCCCCAATG-3' R: 5'-AGTCAAGTCCAGGGAGGTCA-3'	115
c-jun		F:5'- TACCGGCCAGCAACT TTC -3' R: 5'-TAGGCGCAGAAGAGGTTTTG-3'	115
eNOS	endothelial nitric oxide synthase	F:5'-TGACCCTCACCGATACAACA-3' R: 5'-CGGGTGTCTAGATCCATGC-3'	5
ET-1	endothelin-1	F:5'-TGTCTACTTCTGCCACCTGGA-3' R:5'-CCTAGTCCATACGGGACGAC-3'	115
GAPDH	glyceraldehyde-3-phosphate dehydrogenase	F:5'- AGCTGGTCATCAATGGGAAA -3' R: 5'- CGGCAGGTCCTTCTCTATCA -3'	9
SOD1	superoxide dismutase 1	F:5'- GGTCCAGCGGATGAAGAG -3' R:5'- GGACACATTGGCCACACC - 3'	5

4.8. Western blot analysis

LV tissue samples were homogenized in radioimmunoprecipitation assay lysis buffer (RIPA; 50 mmol/l Tris HCl pH 8, 150 mmol/l NaCl, 1 % NP-40, 0.5 % sodium deoxycholate, 0.1 % SDS) containing Complete Protease Inhibitor Cocktail (Roche). Protein concentration was determined using the Pierce® BCA Protein Assay Kit

(Thermo Scientific, Rockford, IL, USA). In case of experiments on the effect of cinaciguat, samples were mixed with 2× Laemmli buffer and boiled at 95 ºC for 5 min. In case of experiments investigating the effect of vardenafil, samples were mixed with NuPAGE® Sample Reducing Agent (10X) (Thermo Fisher Scientific) and NuPAGE® LDS Sample Buffer (4X) (Thermo Fisher Scientific) according to the manufacturer's instructions. In case of the comparative investigation, proteins were extracted with a solution containing 8 mol/l urea, 5 mmol/l EDTA, 0.002 % Trasylol, 0.05 mmol/l PMSF, 0.003 % Triton X-100 and protease inhibitors (Roche).

Equal amounts of protein (10–30 µg) were loaded and separated on commercial available precast 4–12% SDS-PAGE gel (NuPAGE® Novex® Bis-Tris Mini Gel, Thermo Fisher Scientific). Afterwards, proteins were transferred to nitrocellulose membrane by semi-dry electroblotting system (iBlot™ Gel Transfer Device, Thermo Fisher Scientific). Membranes were blocked either in 5 % non-fat milk in Tris-buffered saline containing 0.1 % Tween-20 or in 5 % bovine serum albumine in TTBS for 1 h. After blocking, membranes were incubated overnight at 4 ºC with primary antibodies (diluted in 1% bovine serum albumine in TTBS) against various target proteins as listed in Table 2. The ratio of the vasodilator-stimulated phosphoprotein (VASP) and phospho-VASP was used as a marker of PKG activity. After washing, membranes were incubated in horseradish peroxidase (HRP) – conjugated secondary antibody dilutions at room temperature for 1 h (anti-rabbit IgG, anti-mouse IgG, anti-goat IgG appropriately, 1:2000, Cell Signaling, Danvers, MA, USA). Immunoblots were developed using Pierce® ECL Western Blotting Substrate Kit (Thermo Scientific). Protein band densities were quantified using GeneTools software (Syngene, Frederick, MD, USA). GAPDH or α–tubulin (Tubulin) was used to assess equal protein loading.

Table 2. Primary antibodies used in Western blot procedures

Target protein	Abbreviation	Primary antibody	Dilution	Molecular mass
endothelial nitric oxide synthase	eNOS	SC-654 (SantaCruz Biotechnology, Santa Cruz, CA, USA)	1:1000	140 kDa

soluble guanylate cyclase β1	sGC β1	NB100-91798 (Novus Biologicals, Cambridge, UK)	1:1000	70 kDa
phosphodiesterase 5A	PDE5A	ALX-210-099 (Enzo Life Sciences, Farmingdale, NY, USA)	1:2000	130 kDa
protein kinase G	PKG	ADI-KAP-PK005-F (Enzo Life Sciences)	1:2000	75 kDa
vasodilator-stimulated phosphoprotein	VASP	3112 (Cell Signaling, Danvers, MA, USA)	1:1000	50 kDa
phospho-VASP	p-VASP	3114 (Cell Signaling)	1:2000	50 kDa
matrix metallopeptidase 2	MMP-2	NB200-193 (Novus Biologicals)	1:5000	62 kDa
matrix metallopeptidase 9	MMP-9	SC-6840 (SantaCruz Biotechnology)	1:1000	92 kDa
transforming growth factor β1	TGF-β1	SC-146 (SantaCruz Biotechnology)	1:250	25 kDa
cleaved caspase-3		9662 (Cell Signaling)	1:2000	17 kDa
poly (ADP-ribose) polymerase	PARP1	ab137653 (Abcam, Cambridge, UK)	1:1000	113/85 kDa
phospholamban	PLB	8495 (Cell Signaling)	1:1000	12/24 kDa

phospho-phospholamban	p-PLB	8496 (Cell Signaling)	1:1000	12/24 kDa
α-tubulin	Tubulin	#T5168 (Sigma Aldrich)	1:10000	50 kDa
glyceraldehyde-3-phosphate dehydrogenase	GAPDH	MAB374 (Millipore, Billerica, MA, USA)	1:10000	38 kDa

4.9. Histopathology

Myocardial samples were collected for histological examination immediately after invasive hemodynamics, samples were fixed in 4 % buffered paraformaldehyde (PFA) for 24 h, embedded in paraffin and 5 µm thick sections were cut. Hematoxylin and eosin (HE), Masson's trichrome (MT) and picrosirius red stainings were carried out to examine histopathological characteristics and fibrotic remodeling of the LV in the study groups. Light microscopic examination was performed with a Zeiss microscope (Axio Observer.Z1, Carl Zeiss, Jena, Germany) and digital images were aquired using an imaging software (QCapture Pro 6.0, QImaging, Canada). To evaluate cardiomyocyte hypertrophy we measured transverse transnuclear widths (cardiomyocyte diameter) of 100 randomly selected, longitudinally oriented, mono-nucleated cardiomyocytes of the LV on each HE stained myocardium sections cut on the same plane. The extent of fibrotic remodeling was evaluated on MT stained sections. Semiquantitative scoring of fibrotic area was performed by two blinded observers on 20 fields of each MT stained sections under light microscopy. In brief, according to the area of collagen fibers relative to the myocardium, a fibrotic area score was assigned (Scores: 0-3; 0: 0-25 %, 1: 26-50 %, 2: 51-75 %, 3: 75-100 %) and the value of 20 fields were averaged for one sample. Additionally, picrosirius positive area was determined by Image J (NIH, Bethesda, MD, USA) using RGB stack images (green) and thresholding. Picrosirius area was calculated relative to the total area of the tissue.

4.10. Immunohistochemistry

Immunohistochemistry was performed as follows: after antigen retrieval (citric acid buffer) slides were incubated with primary antibodies against the fibrosis marker fibronectin (rabbit polyclonal anti-fibronectin, 1:1000, Sigma-Aldrich), the profibrotic mediator TGF-β1 (rabbit polyclonal anti-TGF-β1, 1:100; Santa Cruz Biotechnology, Santa Cruz, CA, USA) and the sGC-derived second messenger cGMP (rabbit polyclonal anti-cGMP 1:2000, AbD Serotec, Düsseldorf, Germany). After that, slides were incubated with the secondary anti-rabbit antibodies (Biogenex SuperSensitive Link HK-9R, BioGenex, San Ramon, CA, USA) and developed using Fast Red (Dako, Glostrup, Denmark). Semiquantitative scoring was performed (area score 0: up to 10 % positive cells, 1: 11-50 % positive cells, 2: 50-80 % positive cells, 3: above 80 % positive cells; intensity score 1: weak, 2: mild, 3: strong, 4: very strong staining) by two blinded observers. In case of fibronectin area score, in case of TGF-β1 and cGMP area-intensity score (area score × intensity score) were calculated. 3-nitrotyrosine (3-NT) immunohistochemistry was performed in order to assess nitro-oxidative stress. After deparaffination and blocking, 5 μm thin LV sections were incubated with primary antibody against 3-NT (1:80, #10189540, Cayman Chemical, Ann Arbor, MI, USA) at 4 °C overnight. After washing, sections were treated with secondary anti-rabbit antibody (#MP-7401, ImmPRESS™ HRP Anti-Rabbit IgG (Peroxidase) Polymer Detection Kit, Vector Laboratories, Burlingame, CA, USA) for 30 min at room temperature and developed using black colored nickel-cobalt enhanced diaminobenzidine (Vector Laboratories, 6 min, room temperature). Images of four identical area of each section were taken using light microscope at 200x magnification (Zeiss AxioImager.A1 coupled with Zeiss AxioCAm MRc5 CCD camera, Carl Zeiss). 3-NT positive area was determined by color thresholding with ImageJ software (NIH) by two independent investigator. The percentage of positively stained tissue area to total area of each slide was calculated. In case of the comparative study of T1DM and T2DM, we performed immunohistochemical staining for 3-NT. Semiquantitative histomorphological assessment was performed based on the intensity and distribution of labeling using conventional microscopy. After initially evaluating all corresponding tissue sections (magnification 200x), the tissue section with the most intense labeling signals were used

as a reference for maximum labeling intensity. Each specimen was characterized with the average of 4 adjacent fields. 3-NT levels were scored as follows: 0: complete absence of immunoreactivity, 1: weak area of staining, 2: intermediate staining, 3: extensive staining. Using the Cell^A software (Olympus Soft Imaging Solutions GmbH, Münster, Germany), we measured the area of the objects in each class in each field, assigned an area score (1 = <10 % positive cells, 2 = 11-50 % positive cells, 3 = 51-80 % positive cells, 4 = >80 % positive cells), and calculated an average score for the whole picture (intensity score multiplied by area score, 0-12). The evaluation was conducted by an investigator blinded to the experimental groups.

4.11. Detection of apoptosis by terminal deoxynucleotidyl transferase dUTP nick end labeling (TUNEL) assay

Paraffin embedded, 5 µm thick heart tissue sections were used to detect DNA strand breaks in LV myocardium. TUNEL assay was performed using a commercial available kit (DeadEnd™ Colorimetric TUNEL System, Promega, Mannheim, Germany) according to the manufacturer's protocol. Sections were rehydrated, treated with 20 µg/ml Proteinase K to retrieve antigenic epitopes for antibody labeling (at room temperature, 10 min). After washing, sections were refixed in 4 % PFA and treated with a mixture of 98 µl Equilibration Buffer, 1 µl Biotinylated Nucleotide Mix and 1 µl recombinant Terminal Deoxynucleotidyl Transferase (rTdT) enzyme (at 37 ºC, 60 min) to incorporate biotinylated nucleotides at the 3'-OH DNA ends. After washing, 0.3 % hydrogen peroxide (H_2O_2) was used to quench endogenous peroxidase activity.
HRP-labeled streptavidin and 3,3'-diaminobenzidine was used to detect incorporated nucleotides. TUNEL positive cell nuclei were counted by two blinded observers in 20 fields of each section at 400x magnification.

4.12. Statistical analysis

Data are presented as means and standard errors of the mean (SEM). Normal distribution was tested by Shappiro-Wilks normality test. A p value <0.05 was used as a criterion of significance.

4.12.1. Comparative investigation of T1DM and T2DM-related diabetic cardiomyopathy

An unpaired two-sided Student's t-test was used to compare parameters of diabetic and control animals in both models. To compare diabetes-induced alterations between the two models individual data of each animal was normalized to the average value of the corresponding control group.

4.12.2. Experiments on the effect of sGC activation in T1DM-related diabetic cardiomyopathy

Two-way analysis of variance (ANOVA) with "T1DM" and "Cinaciguat" as independent factors was carried out in order to examine the main effect of the independent variables and the interaction between them. Data that did not show normal distribution were transformed logarithmically before performing two-factorial ANOVA. Tukey HSD post hoc test was used to assess intergroup differences and the results are shown on the figures. Where interaction $p<0.05$ the observed effects of the independent factors are in relationship and the effect of one independent variable may depend on the level of the other independent variable.

4.12.3. Experiments on the effect of PDE5A inhibition in T2DM-related diabetic cardiomyopathy

Two-way analysis of variance (ANOVA) with "T2DM" and "Vardenafil" as independent factors was carried out in order to examine the main effect of the independent variables and the interaction between them. Tukey HSD post hoc test was used to assess intergroup differences and the results are shown on the figures. Where interaction $p<0.05$ the observed effects of the independent factors are in relationship and the effect of one independent variable may depend on the level of the other independent variable.

4.13. Drugs

The sGC activator cinaciguat (BAY 58-2667; 4-(((4-carboxybutyl)[2-(2-([4-(2-phenylethyl)phenyl]methoxy)phenyl)ethyl]amino)methyl)benzoic acid) was provided by Bayer HealthCare (Wuppertal, Germany) for oral application. Cinaciguat was suspended in 0.5% methylcellulose solution. The PDE5A inhibitor vardenafil (2-[2-ethoxy-5-(4-ethylpiperazin-1-yl)sulfonylphenyl]-5-methyl-7-propyl-1H-imidazo[5,1-f][1,2,4]triazin-4-one) was a gift from Bayer HealthCare and was dissolved in 0.01 mol/l citrate buffer for per os application.

5. Results

5.1. Comparative investigation of T1DM- and T2DM-related diabetic cardiomyopathy

Summary of the results is shown in Table 3.

5.1.1. *Heart weight (HW), body weight and glucose levels*

Compared with the corresponding control group, DM was associated with decreased body weight and increased blood and urine glucose levels in both models (Table 3). BG levels did not significantly differ between the two diabetic groups. Heart weight to body weight ratio showed a marked tendency towards increased values in the diabetic animals of the type 2 DM model, while it reached statistical significance in the type 1 DM model (Table 3).

Table 3. Blood and urine glucose levels, body weight and heart weight to body weight ratios (HW/BW) and mean arterial pressure (MAP)
Groups: Sprague-Dawley (SD), streptozotocin (STZ)-diabetic SD, ZDF lean and ZDF diabetic rats. *: $p<0.05$ vs. corresponding non-diabetic group.

Variable	SD control	SD STZ diabetic	ZDF lean	ZDF diabetic
Blood glucose (mmol/l)	6.54±0.16	26.08±0.87*	6.28±0.29	25.99±2.08*
Urine glucose (qualitative)	negative	positive	negative	positive
Body weight (g)	431.3±5.9	330.0±10.5*	440.0±4.8	353.3±9.5*
HW/BW (g/kg)	2.92±0.06	3.51±0.14*	3.46±0.05	3.74±0.23
MAP (mmHg)	77±4	73±3	109±7	90±5

5.1.2. *Cardiac contractility and ventricular stiffness*

MAP did not significantly differ between diabetic rats and corresponding controls (Table 3.). P-V loop derived load-dependent and -independent contractility parameters (EF and E_{es}) were significantly lower in STZ-induced diabetic animals compared to non-diabetic controls, suggesting impaired systolic performance in type 1 DM. In contrast, compared with the corresponding control, type 2 diabetic ZDF rats showed unaltered LV contractility (Figure 5A).

LVEDP and the slope of EDPVR were significantly increased in diabetic animals of the type 2 DM model, indicating a marked increase in end-diastolic stiffness. These changes could be observed only to a lower extent in type 1 diabetic rats (Figure 5B).

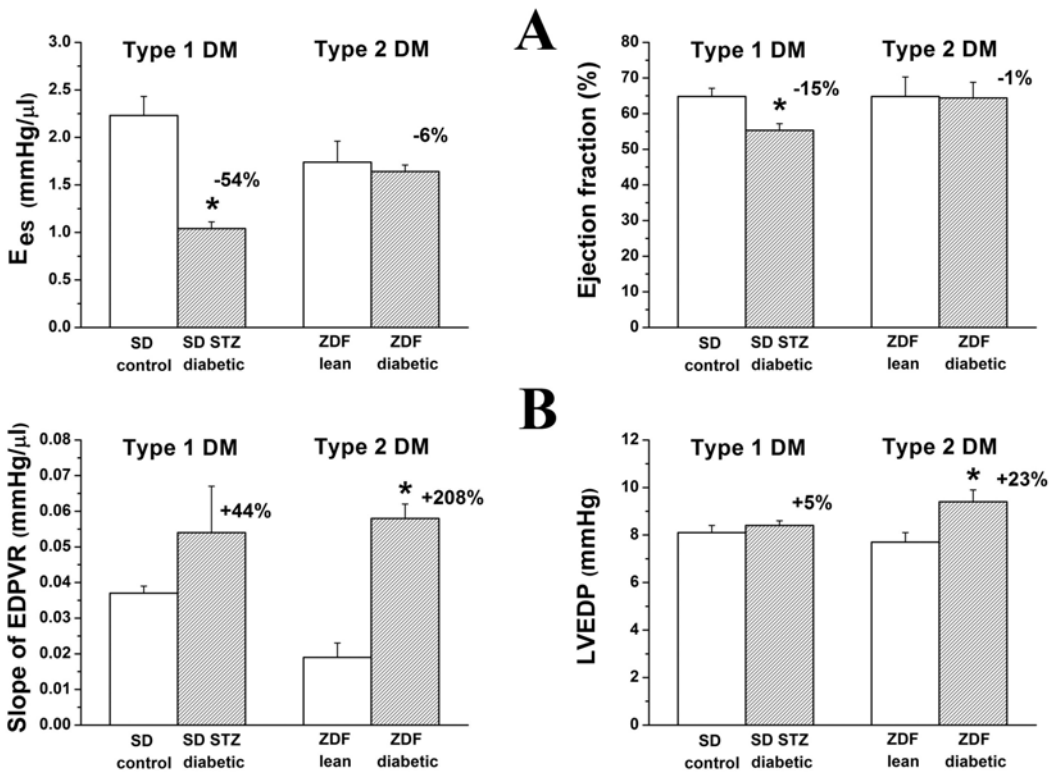

Figure 5. Cardiac function
Left ventricular contractility indices (A): slope of end-systolic pressure-volume relationship (E_{es}) and ejection fraction (EF) in the groups of SD control, STZ-induced diabetic SD, ZDF lean, and ZDF diabetic rats. Parameters of left ventricular stiffness (B): slope of end-diastolic pressure-volume relationship (EDPVR) and end-diastolic pressure (LVEDP) in the groups of SD control, streptozotocin (STZ)-induced diabetic SD, Zucker Diabetic Fatty (ZDF) lean, and ZDF diabetic rats. Percent changes between

diabetic and corresponding non-diabetic control groups are indicated in both DM models. *p<0.05 vs. the corresponding non-diabetic group.

5.1.3. *Histopathology*

The characteristics of diabetic cardiomyopathy were found in LV sections of the diabetic groups with hematoxylin-eosin staining (Figure 6A). Disarray and collapse of myofibers, myocardial degeneration could be observed in the LV myocardium of diabetic rats in both models. Mean cardiomyocyte width, as a marker of cardiomyocyte hypertrophy was significantly increased in both diabetic groups when compared to the corresponding controls (Figure 6A and 7A).

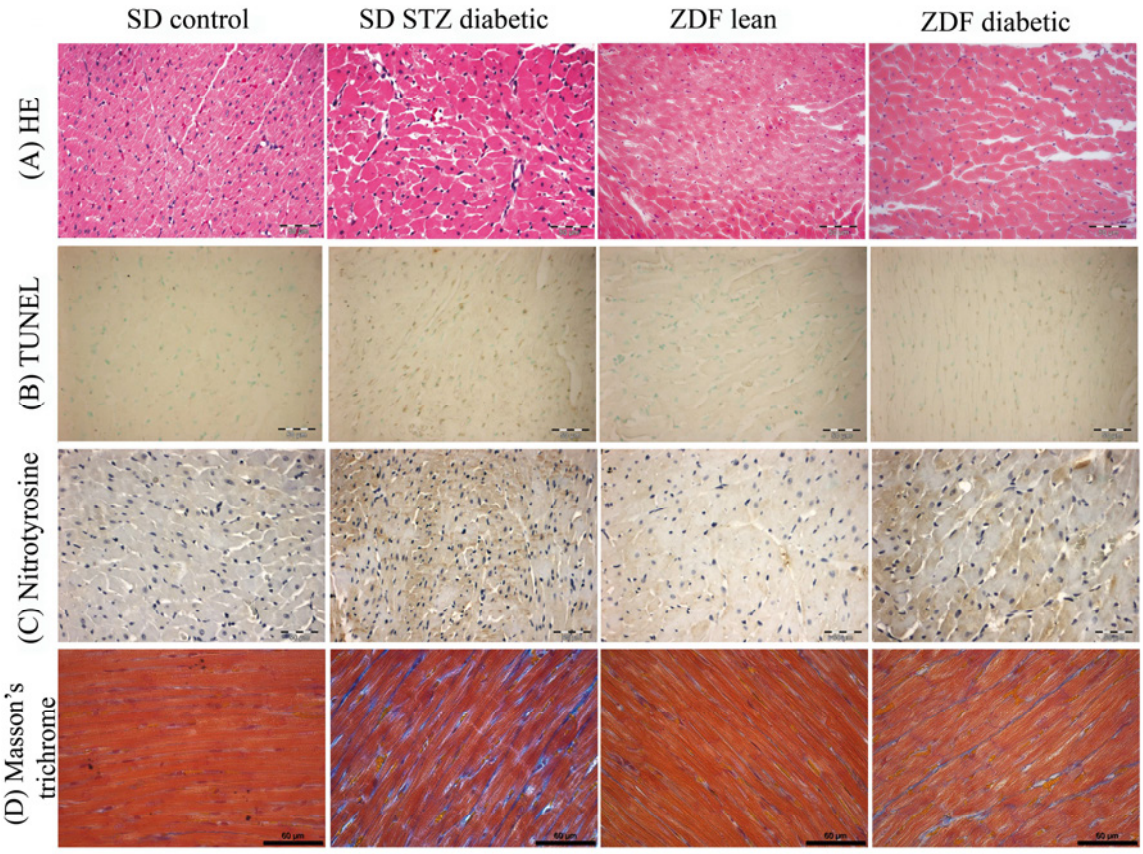

Figure 6. Histopathological changes of the myocardium in type 1 and type 2 diabetes mellitus (DM) models
Representative images of conventional histopathological examination (hematoxylin-eosin (HE) staining; scale bar: 50 µm, magnification: 200x, A), TUNEL staining (brown cell nuclei, scale bar: 50 µm, magnification: 200x, B), immunohistochemistry for the nitro-oxidative stress marker nitrotyrosine (brown staining, scale bar: 50 µm, magnification: 400x, C) and Masson's trichrome staining for fibrosis detection (blue

staining, scale bar: 60 μm, magnification: 400x, D) of left ventricular myocardium in the groups of SD control, streptozotocin (STZ)-induced diabetic SD, Zucker Diabetic Fatty (ZDF) lean, and ZDF diabetic rats.

5.1.4. *DNA strand breaks and nitro-oxidative stress*

Compared with the corresponding controls, diabetic hearts were associated with increased density of TUNEL-positive nuclei, indicating DNA-fragmentation (Figure 6B) and increased immunoreactivity against the nitro-oxidative stress marker 3-NT, as evidenced by increased brown staining (Figure 6C). Moreover, both TUNEL-positivity and nitro-oxidative stress were found to be more pronounced in type 1 when compared with the type 2 DM group (Figure 7B and C).

Quantitative real-time PCR from LV myocardial RNA extracts revealed that mRNA-expression for endogenous antioxidants cytosolic superoxide dismutase 1 (SOD1), catalase, glutathione reductase (GSR) and thioredoxin were significantly upregulated in type 1 DM, while these changes were less pronounced or absent in the type 2 DM model. The mRNA-expression for the mitochondrial superoxide dismutase 2 (SOD2) was not altered in any groups studied. (Figure 8. right panel)

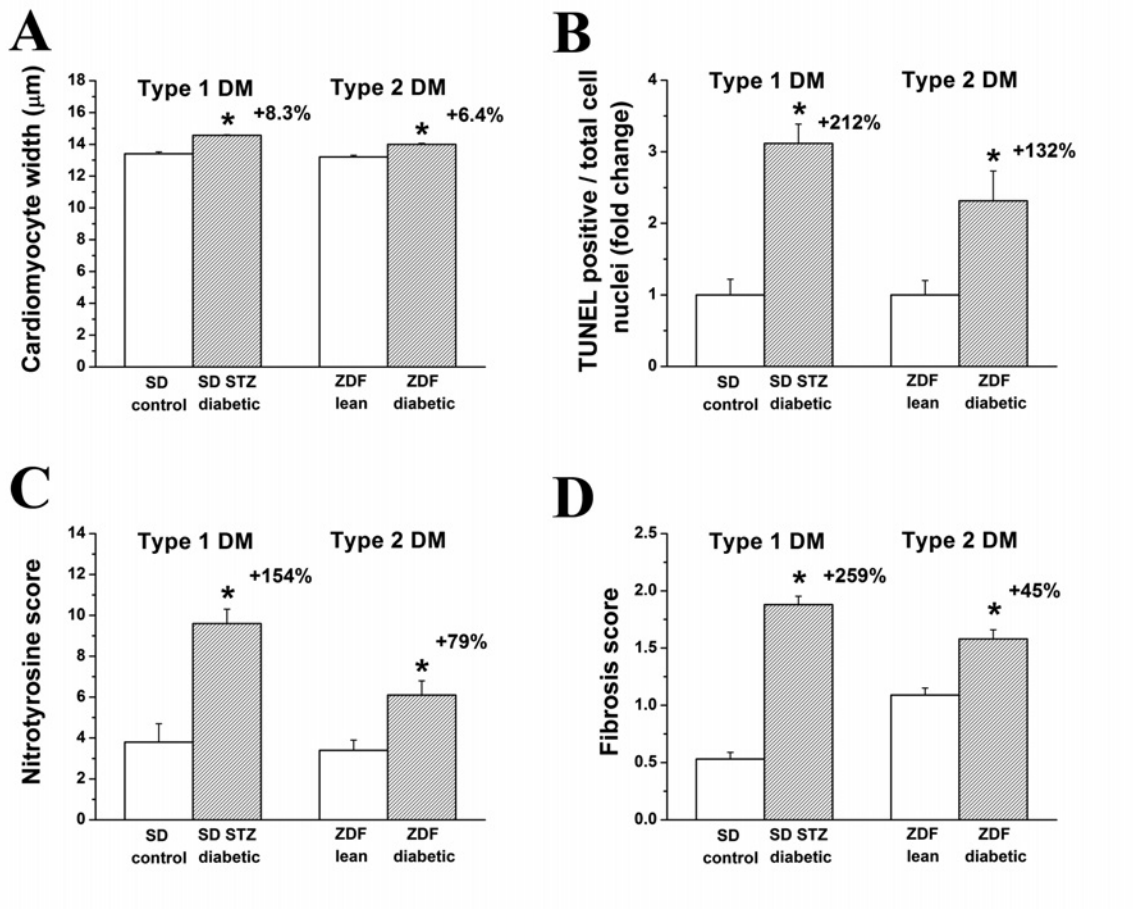

Figure 7. Quantification of the histopathological changes
Mean cardiomyocyte width as marker of myocardial hypertrophy (A), fold change in the number of TUNEL-positive/total cardiomyocyte nuclei (B), semiquantitaive histomorphological scoring of nitrotyrosine immunostaining (C) and Masson's trichrome fibrosis staining (D) in the groups of SD control, streptozotocin (STZ)-induced diabetic SD, Zucker Diabetic Fatty (ZDF) lean, and ZDF diabetic rats. Percent changes between diabetic and corresponding non-diabetic control groups are indicated in both DM models. *$p<0.05$ vs. the corresponding non-diabetic group.

5.1.5. *Myocardial fibrosis*

Myocardial fibrotic remodeling, as reflected by Masson's trichrome staining of myocardial sections was significantly more pronounced in the type 1 DM model, when compared to type 2 DM (Figure 6D). The semiquantitative scoring of the staining supported the above results as the Fibrosis score was increased in both models and was more pronounced in type 1 DM (Figure 7D).

5.1.6. *Myocardial expression of genes involved in the development of diabetic cardiomyopathy*

Quantitative real-time PCR from LV myocardial RNA extracts revealed that mRNA-expression for α-myosin heavy chain (α-MHC) was significantly decreased whereas β-MHC and endothelin-1 mRNA-levels were increased in both diabetic groups compared to corresponding controls (Figure 8 left panel). Whereas c-fos, c-jun and caspase-12 mRNA-expression were significantly upregulated, collagen-1, collagen-3 and endothelial NOS mRNA-levels were downregulated only in type 1 DM when compared with the control group (Figure 8 left panel). Atrial natriuretic factor (ANF) mRNA-expression was up-regulated in both types of DM, but the change reached the level of statistical significance only in the type 2 model (Figure 8 left panel). The gene expression changes for α-MHC, β-MHC, c-fos, c-jun, caspase-12, collagen-1, collagen-3 and endothelial NOS were significantly more pronounced in type 1 when compared to the type 2 DM group (Figure 8 left panel).

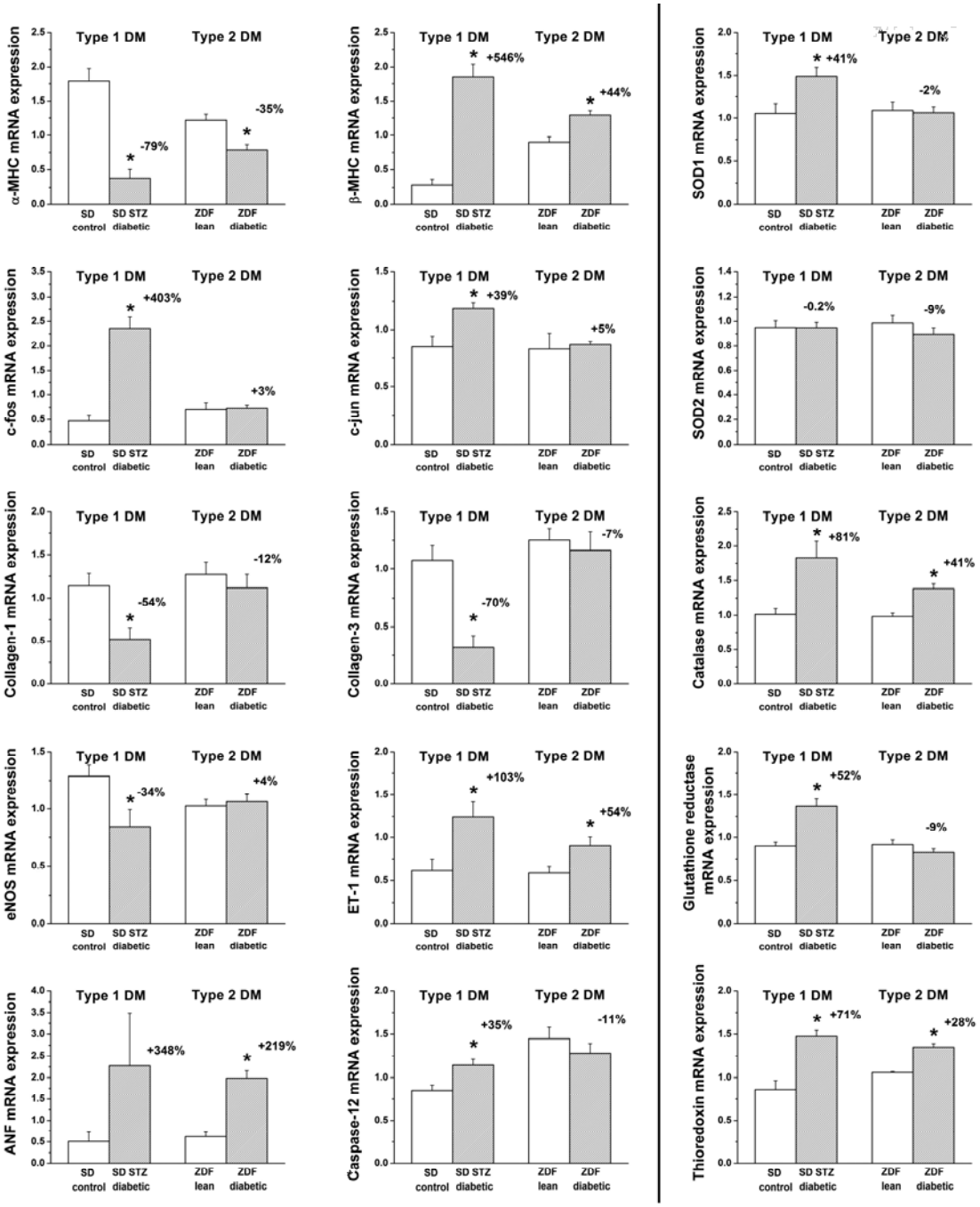

Figure 8. Gene expression results

Relative mRNA expression for (left and middle panels) hypertrophy markers α myosin heavy chain (MHC), β-MHC, early genes of the hypertrophic transcriptional program c-fos and c-jun; extracellular matrix components collagen-1 and 3, vascular endothelial marker endothelial nitric oxide synthase (eNOS) and endothelin-1 (ET-1); atrial natriuretic factor (ANF) and pro-apoptotic caspase-12, as well as for (right panel) endogenous antioxidants superoxide dismutase 1 (SOD1) and 2 (SOD2), catalase, glutathione reductase and thioredoxin in the groups of SD control, streptozotocin (STZ)-induced diabetic SD, Zucker Diabetic Fatty (ZDF) lean and ZDF diabetic rats.

Percent changes between diabetic and corresponding non-diabetic control groups are indicated in both DM models. *p<0.05 vs. the corresponding non-diabetic group.

5.1.7. *Western blot analysis of TGF-β1*

In Western blots, we detected TGF-β1 protein in rat myocardium as a single band at 25 kDa. Densitometric analysis of the bands revealed a significant increase in relative TGF-β1 protein content in myocardium from type 1 diabetic rats in comparison with the corresponding controls. In contrast, significantly decreased TGF-β1 protein expression could be detected in the type 2 DM model (Figure 9).

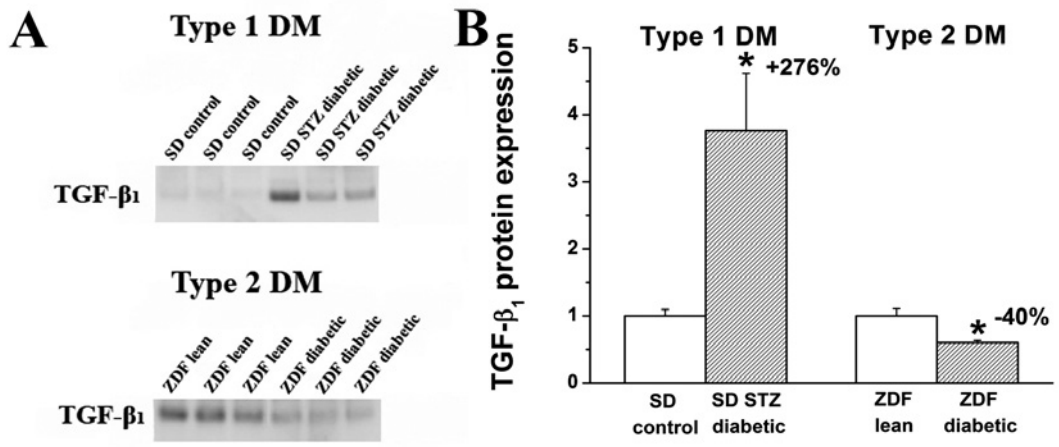

Figure 9. Protein expression of transforming growth factor (TGF)-β1
Representative immunoblot analysis for transforming growth factor (TGF)-β1 (A) and relative myocardial TGF-β1 protein band densities (B) in the groups of SD control, streptozotocin (STZ)-induced diabetic SD, Zucker Diabetic Fatty (ZDF) lean, and ZDF diabetic rats. Percent changes between diabetic and corresponding non-diabetic control groups are indicated in both DM models. *p<0.05 vs. the corresponding non-diabetic group.

5.2. Experiments on the effect of sGC activation in T1DM-related diabetic cardiomyopathy

5.2.1. *Body weight, heart weight and glucose levels*

All animals survived the study period and reached the end-point of the investigation. HW and BW significantly decreased in both diabetic groups while HW to BW ratio

increased in the diabetic groups (Table 4.). When compared with controls, DM led to significantly increased BG levels and daily water intake. Cinaciguat treatment in diabetic rats did not influence BG levels, but led to attenuated water intake (Table 4.). Time-course of body weight changes is available on Figure 10.

Table 4. Basic characteristics
The values of blood glucose, daily water intake, heart weight (HW), body weight (BW) and heart weight to body weight ratio are shown. Groups: vehicle-treated controls (Co), cinaciguat-treated controls (CoCin), vehicle-treated diabetic (DiabCo) and cinaciguat-treated diabetic (DiabCin) groups. *p<0.05 vs. Co, #p<0.05 vs. DiabCo

Variable	Co	CoCin	DiabCo	DiabCin
Blood glucose (mmol/l)	5.8±0.1	6.2±0.1	30.8±0.5*	29.3±1.4*
Water intake (ml/gBW/day)	0.078±0.002	0.090±0.002	0.787±0.006*	0.597±0.013*#
HW (g)	1.20±0.06	1.24±0.07	0.91±0.04*	0.84±0.03*
BW (g)	480.7±17.6	477.8±20.9	293.5±11.1*	247.6±14.8*
HW/BW (g/kg)	0.249±0.008	0.259±0.008	0.311±0.009*	0.348±0.015*

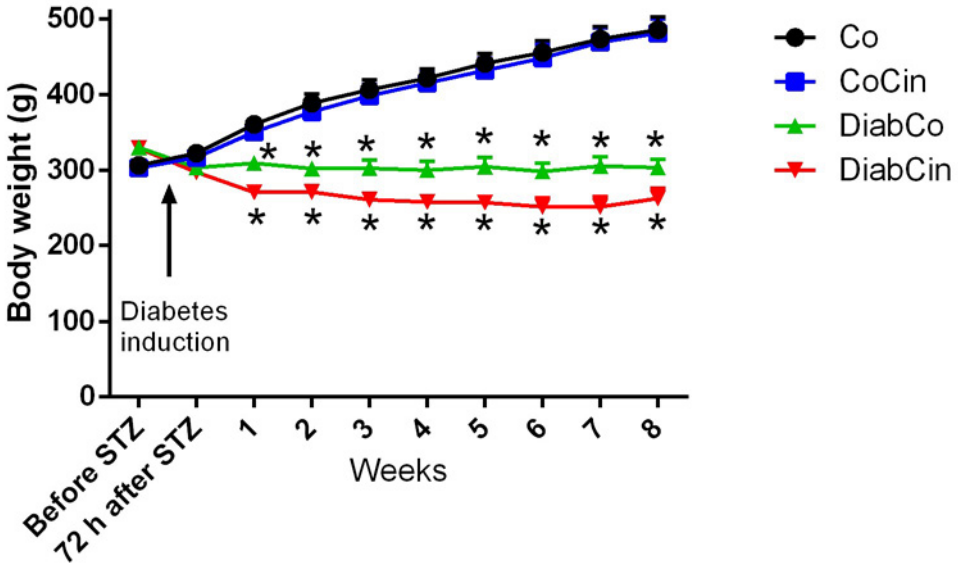

Figure 10. Body weight changes in T1DM
Groups: vehicle-treated control (Co), cinaciguat-treated control (CoCin), vehicle-treated diabetic (DiabCo) and cinaciguat-treated diabetic (DiabCin). *p<0.05 vs. Co

5.2.2. *Effects of cinaciguat on plasma and myocardial cGMP levels in DM*

Cinaciguat treatment had no effect on plasma cGMP levels in control animals (Figure 11A), however it resulted in a pronounced increase of plasma cGMP in DM (Figure 11A). According to cGMP immunohistochemistry, the cGMP content of LV myocardium was significantly lower in DM than in controls (Figure 11B and C). However, chronic treatment with cinaciguat restored cGMP to the control level (Figure 11B and C).

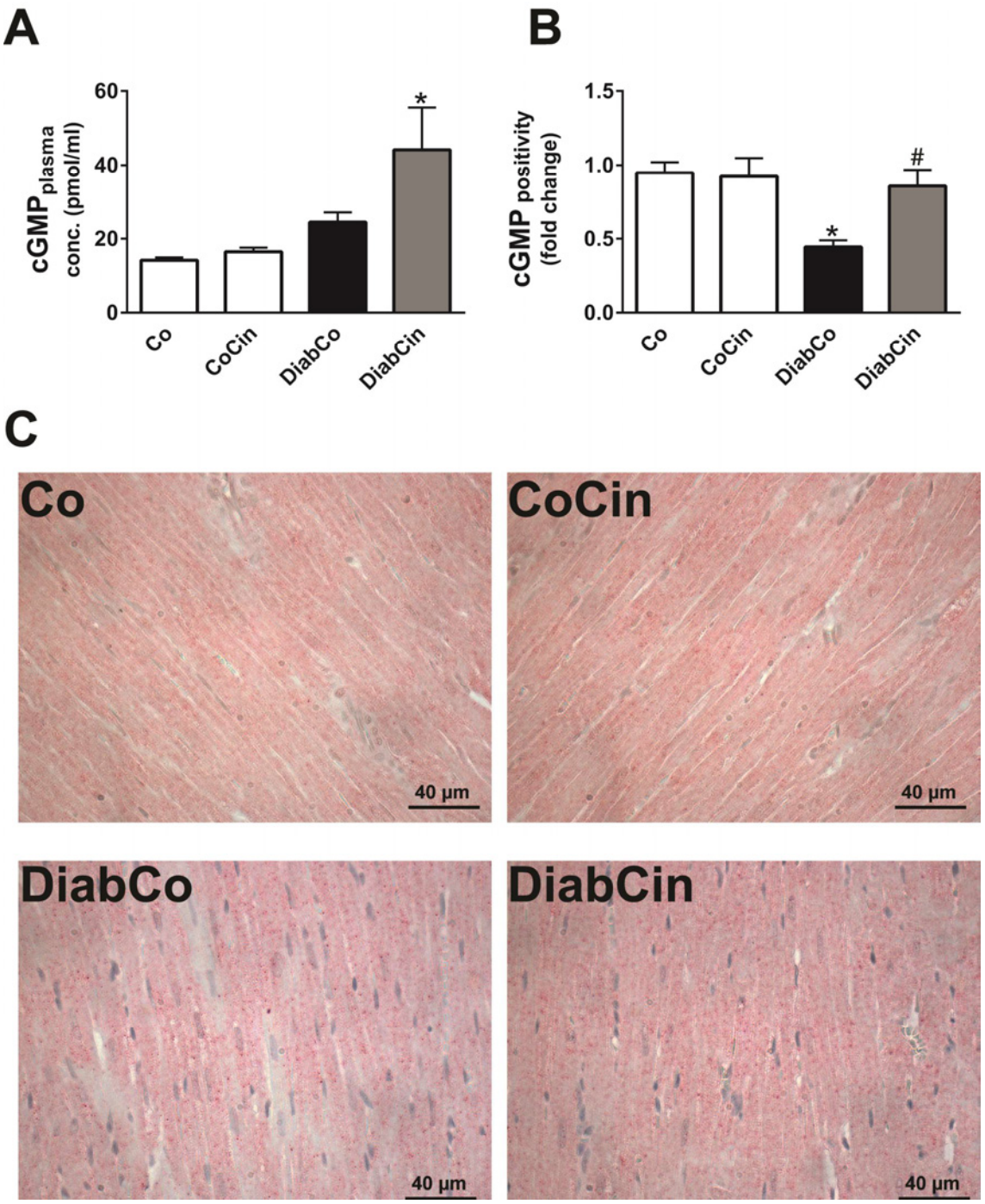

Figure 11. Plasma and myocardial cGMP content
(A) Result of plasma cGMP enzyme immunoassay. (B) Quantification of cGMP immunohistochemistry (C) Representative images of cyclic guanosine monophosphate (cGMP) immunohistochemistry. Magnification: 400x, Scale bar: 40 µm. Groups: vehicle-treated control (Co), cinaciguat-treated control (CoCin), vehicle-treated diabetic (DiabCo) and cinaciguat-treated diabetic (DiabCin). *$p<0.05$ vs. Co, #$p<0.05$ vs. DiabCo

5.2.3. *Effects of diabetes mellitus and cinaciguat treatment on myocardial oxidative stress*

DM was associated with increased 3-NT immunoreactivity in LV myocardium referring to pronounced nitro-oxidative stress, which was significantly alleviated by cinaciguat treatment (Figure 12A and B). Increased expression of HSP70a1, catalase, gluthatione-reductase and thioredoxin-1 was found in DM (Figure 12C). HSP70a1 and gluthatione-reductase mRNA expression in the DiabCin group remained on the level of healthy controls (Figure 12C). SOD-2 expression did not show any difference among the groups (Figure 12C).

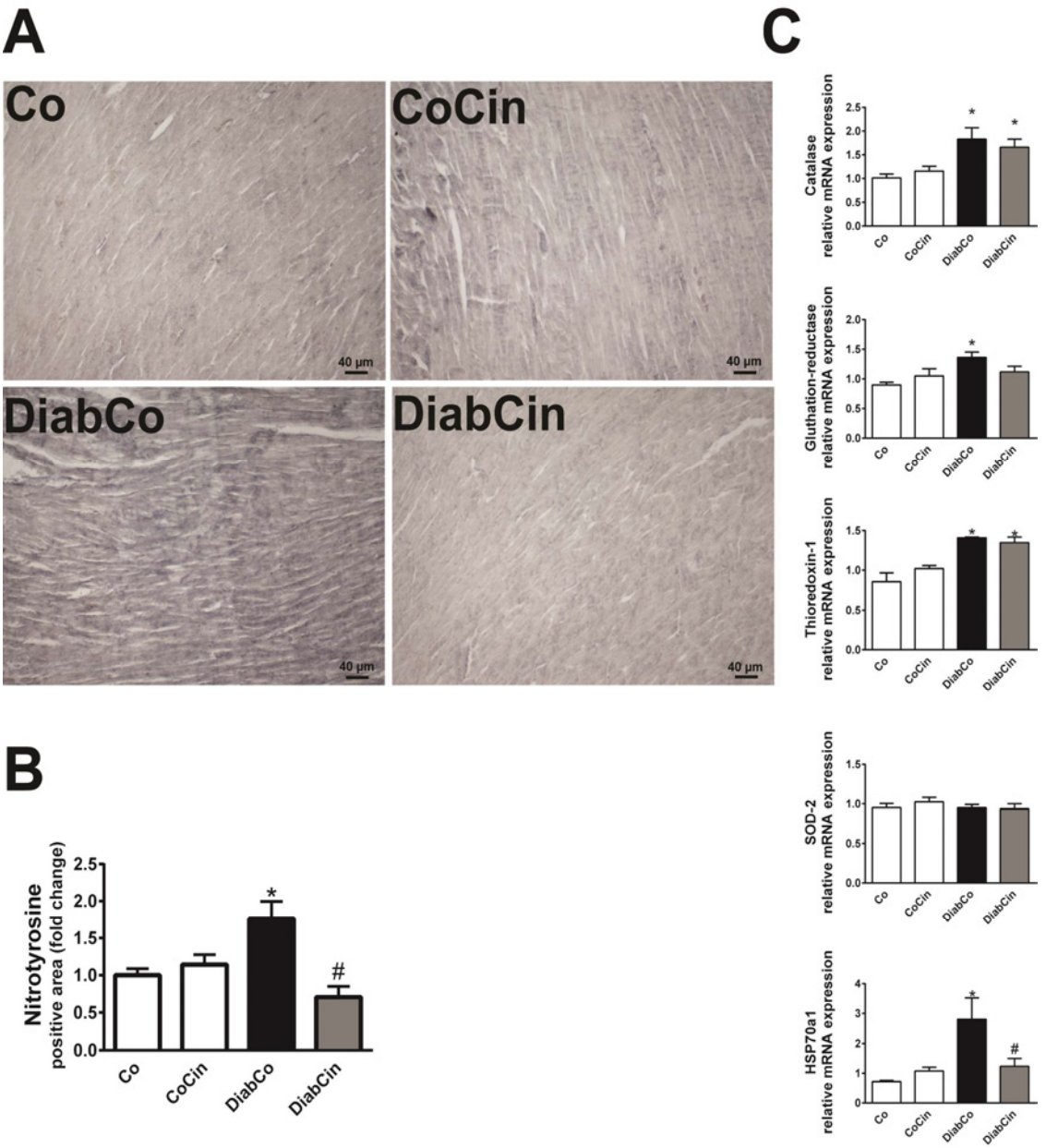

Figure 12. Cinaciguat treatment alleviates DM-related oxidative stress
(A) Representative images of nitrotyrosine (NT) immunohistochemistry. Magnification: 200x, Scale bar: 40 µm (B) Quantification of NT immunohistochemistry. (C) Relative mRNA expression of catalase, gluthatione-reductase, heat shock 70kD protein 1A (HSP70a1), superoxide dismutase (SOD)-2 and thioredoxin-1. Groups: vehicle-treated control (Co), cinaciguat-treated control (CoCin), vehicle-treated diabetic (DiabCo) and cinaciguat-treated diabetic (DiabCin). *p<0.05 vs. Co, #p<0.05 vs. DiabCo

5.2.4. *Cinaciguat protects against DM related alteration of the NO-sGC-cGMP-PKG signaling*

Protein expression of eNOS and sGC β1 did not differ between healthy and diabetic rats (Figure 13A) while eNOS gene expression was significantly lower in both diabetic groups (Figure 13B). We detected elevated PDE-5 and PKG protein expression in the DiabCo group (Figure 13A) whereas the p-VASP/VASP ratio (marker of PKG activity) was significantly reduced, showing severe deterioration of PKG signaling in DM (Figure 13A). Application of cinaciguat in diabetic animals significantly reduced the expression of PDE-5, markedly increased PKG activity (as indicated by elevated p-VASP/VASP ratio) (Figure 13A), while the expression of PKG did not differ between the two diabetic groups (Figure 13A).

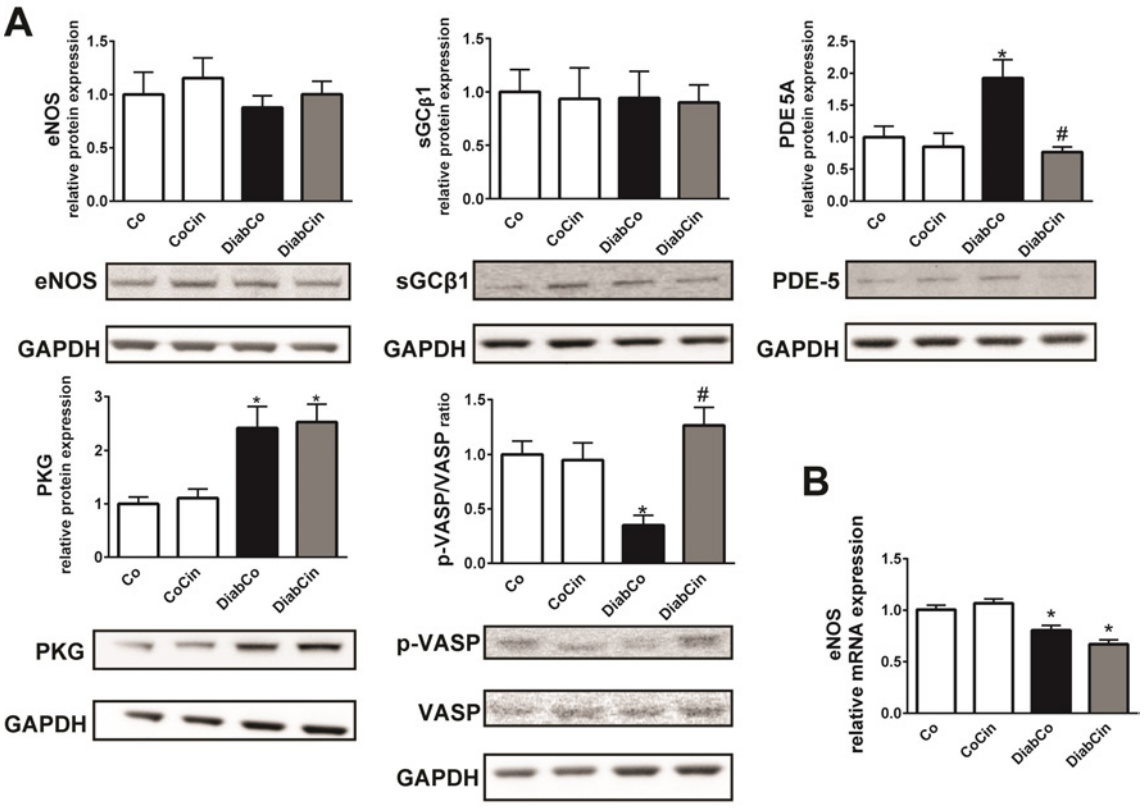

Figure 13. The effect of DM and cinaciguat on myocardial NO-sGC-cGMP-PKG signaling
(A) Relative protein expression and representative immunoblot bands of endothelial nitric oxide synthase (eNOS), soluble guanylate cyclase β1 (sGC β1), phosphodiesterase-5A (PDE5A), protein kinase G (PKG), vasodilator-stimulated

phosphoprotein (VASP) to phospho-VASP (p-VASP) ratio. (B) Relative gene expression of the endothelial nitric oxide synthase (eNOS). Groups: vehicle-treated control (Co), cinaciguat-treated control (CoCin), vehicle-treated diabetic (DiabCo) and cinaciguat-treated diabetic (DiabCin). *<p0.05 vs. Co, #p<0.05 vs. DiabCo

5.2.5. *Cinaciguat treatment protects against DM related fibrotic remodeling of the myocardium*

DM was associated with dysregulation of the MMP system indicated by markedly increased MMP-9/TIMP-1 and reduced MMP-2/TIMP-2 gene expression ratios (Figure 14A). These alterations were attenuated in the DiabCin group (Figure 14A). Although fibronectin expression did not change, Col1a1 and Col3a1 expression levels were significantly lower in both diabetic groups (Figure 14A). The profibrotic TGF-β1 showed increased expression in the diabetic animals, which was significantly ameliorated by cinaciguat (Figure 14C). Expression of MMP-9 showed a 2-fold increase in DM, while MMP-2 remained unchanged (Figure 14C). Cinaciguat did not significantly alter these parameters (Figure 14C). We found severe interstitial fibrosis in the myocardium of diabetic animals indicated by increased MT staining (Figure 15). Additionally, elevated immunoreactivity was observed against the profibrotic mediator TGF-β1 and fibrosis marker fibronectin in the diabetic heart (Figure 15). Application of cinaciguat reduced MT staining intensity in the heart of diabetic animals (Figure 15) while TGF-β1 immunoreactivity strongly tended to decrease (p=0.051) (Figure 15).

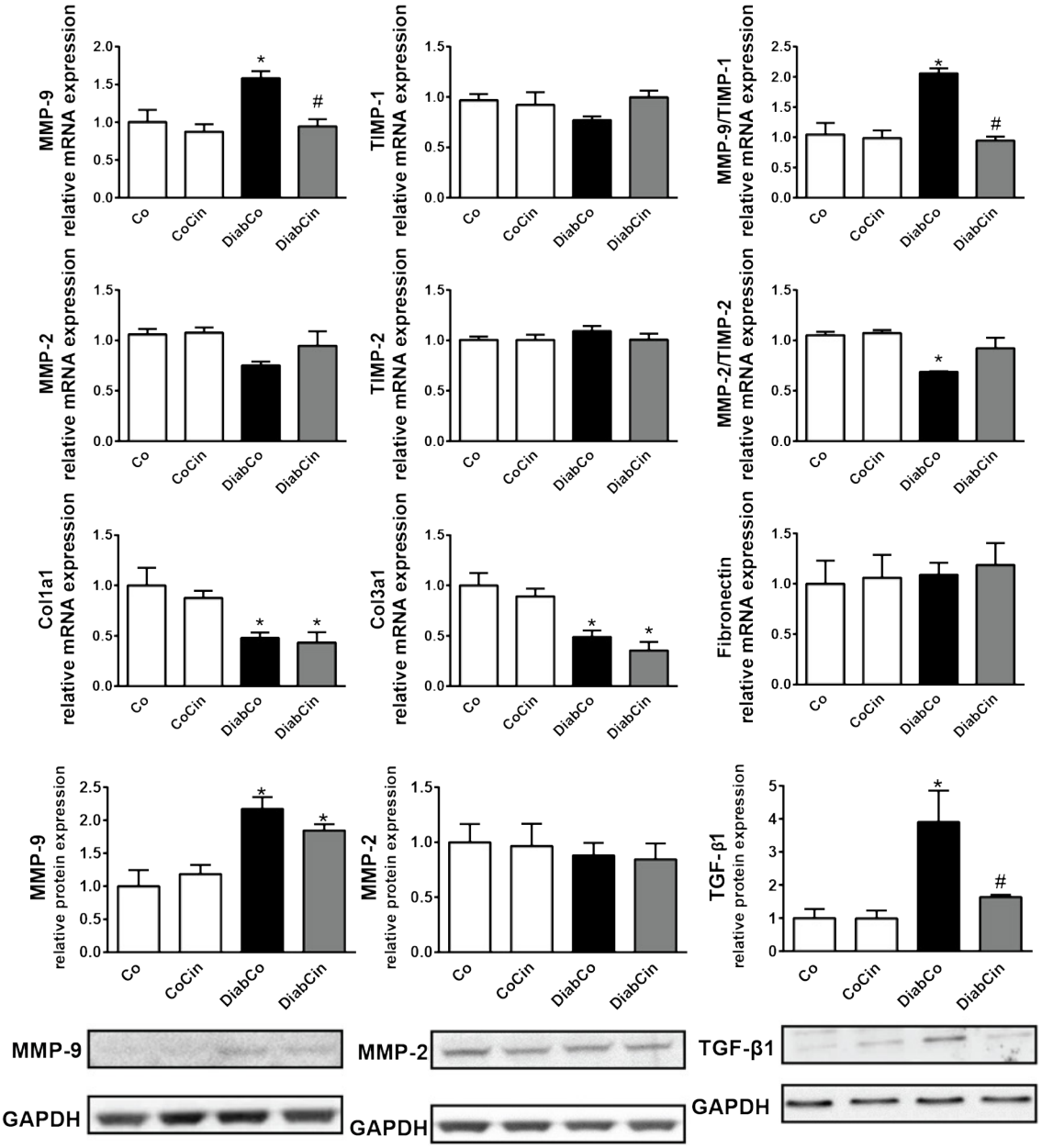

Figure 14. Effects of DM and cinaciguat on myocardial fibrotic remodeling
Relative gene expression and protein expression values of matrix metallopeptidase (MMP)-9, tissue inhibitor of MMP (TIMP)-1, MMP-9/TIMP-1 ratio, MMP-2, TIMP-2, MMP-2/TIMP-2 ratio, collagen 1a1 (Col1a1), 3a1 (Col3a1), fibronectin and transforming growth factor (TGF)-β1. Figure shows the representative immunoblot bands of TGF-β1, MMP-2 and MMP-9. Groups: vehicle-treated control (Co), cinaciguat-treated control (CoCin), vehicle-treated diabetic (DiabCo) and cinaciguat-treated diabetic (DiabCin). *p<0.05 vs. Co, #P<0.05 vs. DiabCo

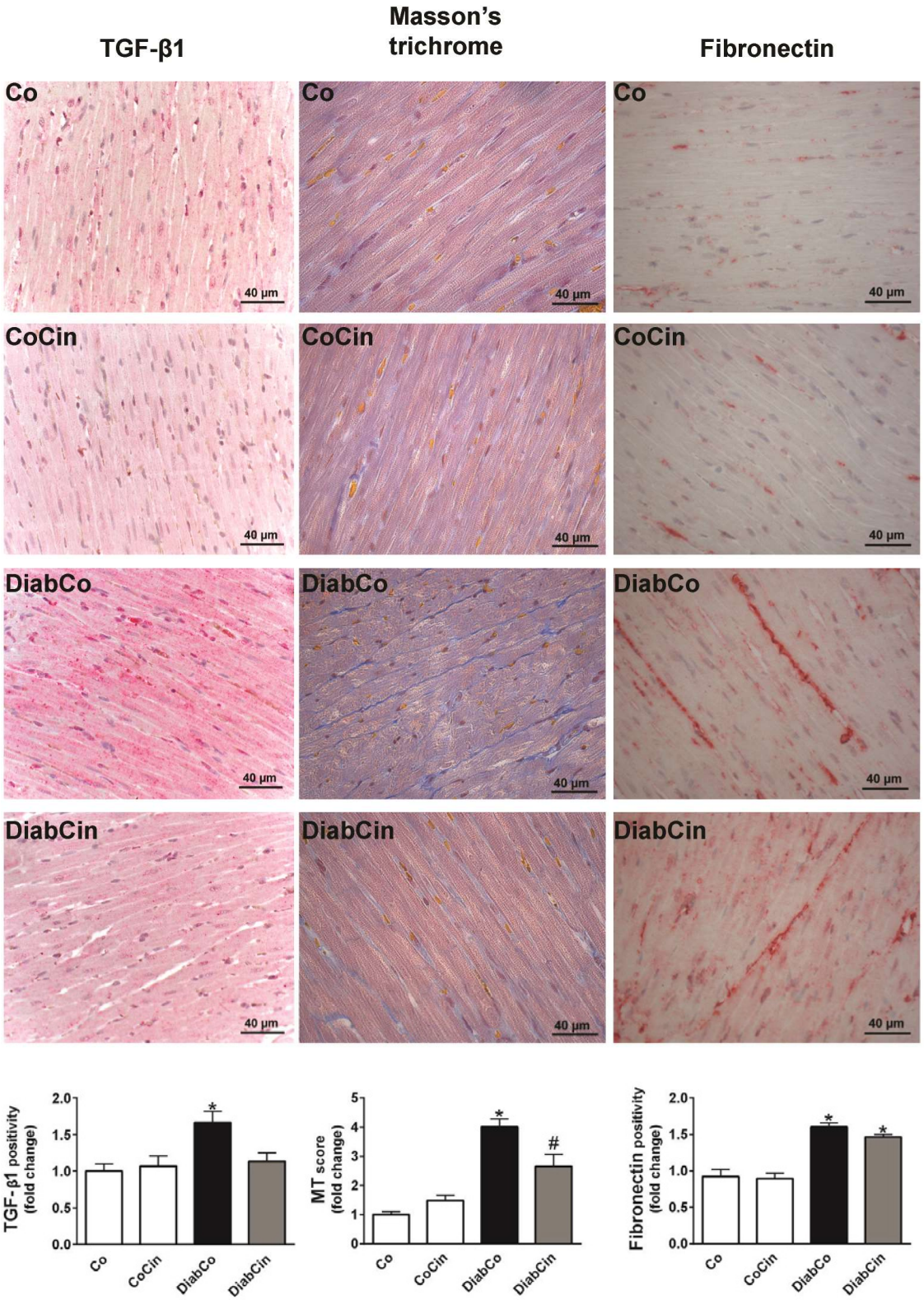

Figure 15. Histology of myocardial remodeling in DM and in cinaciguat treatment
Representative images of Masson's trichrome (MT) staining and representative immunohistochemical images of profibrotic mediator transforming growth factor (TGF)–β1 and fibrosis marker fibronectin. Quantification of MT staining, TGF-β1 and fibronectin immunohistochemistry are shown. Magnification: 400x, Scale bar: 40 µm.

Groups: vehicle-treated control (Co), cinaciguat-treated control (CoCin), vehicle-treated diabetic (DiabCo) and cinaciguat-treated diabetic (DiabCin). *p<0.05 vs. Co, #p<0.05 vs. DiabCo

5.2.6. *DM-related myocardium hypertrophy and apoptosis is alleviated by cinaciguat*

Myocardial mRNA expression data from LV myocardium of diabetic rats showed a marked increase of ANF and the β-MHC/α-MHC ratio (Figure 16). Treatment with cinaciguat caused a significant decrease of ANF expression in DM (Figure 16) while β-MHC/α-MHC ratio showed a slight decrease (Figure 16). When compared with controls, increased cardiomyocyte width was observed in the DiabCo group indicative of cardiomyocyte hypertrophy. This increase was completely prevented by cinaciguat (Figure 17A and C). The mRNA expression levels of proapoptotic BAX and antiapoptotic Bcl-2 did not differ among the study groups resulting in unchanged BAX/Bcl-2 ratio (Figure 16). DM was associated with increased TUNEL positivity in LV myocardium referring to pronounced DNA fragmentation (Figure 17B and C). TUNEL positivity was effectively reduced in the DiabCin group (Figure 17B and C).

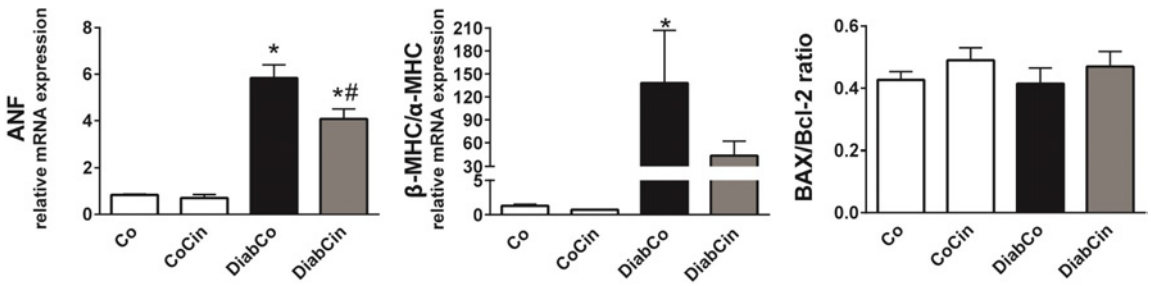

Figure 16. Effects of diabetes and cinaciguat on hypertrophy and apoptosis markers
Relative mRNA expression of pathological hypertrophy markers atrial natriuretic factor (ANF), β myosin heavy chain (MHC) to α-MHC ratio and the apoptosis marker Bcl2-associated X protein (BAX) to B-cell CLL/lymphoma 2 (Bcl-2) ratio. Groups: vehicle-treated control (Co), cinaciguat-treated control (CoCin), vehicle-treated diabetic (DiabCo) and cinaciguat-treated diabetic (DiabCin). *p<0.05 vs. Co, #p<0.05 vs. DiabCo

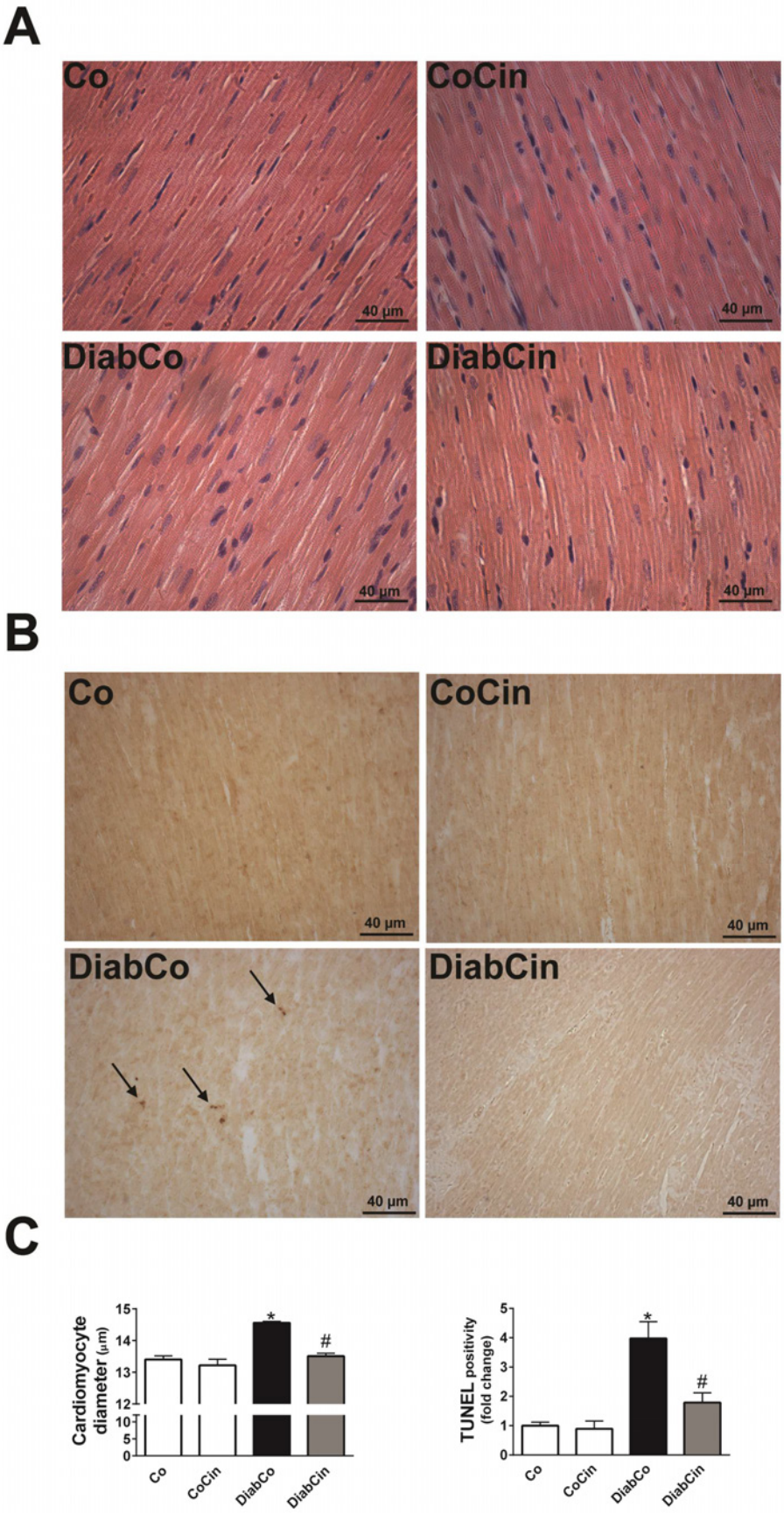

Figure 17. Effects of diabetes and cinaciguat on myocardial hypertrophy and apoptosis

(A) Representative images of hematoxylin – eosin stained sections and (B) TUNEL assay of the left ventricle. Magnification: 400x, Scale bar: 40 μm. (C) Mean cardiomyocyte diameter (as marker of cardiomyocyte hypertrophy) and quantification of TUNEL-positive cardiomyocyte nuclei. Groups: vehicle-treated control (Co), cinaciguat-treated control (CoCin), vehicle-treated diabetic (DiabCo) and cinaciguat-treated diabetic (DiabCin). *p<0.05 vs. Co, #p<0.05 vs. DiabCo

5.2.7. *In vivo cardiac function is improved by cinaciguat in DM*

In comparison with non-diabetic controls, the DiabCo group showed remarkably reduced MAP, LVSP, EF, SW, dP/dt_{max} and impaired dP/dt_{min} values, while LVEDP and Tau_W increased, indicating LV systolic and diastolic dysfunction (Table 5.). HR significantly decreased in the diabetic groups while CO was not significantly different among the study groups (Table 5.). MAP, LVSP, SW, dP/dt_{max} and dP/dt_{min} remained unchanged in the DiabCin group, however drug treatment markedly improved LVEDP and Tau_W in DM (Table 5.). As a result of cinaciguat treatment EF tended towards improvement (p=0.054) in DM (Table 5.).

The values of load-independent, P-V-loop derived contractility indexes (E_{es}, PRSW) were significantly reduced in diabetic animals indicating severe contractile dysfunction (Figure 18A and B) Treatment with cinaciguat led to a significant increase in PRSW (Figure 18B.) while E_{es} showed a strong tendency towards improvement in DM (P=0.092) (Figure 18B).

In comparison with the Co group, the slope of EDPVR tended to increase (P=0.063) in diabetic animals, which was significantly reduced by cinaciguat (Figure 16B). Cinaciguat had no hemodynamic effects in non-diabetic rats.

Table 5. Basic hemodynamic data in T1DM
Heart rate (HR), mean arterial pressure (MAP), maximal left ventricular (LV) systolic pressure (LVSP), stroke work (SW), cardiac output (CO), ejection fraction (EF), maximal slope of systolic pressure increment (dP/dt_{max}) and diastolic pressure decrement (dP/dt_{min}), LV end-diastolic pressure (LVEDP) and time constant of LV pressure decay (Tau_W) are shown. Groups: vehicle-treated controls (Co), cinaciguat-treated controls (CoCin), vehicle-treated diabetic (DiabCo) and cinaciguat-treated diabetic (DiabCin) animals. *p<0.05 vs. Co, #p<0.05 vs. DiabCo

Variable	Co	CoCin	DiabCo	DiabCin
HR (beats/min)	231±11	246±12	208±8*	204±10*
MAP (mmHg)	80.0±2.0	81.0±3.5	63.7±2.5*	64.4±3.1*
LVSP (mmHg)	99.5±2.6	103.5±2.1	85.5±1.3*	82.3±2.3*
SW (mmHg*µl)	14561±1060	13293±948	9789±592*	12032±1067
CO (µl/min)	42347±2472	41306±2804	33360±2162	38605±4288
EF (%)	70.42±2.50	68.17±2.70	58.09±2.54*	68.02±2.56
dP/dt_{max} (mmHg/s)	6539±240	6804±188	4933±207*	4785±230*
dP/dt_{min} (mmHg/s)	-6135±362	-6570±446	-3883±133*	-3723±248*
LVEDP (mmHg)	7.0±0.6	7.2±0.4	9.7±0.7*	6.8±0.3#
Tau_W (ms)	10.3±0.3	10.1±0.3	17.3±0.8*	14.9±0.6*#

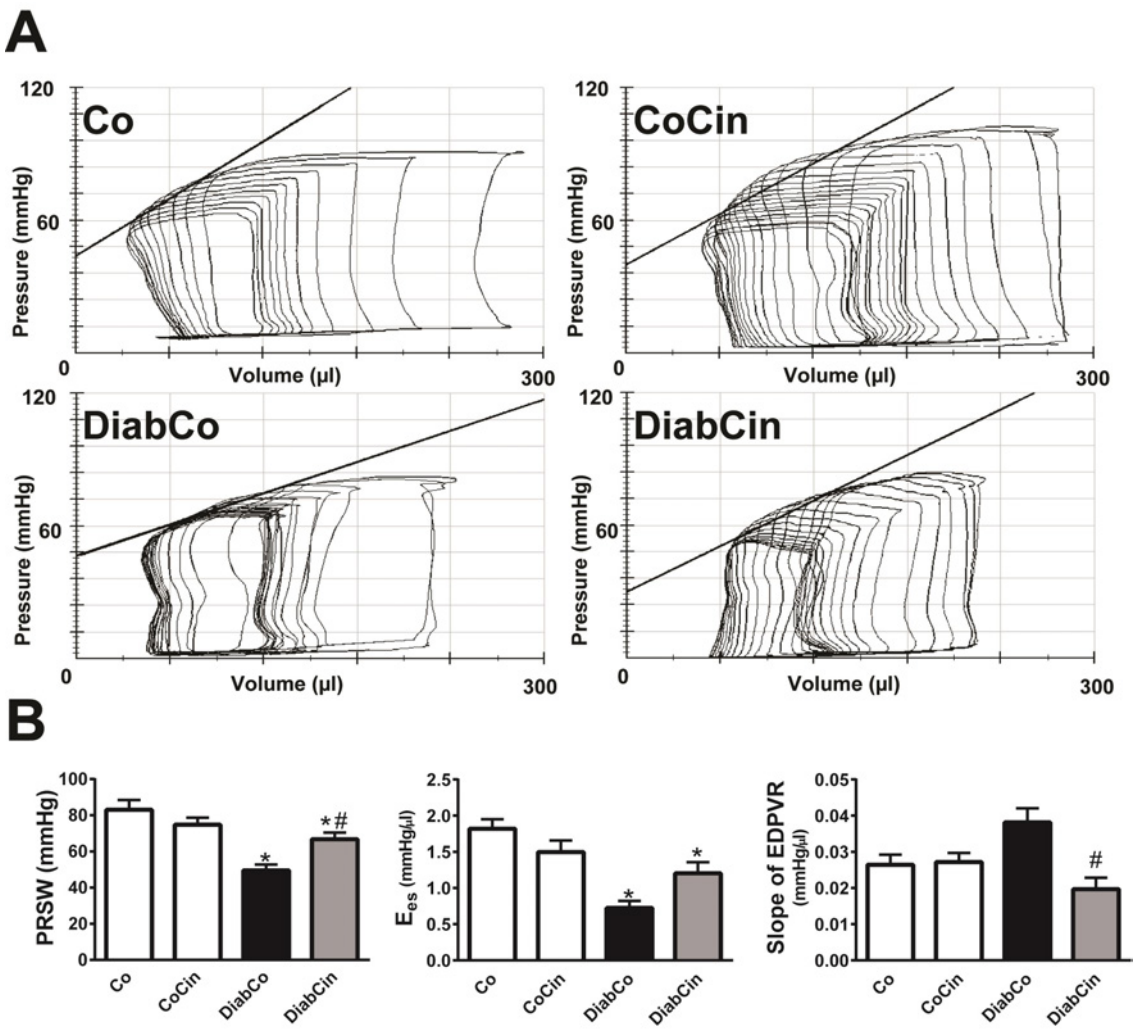

Figure 18. Effect of cinaciguat on left ventricular (LV) contractility and cardiac stiffness in diabetes mellitus (DM)
(A) Representative pressure-volume (P-V) loops, (B) preload recruitable stroke work (PRSW), slope (E_{es}) of LV end-systolic P-V relationship and the slope of LV end-diastolic P-V relationship (EDPVR) are presented in vehicle-treated control (Co), cinaciguat-treated control (CoCin), vehicle-treated diabetic (DiabCo) and cinaciguat-treated diabetic (DiabCin) groups. *$p<0.05$ vs. Co, #$p<0.05$ vs. DiabCo

The results of the two-factorial ANOVA main effects and interaction are depicted in Table 6.

Table 6. Two-way ANOVA results

Variable	Two-way ANOVA P values		
Basic characteristics	**Factor „T1DM”**	**Factor „Cinaciguat”**	**Interaction**
Blood glucose (mmol/l)	<0.001	0.460	0.209
Water intake (ml/gBW/day)	<0.001	<0.001	<0.001
HW (g)	<0.001	0.805	0.278
BW (g)	<0.001	0.150	0.202
HW/BW	<0.001	0.026	0.196
Hemodynamics			
HR (beats/min)	0.003	0.608	0.351
MAP (mmHg)	<0.001	0.845	0.969
LVSP (mmHg)	<0.001	0.858	0.102
SW (mmHg*µl)	0.003	0.611	0.072
CO (µl/min)	0.057	0.484	0.297
EF (%)	0.021	0.146	0.024
dP/dt_{max} (mmHg/s)	<0.001	0.791	0.350
dP/dt_{min} (mmHg/s)	<0.001	0.679	0.374
LVEDP (mmHg)	0.026	0.082	0.034
Tau_W (ms)	<0.001	0.016	0.054
PRSW (mmHg)	0.275	<0.001	0.004
E_{es} (mmHg/µl)	0.570	<0.001	0.006
EDPVR (mmHg/µl)	0.007	0.499	0.004

Histology/immunohistochemistry			
Cardiomyocyte diameter (μm)	<0.001	<0.001	0.003
cGMP positivity	0.005	0.046	0.025
Nitrotyrosine positivity	0.353	0.006	<0.001
TGF-β1 positivity	0.009	0.086	0.029
Masson's trichrome score	<0.001	0.103	0.002
Fibronectin positivity	<0.001	0.250	0.437
TUNEL positivity	<0.001	0.005	0.010
Gene expression results			
Catalase	<0.001	0.933	0.342
Glutathione-reductase	0.010	0.616	0.046
HSP70a1	0.009	0.132	0.022
SOD-2	0.412	0.581	0.428
Thioredoxin-1	<0.001	0.482	0.128
eNOS	<0.001	0.422	0.039
MMP-9	0.011	0.004	0.038
MMP-2	0.032	0.280	0.359
TIMP-1	0.483	0.303	0.133
TIMP-2	0.369	0.397	0.400
MMP-9/TIMP-1	0.001	<0.001	<0.001
MMP-2/TIMP-2	0.001	0.066	0.116
Col1a1	<0.001	0.409	0.704
Col3a1	<0.001	0.171	0.868

Fibronectin	0.599	0.699	0.927
ANF	<0.001	0.017	0.036
β-MHC/α-MHC ratio	0.009	0.145	0.149
BAX/Bcl-2 ratio	0.703	0.175	0.922
Western blotting			
eNOS	0.422	0.414	0.930
sGC β1	0.848	0.820	0.961
PDE5A	0.054	0.005	0.024
PKG	<0.001	0.694	0.997
p-VASP/VASP ratio	0.243	0.006	0.003
MMP-9	<0.001	0.707	0.178
MMP-2	0.453	0.826	0.994
TGF-β1	0.004	0.048	0.050
Biochemistry			
Plasma cGMP (pmol/ml)	0.002	0.058	0.130

5.3. Experiments on the effect of PDE5A inhibition in T2DM-related diabetic cardiomyopathy

5.3.1. *The effect of vardenafil on basic characteristics in T2DM*

The BW, HW and HW/BW ratio did not differ statistically at the end of the study period (Table 7.) Both ZDF and ZDF+Vard animals had significantly elevated BG levels throughout the study period (Figure 19.). ZDF lean control animals reached the body

weight of the ZDF groups at the 24th week, due to their constant body weight gain (Figure 20.).

Table 7. Basic characteristics of the study groups
The table shows the basic characteristics of the study groups: body weight (BW), heart weight (HW), HW/BW ratio (HW/BW), HW/tibia length ratio (HW/TL). Groups: vehicle-treated controls (ZDFLean), vardenafil-treated controls (ZDFLean+Vard), vehicle-treated diabetic (ZDF) and vardenafil-treated diabetic (ZDF+Vard). *p<0.05 vs. ZDFLean; #p<0.05 vs. ZDF

Variable	ZDFLean	ZDFLean+Vard	ZDF	ZDF+Vard
BW (g)	421±9	419±12	395±25	405±28
HW (g)	1.46±0.03	1.55±0.02	1.55±0.03	1.51±0.04
HW/BW (g/kg)	3.46±0.05	3.71±0.13	3.98±0.25	3.79±0.24
HW/TL (g/cm)	0.346±0.007	0.364±0.005	0.389±0.007*	0.377±0.010

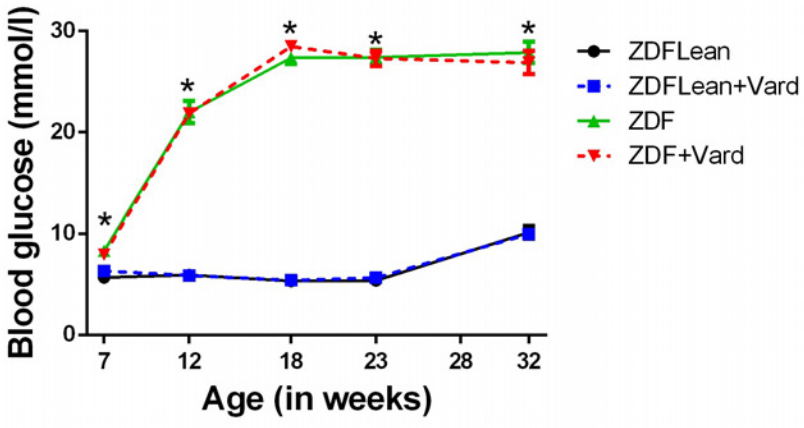

Figure 19. Blood glucose values in the study groups
Groups: vehicle-treated controls (ZDFLean), vardenafil-treated controls (ZDFLean+ Vard), vehicle-treated diabetic (ZDF) and vardenafil-treated diabetic (ZDF+Vard). *p<0.05 vs. ZDFLean

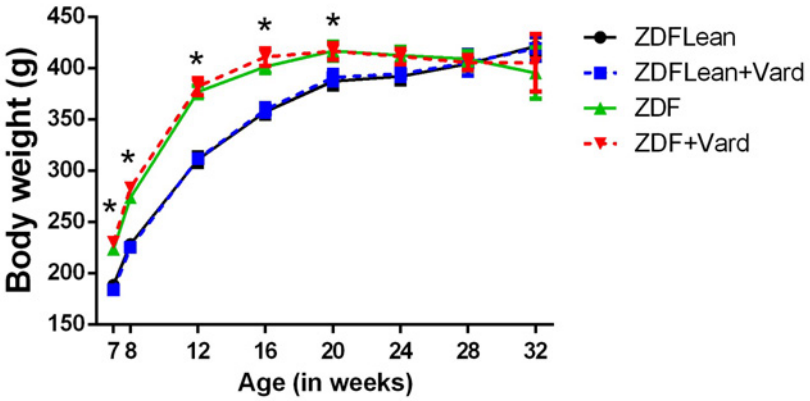

Figure 20. Body weight changes in T2DM
Groups: vehicle-treated controls (ZDFLean), vardenafil-treated controls (ZDFLean+ Vard), vehicle-treated diabetic (ZDF) and vardenafil-treated diabetic (ZDF+Vard). *p<0.05 vs. ZDFLean

5.3.2. *Vardenafil prevented T2DM-associated LV dysfunction in vivo*

HR and MAP did not differ among the groups (Table 8.). The slope of EDPVR (LV stiffness parameter) and Tau_W showed a significant increase in ZDF (Figure 21A and B). Vardenafil treatment markedly improved the slope of EDPVR, while Tau_W tended to decrease in ZDF rats (Figure 21B). Two-way ANOVA revealed that T2DM significantly affects the EDPVR and Tau_W as they have been shown to differ statistically between T2DM and non-diabetic animals. In spite of the marked diastolic dysfunction in T2DM, conventional systolic parameters, such as EF, CO, dP/dt_{max}, SW did not differ among our study groups (Table 8.). Moreover, reliable load-independent systolic parameters E_{es} and PRSW remained unchanged (Figure 21C).

Table 8. Hemodynamic parameters of the study groups
Heart rate (HR), mean arterial pressure (MAP), ejection fraction (EF), cardiac output (CO), maximal and minimal slope of dP/dt (dP/dt_{max} and dP/dt_{min}), stroke work (SW) are shown. Groups: vehicle-treated controls (ZDFLean), vardenafil-treated controls (ZDFLean+Vard), vehicle-treated diabetic (ZDF) and vardenafil-treated diabetic (ZDF+Vard). *p<0.05 vs. ZDFLean; #p< 0.05 vs. ZDF

Variable	ZDFLean	ZDFLean+Vard	ZDF	ZDF+Vard
HR (beats/min)	326±4	327±8	310±6	319±8
MAP (mmHg)	96±3	96±3	99±2	105±2
EF (%)	65±2	66±2	61±2	64±4
CO (ml/min)	67±5	70±5	55±5	58±9
dP/dt_{max} (mmHg/s)	9426±453	9061±270	8478±234	9994±634
dP/dt_{min} (mmHg/s)	-9799±549	-9706±424	-9039±639	-9463±1084
SW (mmHg*µl)	19378±1125	20567±1231	17279±1392	17848±2576

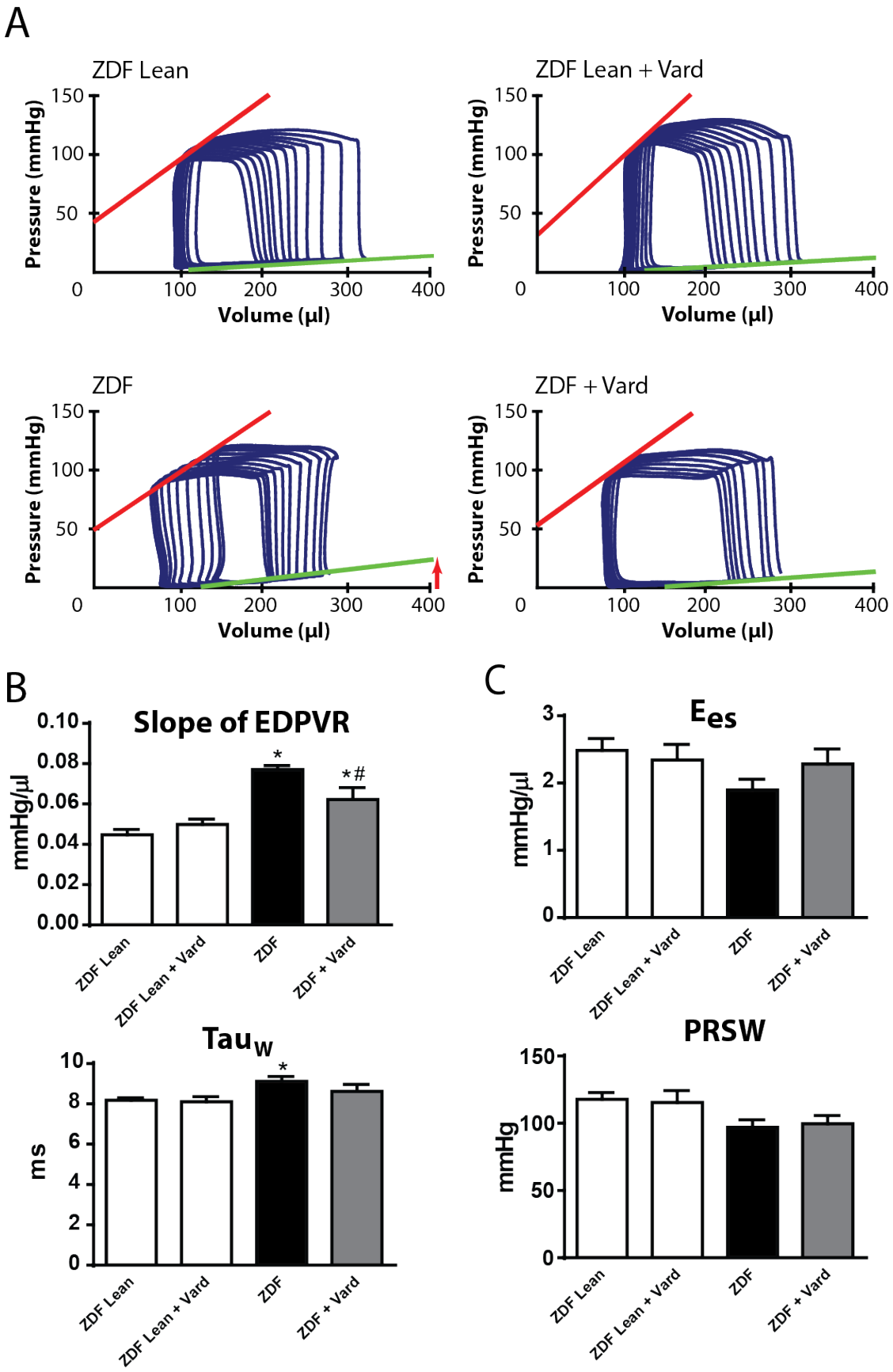

Figure 21. The effect of vardenafil on the hemodynamic alterations in T2DM animals

(A) Representative left ventricular (LV) pressure-volume (P-V) loops. (B) Graphs represent the value of the slope of end-diastolic P-V relationship (EDPVR) and Tauw. (C) Graphs of the slope (E_{es}) of the LV end-systolic P-V relationships and the value of preload-recruitable stroke work (PRSW). The arrow indicates the increase of EDPVR (a marker of cardiac stiffness) in ZDF. Groups: vehicle-treated controls (ZDFLean), vardenafil-treated controls (ZDFLean+Vard), vehicle-treated diabetic (ZDF) and vardenafil-treated diabetic (ZDF+Vard). *p< 0.05 vs. ZDFLean; #p< 0.05 vs. ZDF

5.3.3. *Vardenafil prevented T2DM-associated stiffening of LV cardiomyocytes*

$F_{passive}$ (at different SLs; marker of cardiomyocyte stiffness) increased significantly in ZDF rats (Figure 22A). Vardenafil prevented the diabetes-associated increase of $F_{passive}$ (Figure 22A), however, it had no effect on F_{max} (Figure 22B).

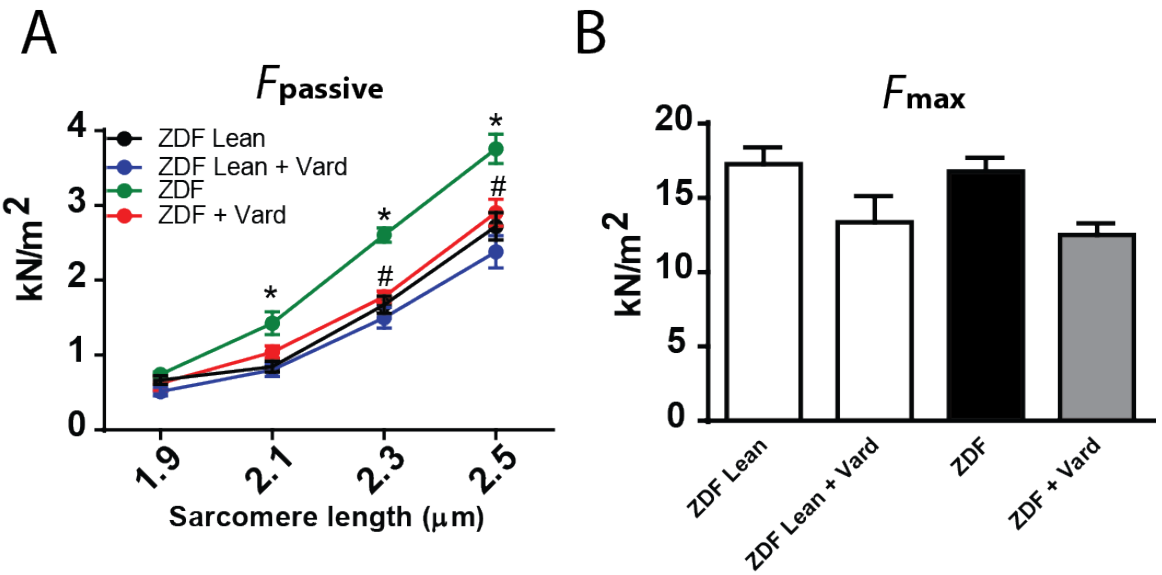

Figure 22. The effect of vardenafil on the cardiomyocyte $F_{passive}$ and F_{max} in T2DM animals
(A) $F_{passive}$ (cardiomyocyte stiffness marker) at different sarcomere lengths and (B) F_{max} are shown. Groups: vehicle-treated controls (ZDFLean), vardenafil-treated controls (ZDFLean+Vard), vehicle-treated diabetic (ZDF) and vardenafil-treated diabetic (ZDF+Vard). *p<0.05 vs. ZDFLean; #p<0.05 vs. ZDF

5.3.4. *Vardenafil decreased myocardial hypertrophy in T2DM rats*

Although HW and HW/BW ratios were not different, HW/TL ratio increased significantly in ZDF compared to ZDFLean (Table 7.). HW/TL ratio of ZDF+Vard tended to decrease when compared to ZDF (Table 7.). Additionally, echocardiography

revealed the signs of myocardial hypertrophy in ZDF indicated by the significantly elevated LVAW and LVPW in systole and diastole, increased RWT, LVmass/TL and LVmass index (Table 9.) All of these parameters were not statistically different in ZDF+Vard when compared to ZDFLean, while LVAWs and LVAWd were markedly reduced in response to vardenafil treatment when compared to ZDF (Table 9.). Beside the robust hypertrophy observed on echocardiographic images (Figure 23A), significant elevation of ANF (Figure 23C) and robust increase of cardiomyocyte diameter/TL (Figure 23B and D) have proven cardiomyocyte hypertrophy. Vardenafil significantly reduced the gene expression level of ANF (Figure 23C) and decreased cardiomyocyte diameter/TL (Figure 23D). Additionally, the slope of EDPVR correlated robustly with the hypertrophy marker cardiomyocyte diameter/TL (Figure 23E).

Table 9. Echocardiography data
Left ventricular (LV) anterior and posterior wall thickness (LVAW, LVPW), LV internal diameter (LVID), relative wall thickness (RWT), LVmass, LVmass/TL ratio and LVmass index are shown. The "s" and "d" refer to end-systolic and end-diastolic, respectively. Groups: vehicle-treated controls (ZDFLean), vardenafil-treated controls (ZDFLean+Vard), vehicle-treated diabetic (ZDF) and vardenafil-treated diabetic (ZDF+Vard). *p< 0.05 vs. ZDFLean; #p< 0.05 vs. ZDF

Variable	ZDFLean	ZDFLean+Vard	ZDF	ZDF+Vard
LVAWs (mm)	2.53±0.04	2.58±0.15	2.90±0.08*	2.48±0.05#
LVAWd (mm)	1.73±0.03	1.76±0.03	1.88±0.01*	1.72±0.03#
LVIDs (mm)	4.91±0.21	4.84±0.16	4.50±0.14	5.04±0.19
LVIDd (mm)	8.08±0.20	7.83±0.15	7.99±0.32	8.08±0.29
LVPWs (mm)	2.63±0.07	2.69±0.10	3.07±0.10*	2.93±0.11
LVPWd (mm)	1.72±0.08	1.91±0.07	2.12±0.10*	2.02±0.10
RWT	0.41±0.02	0.47±0.01	0.50±0.03*	0.47±0.02

LVmass (g)	0.98±0.02	1.01±0.05	1.15±0.05	1.09±0.07
LVmass/TL (g/cm)	0.232±0.005	0.245±0.118	0.299±0.010*	0.271±0.017
LVmass index (g/kgBW)	2.53±0.09	2.66±0.13	3.23±0.23*	2.99±0.23

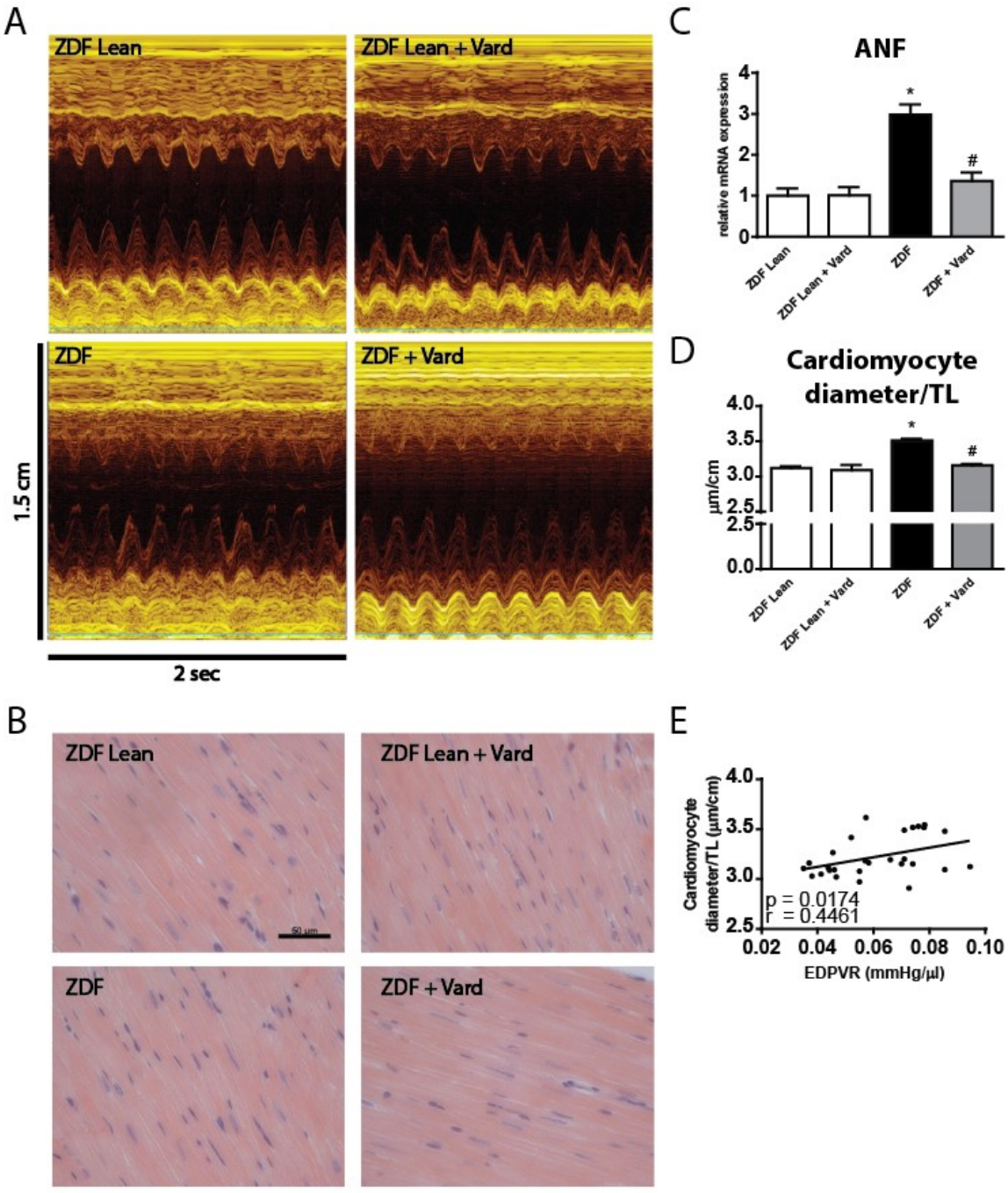

Figure 23. The effect of vardenafil on myocardium hypertrophy in T2DM
(A) Representative M-mode echocardiography images at the mid-papillary level on short axis view. (B) Representative hematoxylin-eosin stained sections. Magnification: 400x; Scale bar: 50 μm. (C) Relative gene expression of atrial natriuretic factor (ANF). (D) Graph shows the quantification of cardiomyocyte diameter/tibia length (TL). (E) Correlation analysis between cardiomyocyte diameter/TL and the slope of EDPVR. Groups: vehicle-treated controls (ZDFLean), vardenafil-treated controls (ZDFLean+ Vard), vehicle-treated diabetic (ZDF) and vardenafil-treated diabetic (ZDF+Vard). *p< 0.05 vs. ZDFLean; #p< 0.05 vs. ZDF

5.3.5. *Vardenafil reduced alterations associated with nitro-oxidative stress in T2DM*

T2DM was associated with markedly elevated 3-NT content of the LV (Figure 24A and B). However, vardenafil effectively prevented the elevation of 3-NT content (Figure 24A and B). In accordance, we observed significant upregulation of different antioxidant enzymes including catalase and thiorexodin-1 in the ZDF group (Figure 24C). Nevertheless, as a result of chronic drug treatment catalase and thioredoxin-1 levels declined significantly in ZDF rats (Figure 24C). Moreover, SERCA2a was markedly downregulated in ZDF rats regardless of our treatment (Figure 24D). Additionally, PLB gene expression tended to decrease in the ZDF group (Figure 24D), however, in the ZDF+Vard group it did not show any difference when compared to ZDFLean animals (Figure 24D). Despite the unchanged PLB/SERCA2a ratio in T2DM (Figure 24D), vardenafil treatment markedly increased the ratio of PLB/SERCA2a in ZDF animals (Figure 24C).

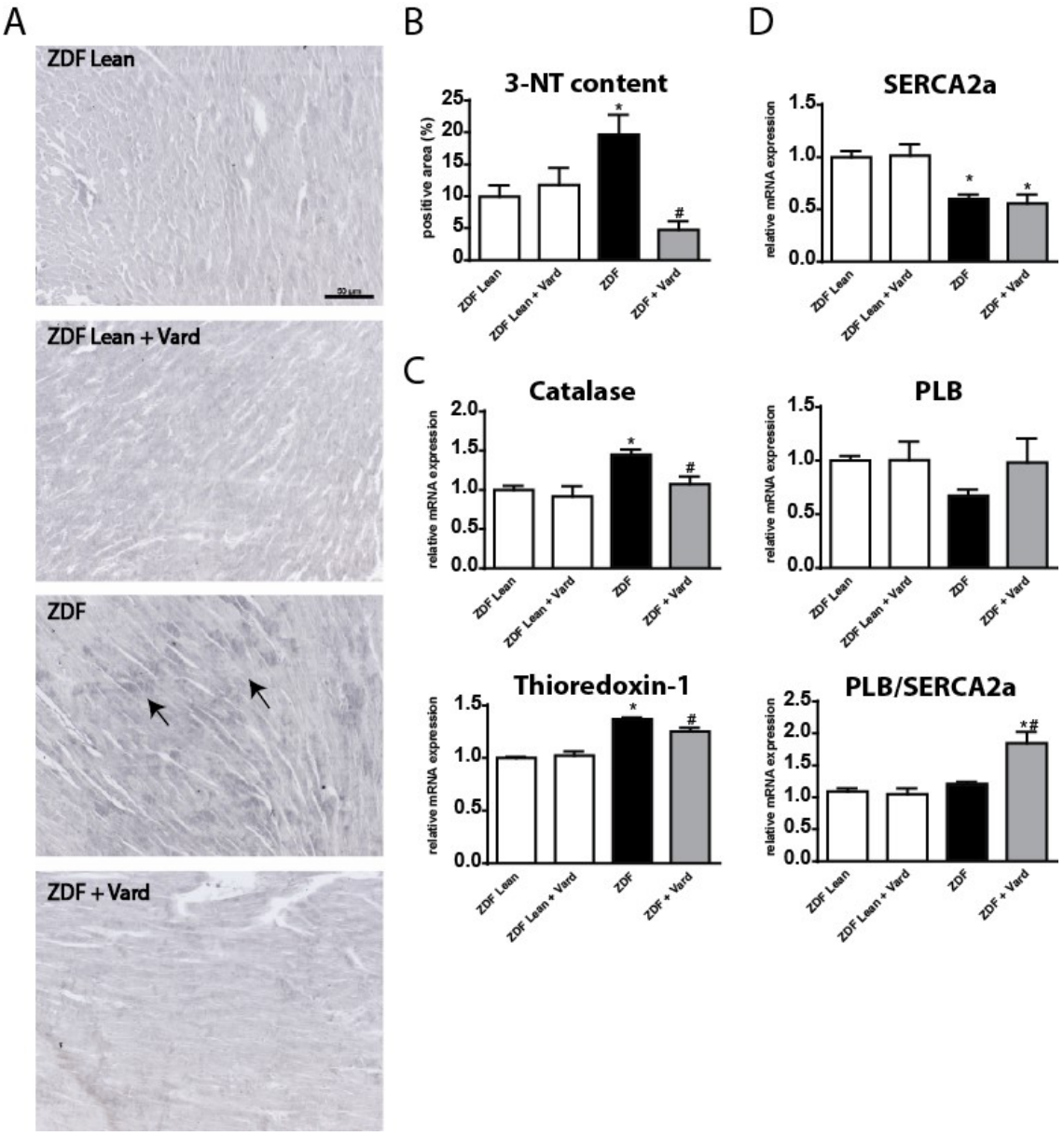

Figure 24. Phosphodiesterase-5A inhibition reduces the extent of cardiac nitro-oxidative stress in T2DM

(A) Representative images of 3-nitrotyrosine (3-NT) stained sections. Magnification: 200x; Scale bar: 50 μm. Arrows indicate the grey colored 3-NT positive area. (B) Quantification of 3-NT positive area in the experimental groups. (C) Relative gene expression levels of catalase, thioredoxin-1, (D) sarcoplasmic reticulum calcium ATPase 2 (SERCA2a), phospholamban (PLB) and the ratio of PLB/SERCA2a are shown. Groups: vehicle-treated controls (ZDFLean), vardenafil-treated controls (ZDFLean+Vard), vehicle-treated diabetic (ZDF) and vardenafil-treated diabetic (ZDF+Vard). *p< 0.05 vs. ZDFLean; #p< 0.05 vs. ZDF

5.3.6. *Vardenafil suppressed myocardial fibrotic remodeling*

MT and picrosirius staining revealed fibrotic remodeling of the myocardium in ZDF animals (Figure 25A, B, C, D). The extent of myocardial fibrosis correlated robustly with the slope of EDPVR (Figure 25E). Fn1 was markedly overexpressed in T2DM (Figure 25F). Additionally, Col1a1 and Col3a1 mRNAs were significantly downregulated in ZDF rats (Figure 25G). Prevention by vardenafil effectively reduced the fibrotic remodeling of the myocardium (Figure 25A, B, C, D) and significantly reduced Fn1 gene expression (Figure 25F) in T2DM. Interestingly, Col1a1 and Col3a1 gene expressions were unaltered by vardenafil in the ZDF+Vard group compared to ZDF (Figure 25G).

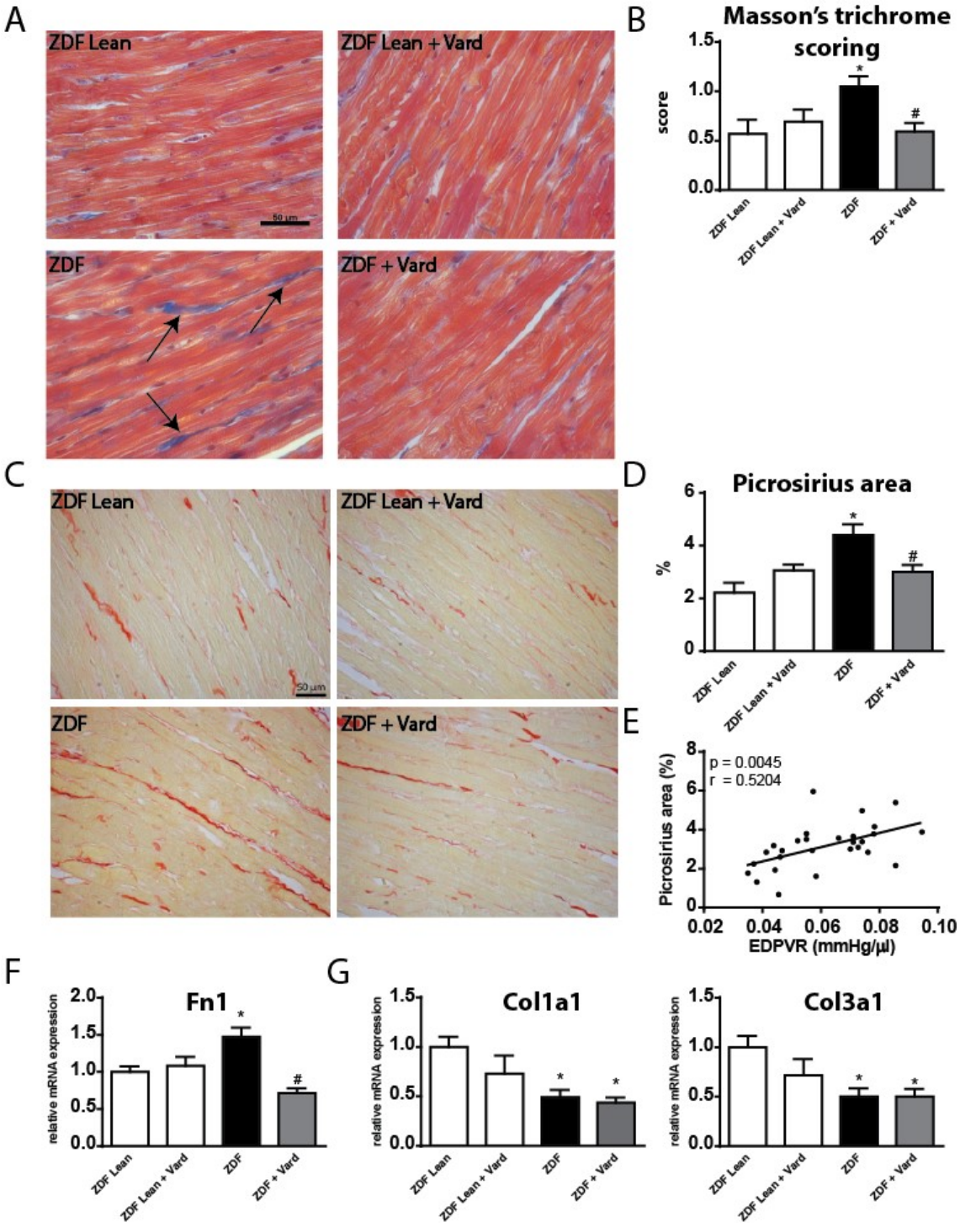

Figure 25. Protective effects of vardenafil on myocardial fibrosis
(A) Representative images and (B) semiquantitative scoring of Masson's trichrome (MT) stained sections. Arrows indicate interstitial fibrosis of the myocardium. Magnification: 400x; Scale bar: 50 µm. (C) Representative images and (D) quantification of picrosirius stained myocardium. Magnification: 400x; Scale bar: 50 µm. (E) Correlation analysis between picrosirius positive area and the slope of EDPVR. (F) Gene expression of fibronectin-1 (Fn1), (G) collagen 1a1 and 3a1 (Col1a1; Col3a1).

Groups: vehicle-treated controls (ZDFLean), vardenafil-treated controls (ZDFLean+ Vard), vehicle-treated diabetic (ZDF) and vardenafil-treated diabetic (ZDF+Vard). *p<0.05 vs. ZDFLean; #p<0.05 vs. ZDF

5.3.7. *Phosphodiesterase-5A inhibiton prevented cardiomyocyte apoptosis in ZDF rats*

Increased cardiomyocyte apoptosis was evidenced by TUNEL assay (Figure 26A and B), by markedly risen cleaved caspase-3 and cleaved PARP1 band densities (Figure 26C and D). However, vardenafil prevented the above alterations by significantly decreasing the number of TUNEL positive nuclei (Figure 26A and B) and cleaved PARP1 band density (Figure 26D). Cleaved caspase-3 band density was not significantly different in ZDF+Vard compared to the ZDFLean (Figure 26C).

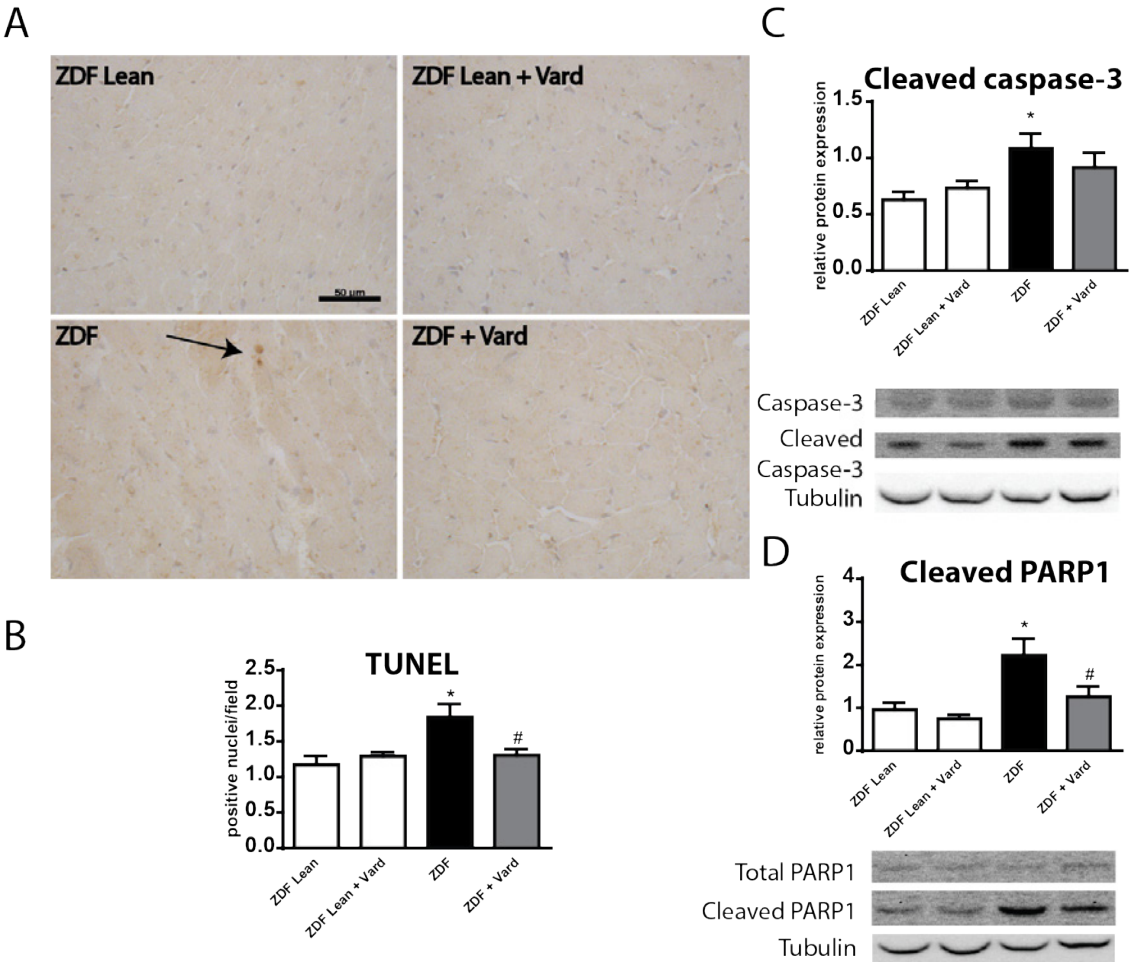

Figure 26. The effects of vardenafil on myocardial DNA fragmentation and apoptosis (A) Representative images of TUNEL assay. Magnification: 200x; Scale bar: 50 μm. (B) Quantification of TUNEL positive nuclei/field. (C) Graphs and representative Western blot bands of cleaved caspase-3 (17kDa) and (D) cleaved poly (ADP-ribose)

polymerase (PARP1; 113/85kDa) levels in the myocardium. Groups: vehicle-treated controls (ZDFLean), vardenafil-treated controls (ZDFLean+Vard), vehicle-treated diabetic (ZDF) and vardenafil-treated diabetic (ZDF+Vard). *p<0.05 vs. ZDFLean; #p<0.05 vs. ZDF

5.3.8. *Vardenafil protected against the disturbances of myocardial cGMP-PKG signaling in ZDF rats*

The PDE5A-cGMP-PKG axis was significantly deteriorated in T2DM as evidenced by the markedly lower cGMP staining intensity of the myocardium (Figure 27A and B), by the increased protein levels of PDE5A and PKG (Figure 27D) and by the lower p-VASP/VASP ratio (as a marker of impaired PKG activity; Figure 27D). Myocardial PDE5A levels in the ZDF+Vard group did not differ from the healthy controls (Figure 27D). Vardenafil effectively increased the cGMP staining intensity of the myocardium of ZDF animals (Figure 27A and B). Furthermore, vardenafil elevated the plasma cGMP content in ZDF rats (Figure 27C) and restored the ratio of p-VASP/VASP (Figure 27D). Interestingly, plasma cGMP level showed a strong tendency toward elevation in ZDFLean+Vard (Figure 27C). Plasma total nitrite/nitrate levels and p-PLB/PLB ratios were not different among the groups (Figure 27E and F).

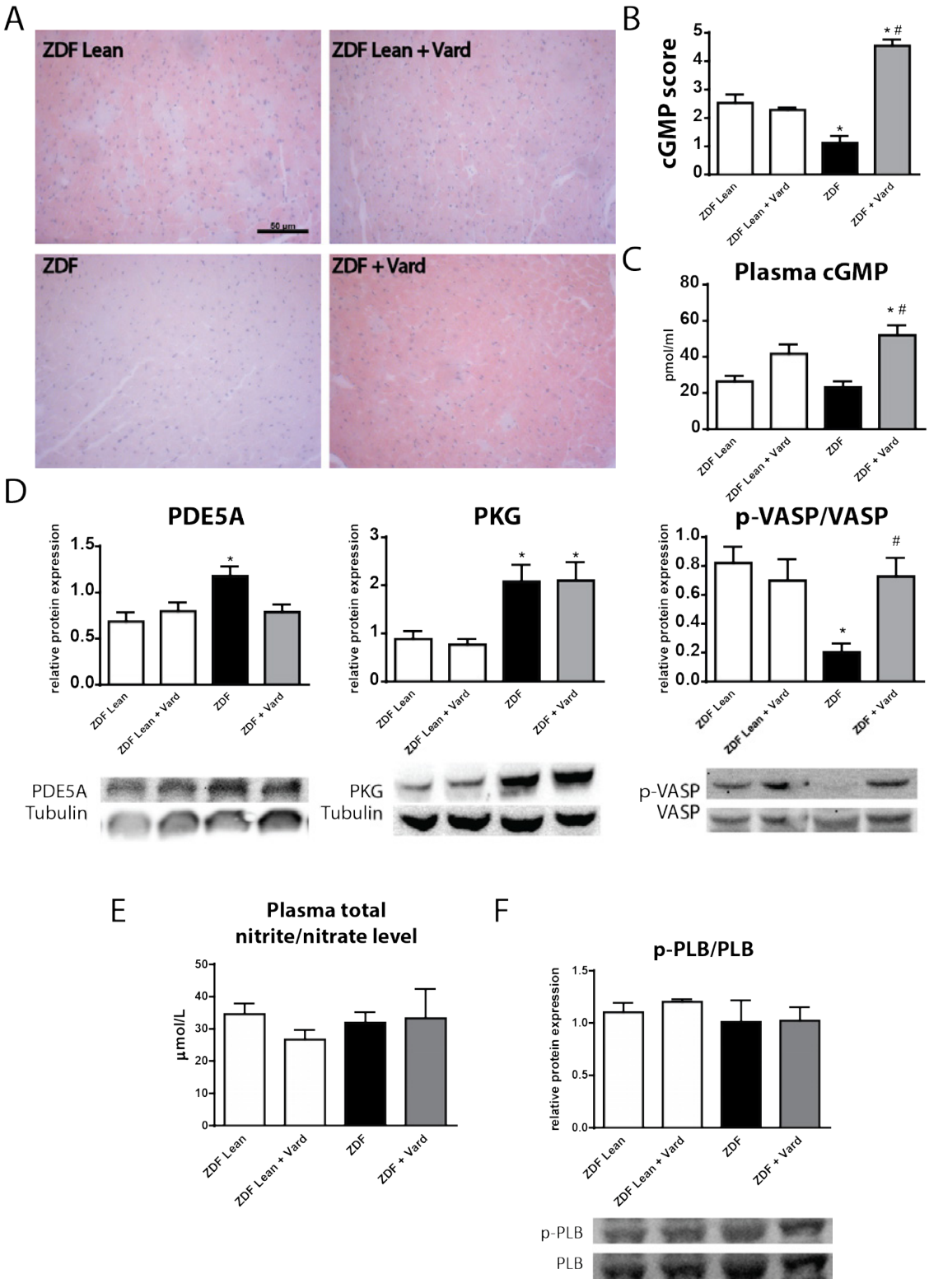

Figure 27. Modulatory effects of vardenafil on the myocardial NO-cGMP signaling in T2DM

(A) Representative images (Magnification: 200x; Scale bar: 50 µm) and (B) quantification of cGMP immunohistochemistry in the study groups. (C) Plasma cGMP

levels in the experimental groups. (D) Graphs and representative Western blot bands of phosphodiesterase-5A (130 kDa, PDE5A), protein kinase G (75 kDa, PKG) and phospho-vasodilator-stimulated phosphoprotein (p-VASP) and VASP (50 kDa) are shown. (E) Graph of total plasma nitrite/nitrate levels and (F) Western blot phosphorylation assay of phospholamban (PLB) (24 kDa). Groups: vehicle-treated controls (ZDFLean), vardenafil-treated controls (ZDFLean+Vard), vehicle-treated diabetic (ZDF) and vardenafil-treated diabetic (ZDF+Vard). *p<0.05 vs. ZDFLean; #p<0.05 vs. ZDF

The results of the two-factorial ANOVA main effects and interaction are depicted in Table 10.

Table 10. Two-way ANOVA results

Variable	**Two-way ANOVA P values**		
Basic characteristics	**Factor „T2DM”**	**Factor „Vardenafil”**	**Interaction**
BW (g)	0.296	0.850	0.750
HW (g)	0.415	0.415	0.052
HW/BW (g/kg)	0.085	0.850	0.196
HW/TL (g/cm)	0.001	0.700	0.064
Blood glucose (mmol/l) (7^{th} week)	<0.001	0.699	0.129
Blood glucose (mmol/l) (12^{th} week)	<0.001	0.904	0.952
Blood glucose (mmol/l) (18^{th} week)	<0.001	0.151	0.196
Blood glucose (mmol/l) (23^{rd} week)	<0.001	0.890	0.713
Blood glucose (mmol/l) (32^{nd} week)	<0.001	0.506	0.632
Echocardiography			
LVAWs (mm)	0.143	0.043	0.013
LVAWd (mm)	0.093	0.049	0.005
LVIDs (mm)	0.564	0.208	0.114

LVIDd (mm)	0.759	0.748	0.484
LVPWs (mm)	0.001	0.681	0.294
LVPWd (mm)	0.007	0.632	0.111
RWT	0.037	0.602	0.019
LVmass (g)	0.028	0.820	0.350
LVmass/TL (g/cm)	0.001	0.521	0.112
LVmass index (g/kgBW)	0.007	0.747	0.313
Hemodynamic parameters			
HR (beats/min)	0.079	0.438	0.560
MAP (mmHg)	0.055	0.299	0.350
EF (%)	0.339	0.476	0.691
CO (ml/min)	0.062	0.603	0.969
dP/dt_{max} (mmHg/s)	0.986	0.180	0.034
dP/dt_{min} (mmHg/s)	0.481	0.815	0.715
SW (mmHg*µl)	0.147	0.589	0.848
EDPVR (mmHg/µl)	<0.001	0.197	0.014
Tau_W (ms)	0.006	0.249	0.382
E_{es} (mmHg/µl)	0.773	0.350	0.226
PRSW (mmHg)	0.009	0.762	0.533
In vitro cardiomyocyte force measurement			
F_{max} (kN/m^2)	0.584	0.003	0.891
$F_{passive}$ (kN/m^2) (SL: 1.9 µm)	0.149	0.038	0.776
$F_{passive}$ (kN/m^2) (SL: 2.1 µm)	0.044	0.416	0.085
$F_{passive}$ (kN/m^2) (SL: 2.3 µm)	<0.001	<0.001	0.007
$F_{passive}$ (kN/m^2) (SL: 2.5 µm)	<0.001	0.006	0.203
Histology/immunohistochemistry			
Cardiomyocyte diameter/TL	<0.001	<0.001	<0.001

(μm/cm)			
3-NT content (%)	0.560	0.009	0.001
Masson's trichrome score	0.117	0.162	0.021
Picrosirius area (%)	0.005	0.427	0.003
TUNEL positive nuclei/field	0.017	0.125	0.021
cGMP score	0.085	<0.001	<0.001
Gene expression results			
ANF	<0.001	0.002	0.002
Catalase	0.004	0.021	0.126
Thioredoxin-1	<0.001	0.090	0.010
SERCA2a	<0.001	0.850	0.708
PLB	0.203	0.248	0.265
PLB/SERCA2a	<0.001	0.006	0.002
Fn1	0.610	0.004	0.001
Col1a1	0.001	0.148	0.333
Col3a1	0.004	0.213	0.216
Protein expression results			
Cleaved caspase 3	0.011	0.771	0.238
Cleaved PARP1	<0.001	0.022	0.036
PDE5A	0.019	0.161	0.016
PKG	<0.001	0.855	0.805
p-VASP/VASP	0.021	0.098	0.013
p-PLB/PLB	0.349	0.701	0.764
Biochemistry			
Plasma cGMP (pmol/ml)	0.421	<0.001	0.127
Plasma total nitrite/nitrate (μmol/l)	0.728	0.570	0.426

6. Discussion

In the present investigation we compared the functional and molecular changes of diabetic heart disease in type 1 and type 2 DM. Moreover, we investigated the potential beneficial effects of sGC activation and PDE5A inhibition in the treatment of diabetic cardiomyopathy. We have shown that there are distinct differences in cardiac function together with different degree of tissue injury and myocardial remodeling between the two types of diabetes. Additionally, massive deterioration of the NO-sGC-cGMP-PKG signaling can be observed in the diabetic cardiomyocytes. Finally, we have shown that both sGC activation and PDE5A inhibition have cardioprotective properties in diabetic cardiomyopathy thus they might become novel therapies for the diabetes-associated heart failure.

6.1. Structural and molecular hallmarks of type 1 and type 2 DM-associated diabetic cardiomyopathy

Although the functional and molecular changes of diabetic cardiomyopathy has been investigated by many authors, the exact pathomechanisms of the disease are still not fully understood. Several key pathophysiological processes play role in the development of the disease such as oxidative imbalance and increased nitro-oxidative stress, cardiomyocyte apoptosis, hypertrophy and myocardial fibrosis (Huynh et al. 2014). Despite the several key features that are contributors to diabetic cardiomyopathy, the most important one is hyperglycemia that presumably leads to severe complications. The imbalance in glucose metabolism triggers numerous mechanisms and signaling pathways which result in cardiac dysfunction (see Section 11.1. Bibliography of the candidate's publications – Articles III., V.).

6.1.1. Nitro-oxidative stress

Hyperglycemia leads to the accumulation of ROS and to the development of severe nitro-oxidative stress in DM and subsequent upregulation of endogenous antioxidant systems and overexpression of heat shock proteins (Snoeckx et al. 2001, Huynh et al.

2014). Several mechanisms have been described to play a role in DM associated nitro-oxidative stress such as the upregulation of NADPH-oxidases and NO synthases (Huynh et al. 2014). In addition to these, in nitro-oxidative stress peroxynitrite is generated as a result of ROS-NO reaction and this significantly contributes to the decreased NO bioavailibility (Pacher et al. 2007). In accordance with this, we observed massive hyperglycemia in both of our diabetes models already at early time-points. Interestingly, plasma nitrite/nitrate levels (reflecting NO bioavailability) were not diminished in type 2 diabetes.

Peroxynitrite is a highly reactive molecule that directly reacts with different cellular elements, enzymes, myofibrillar proteins and the DNA (Pacher et al. 2007). Additionally, in nitro-oxidative stress the non-specific nitration of different cellular proteins occur, e.g. nitration at tyrosine amino-acids (Pacher et al. 2007). Accordingly, the immunohistochemical staining against NT (a marker for nitro-oxidative stress) indicated elevated NT positivity in the diabetic myocardium in both DM models, which is in line with earlier studies (Kajstura et al. 2001, Song et al. 2008). According to the semiquantitative analysis of the staining, more pronounced nitro-oxidative stress could be documented in the type 1 DM model, when compared with type 2 DM. The severe nitro-oxidative stress in the myocardium was further confirmed by the compensatory overexpression of endogenous antioxidant systems (such as the SOD – catalase and glutathione systems or thioredoxin) and by a remarkable heat shock response (increased HSP70a1 level). Increased nitro-oxidative stress can result in triggering pathways of apoptosis, ventricular hypertrophy and fibrotic remodeling (Huynh et al. 2014).

6.1.2. DNA damage and apoptosis

Oxidative stress with the excessive production of ROS and peroxynitrite directly propagates DNA fragmentation and apoptosis (programmed form of cell death) in diabetes leading to the loss of cardiomyocytes (Pacher et al. 2007) and to the development of diabetic cardiomyopathy. Both clinical and experimental studies have shown that progressive loss of cardiomyocytes has causal role in the development of the disease (Fiordaliso et al. 2000, Cai et al. 2003, Huynh et al. 2014). As a result of the constant presence of DNA damage and increased apoptosis ventricular function

becomes decompensated over the course of the disease (Frustaci et al. 2000). Apoptosis contributes also to the fibrotic remodeling of the heart as dead cardiomyocytes are replaced by extracellular matrix components such as fibroblasts and collagen (van Heerebeek et al. 2008, Paulus et al. 2013). There are several measures available to assess the extent of DNA damage and apoptosis including TUNEL assay, caspase 3 and PARP1 cleavage. TUNEL assay is a widely used method to study DNA fragmentation in vivo and in vitro (Loo 2011). Increased DNA fragmentation and elevated rate of apoptosis have been observed (TUNEL-positive cardiomyocyte nuclei, myocardial expression of the pro-apoptotic mediator caspase-12 and increased rate of caspase-3 cleavage and PARP1 cleavage in type 2 DM) in both types of diabetes. DNA fragmentation was more pronounced (indicated by TUNEL assay) in the type 1 DM model. Correspondingly, previous literature data reported the increase in TUNEL positive cardiomyocyte cell nuclei both in T1DM and T2DM animals (Fiordaliso et al. 2000, Ramirez et al. 2013). Interestingly, we did not find any differences in BAX/Bcl-2 ratio in type 1 DM which suggest that classical apoptotic pathways are not involved in the process.

6.1.3. Myocardial hypertrophy

We investigated several markers of myocardial hypertrophy in our studies. The development of diabetic cardiomyopathy was associated with increased cardiomyocyte diameter (histological analysis of the myocardium) in both of our models and it was comparable in both types of diabetes. Interestingly, increasing tendency in heart weight/body weight ratio was observed in diabetes that reached the level of statistical significance only in type 1 diabetes mellitus. It is worth to note that this index is influenced by the changes of body weight (more significantly in the type 1 DM animals). Moreover, our experiments revealed massive cardiac hypertrophy by increased HW/TL ratio and by echocardiography in the type 2 DM model.

Several mechanisms might be in the background of the hypertrophic remodeling in diabetic cardiomyopathy including the transient activation of immediate-early genes that encode transcription factors such as c-jun and c-fos (Nadruz et al. 2005, Min et al. 2009). The above genes were significantly upregulated only in type 1 DM. Accordingly,

c-jun and c-fos have been suggested to activate the fetal gene program (transcription of genes such as ß-MHC or ANF). These genes play significant role in adaptive hypertrophy and are considered markers of pathologic myocardial hypertrophy (Cox et al. 2014). Correspondingly, we observed decreased expression of α-MHC and increased expression of the fetal type ß-MHC (shift in the β/α-MHC expression ratio as a marker of pathological hypertrophy). These changes were more pronounced in type 1 DM. The myocardial overexpression of the hypertrophy marker ANF was found to be comparable in the two DM models. These results clearly reflect the existence of myocardial hypertrophy associated with diabetes in type 1 and also in type 2 DM models, and are in correspondence with previous data (Fredersdorf et al. 2004, Xia et al. 2007, Huynh et al. 2014).

6.1.4. Fibrotic remodeling

Another key component of myocardial remodeling is the excessive fibrosis of the heart in diabetic cardiomyopathy. Oxidative stress and hyperglycemia both stimulate pro-fibrotic signaling and interstitial collagen deposition (Huynh et al. 2014), while cardiomyocyte apoptosis contributes to the replacement fibrosis. As a result of a more pronounced oxidative stress and DNA damage/apoptosis we observed more pronounced myocardial fibrosis (higher level of TGF-ß1; significantly higher fibrosis score values [fibrosis +~260%] in type 1 diabetic animals in comparison to the T2DM model (fibrosis +~45%). Although myocardial fibrosis has been widely described in STZ-induced T1DM (Xia et al. 2007, Taye et al. 2013, Huynh et al. 2014), literature data are controversial regarding myocardial fibrosis in ZDF rats. Myocardial collagen deposition was not presented in 14-week old ZDF diabetic animals (Marsh et al. 2007), however, other investigations demonstrated only perivascular but not interstitial myocardial fibrosis (Fredersdorf et al. 2004) in 19-week old ZDF. In spite of that, cardiac fibrosis was significantly increased in 45-week old ZDF animals (Daniels et al. 2012). Accordingly, fibrotic remodeling was presented in the LV of our ZDF animals (32 weeks of age; higher MT score, picrosirius area and Fn1 gene expression). According to the literature, fibrotic remodeling of the diabetic myocardium is strongly associated with dysregulation of MMPs (Huynh et al. 2014), increased fibroblast proliferation

(Bugger et al. 2014), decreased Col1a1 and Col3a1 mRNA expression (Van Linthout et al. 2008) and TGF-β1 signaling (Cai et al. 2002). Interestingly, Col1a1 and Col3a1 mRNA levels were significantly reduced in both T1DM and T2DM, which is in agreement with previous literature data (Van Linthout et al. 2008). This could be the consequence of a negative feedback mechanism and suggests that an altered rate of collagen degradation rather than enhanced synthesis is responsible for the observed interstitial fibrosis.

It is worth to note, that shorter diabetes duration (8 weeks) resulted in more pronounced fibrosis of the heart in the type 1 model compared to type 2 model (25 weeks of diabetes duration). Differences of the pathophysiological processes (insulinopenia vs. hyperinsulinaemia and insulin resistance and the different time course of DM) might lie in the background of this phenomenon since the degree of hyperglycemia was comparable between the models (Daniels et al. 2012). The expression and bioavailability of different vasoactive factors are altered in diabetic cardiomyopathy including upregulation of ET-1 and decrease of NO (Farhangkhoee et al. 2006). Accordingly, we found marked overexpression of ET-1 in the diabetic heart of both models (more severe in type 1 DM) along with decreased eNOS expression in type 1 DM. Upon this, a more severe cardiac microvascular injury is suggested in T1DM compared to T2DM. The overexpression of ET-1 might have significant effect on fibrotic remodeling by inducing the accumulation of fibroblasts in the myocardium (Widyantoro et al. 2010).

6.1.5. Deterioration of the NO-sGC-cGMP-PKG signaling pathway

Heart failure coupled with different comorbidities including obesity, diabetes mellitus contribute greatly to a pronounced nitro-oxidative stress in the myocardium. The importance of comorbidities and the subsequent deterioration of the NO-cGMP-PKG signaling have been proposed in the development of heart failure by Paulus et al. (Paulus et al. 2013). These together lead to decreased NO bioavailibility, lower cGMP levels with subsequent deactivation of the main effector PKG enzyme. In line with this finding, van Heerebeek et al. found lower myocardial PKG activity in the myocardium of HFpEF patients (van Heerebeek et al. 2012).

Additionally, severe nitro-oxidative stress can lead to the oxidation of the sGC enzyme. This causes the loss of the heme prosthetic group of the enzyme in response and results in NO-insensitive (inactive) form of sGC. Moreover, the imbalance of the different types of phosphodiesterases in the failing heart might contribute to the rapid degradation of intracellular cGMP (Lukowski et al. 2014).

The above observation was confirmed by our results showing reduced myocardial cGMP content in the heart of both T1DM and T2DM rats. Interestingly, sGC β1 and eNOS protein expressions remained unchanged in T1DM. Moreover, increased myocardial PDE5A protein levels (in accordance with previous data (Fang et al. 2013)) in both types of DM might have contributed to the degradation of cGMP. As a result of this we observed significantly lower activity of PKG as indicated by the phosphorylation of its target VASP (lower p-VASP/VASP ratio, an index of PKG activity (Irvine et al. 2012)) in both diabetes models. In spite of that, elevated PKG protein expression was observed, which might reflect an ineffective compensatory mechanism in the heart. Of note, plasma cGMP levels were not altered in the animal models. This could be a consequence of diabetes-associated increase in ANF levels and the subsequent activation of natriuretic peptide receptors and pGC in organs other than the heart. Thus the preserved plasma cGMP is seen as a sign of overspill of cGMP from different tissues (Hamet et al. 1989). Beside plasma cGMP, plasma nitrite/nitrate levels (reflecting NO bioavailability) were also unaltered. (see Section 11.1. Bibliography of the candidate's publications – Articles I., II., IV.)

6.1.6. Characteristics of cardiac dysfunction T1DM and T2DM

Diabetic cardiomyopathy-associated functional alterations are closely related to the above discussed histological and molecular changes of the myocardium (nitro-oxidative stress, apoptosis, hypertrophy and fibrosis) (Huynh et al. 2014). Depending on its type, diabetes mellitus is associated with different characteristics of cardiac dysfunction (systolic and diastolic dysfunction [HFrEF] in type 1 while mainly diastolic dysfunction [HFpEF] in type 2 DM) measured by non-invasive and invasive methods (Litwin et al. 1990, Radovits et al. 2009b) (Franssen et al. 2016a). Based upon our results, the contribution of the above pathophysiological processes to systolic versus diastolic heart

failure might be different. Both cardiomyocyte hypertrophy and cardiac fibrosis are evident in HFpEF, but the latter one coupled with more severe apoptosis has been reported to be more important in systolic heart failure (van Heerebeek et al. 2008, Paulus et al. 2013, Huynh et al. 2014). Moreover, systolic dysfunction is more likely to be associated with greater extent of nitro-oxidative stress (Gonzalez et al. 2011, Paulus et al. 2013).

Accordingly, our current results on in vivo cardiac function showed corresponding differences in the characteristics of type 1 and type 2 diabetic cardiac dysfunction. We observed a significant reduction of MAP (probably as a consequence of diabetic polyuria (Wang et al. 2008)) in T1DM, while it did not change in T2DM. We found marked impairment of LV contractility and systolic function (as reflected by decreased LVSP, SW, EF and dP/dt_{max}, E_{es} and PRSW), severe deterioration of diastolic function (decreased LV active relaxation [impaired dP/dt_{min}, prolonged Tau]) and elevated LV diastolic stiffness (elevated LVEDP, tendency toward elevation of EDPVR) in T1DM. Despite the characteristic of cardiac dysfunction in T1DM, T2DM was associated with preserved systolic function (EF, E_{es}, PRSW) but impaired diastolic function (prolonged Tau) and increased LV stiffness (increased LVEDP and slope of EDPVR). Additionally, in vitro cardiomyocyte stiffness (as evidenced by the increased $F_{passive}$) was also present in T2DM. Diastolic dysfunction (slope of EDPVR) strongly correlated with both cardiac hypertrophy and fibrosis in the T2DM model. Disturbed calcium homeostasis might be a possible contributor to the prolonged relaxation time in T2DM (Zarain-Herzberg et al. 2014). According to this, we observed lower SERCA2a gene expression in the myocardium of ZDF rats. (see Section 11.1. Bibliography of the candidate's publications – Articles I., II., IV.)

6.1.7. Effects of sGC activation by cinaciguat on diabetic cardiomyopathy in T1DM

It has been described that cinaciguat, a sGC activator compound have disease specific effects as it preferentially activates the inactive, oxidized form of the enzyme. This form is mainly present in diseased conditions (including diabetes mellitus). Thus, cinaciguat restores the enzyme's cGMP producing ability in various pathological conditions where

oxidative stress is occured (Stasch et al. 2006, Radovits et al. 2011, Korkmaz et al. 2013). Accordingly, cinaciguat application resulted in massive cytoprotective effects in diabetes mellitus: it has lowered diabetes-induced nitro-oxidative burden (reduced level of NT positivity) and it has normalized the expression of endogenous antioxidant and heat shock protein systems. Moreover, cinaciguat treatment reduced diabetes-associated DNA fragmentation and apoptosis (decreased TUNEL positivity). Regarding other pathophysiological processes in type 1 diabetes, we observed anti-hypertrophic and anti-fibrotic properties of the compound. Pharmacological activation of sGC reduced hypertrophy on the histological/tissue level (decreased cardiomyocyte diameter) as well as on the molecular level (significantly reduced ANF gene expression, strong tendency towards reversed shift in β/α-MHC ratio). These results further confirm the data from a recent publication where cinaciguat has been proven to act as anti-hypertrophic and anti-fibrotic agent (Irvine et al. 2012). Another hallmark, fibrotic remodeling was also prevented by the application of this compound. Our data revealed that our treatment strategy improved MMP dysregulation (normalized MMP-9/TIMP-1 and MMP-2/TIMP-2 ratios) and decreased myocardial level of TGF-β1.

Several possible explanations are available for the above discussed anti-oxidative, anti-hypertrophic and anti-fibrotic properties. One of them is that cinaciguat and the subsequent activation of cGMP signaling might induce the down-regulation of NADPH-oxidases, as proposed by a recent experimental work (Koka et al. 2013). By reducing oxidative damage to the myocardium pathologically high levels of PDE5A reversed. This could have contributed to the accumulation of cGMP in the diabetic myocardium and plasma, too. The augmented cGMP production consequently reinforced the impaired PKG activity (increased myocardial p-VASP/VASP ratio) that further contributed to the protective effects of cinaciguat in T1DM. Regarding anti-fibrotic effects, a possible explanation could be the cross-talk of sGC-cGMP axis and TGF-β-dependent extracellular signal-regulated kinase pathway (Beyer et al. 2014).

Cinaciguat, via the activation of sGC, was able to improve diabetes mellitus-related cardiac dysfunction. Not only systolic function and contractility (increased PRSW, EF and SW) but also diastolic function (improved active relaxation and decreased LV stiffness) improved significantly (see Section 11.1. Bibliography of the candidate's publications – Articles II., IV.).

6.1.8. Effects of PDE5A inhibition by vardenafil on T2DM-associated heart failure

Improvement of NO-cGMP-PKG signaling by preserving intracellular cGMP levels could provide a useful tool in the treatment of heart failure. PDE5A inhibitors block one of the main regulator of cGMP degradation, the PDE5A enzyme. Thus, they are able to preserve or increase intracellular cGMP concentration (Zhao et al. 2016). Correspondingly, dysfunction of cardiomyocytes has been reported to predominate the initial phase of HFpEF thus improving cGMP signaling might be useful to reduce cardiomyocyte stiffness (Franssen et al. 2016b). On the other hand, sildenafil has been proven to exert anti-remodeling effect in diabetic cardiomyopathy in type 2 diabetic patients (Giannetta et al. 2012). Moreover, Koka et al. showed beneficial effects of tadalafil on systolic performance and mitochondrial function in the obese *db/db* mice (Koka et al. 2014). In spite of the promising preclinical data, a clinical trial that investigated beneficial effects of the PDE5A inhibitor sildenafil in HFpEF patients (RELAX Study) showed no improvement in exercise capacity and on the clinical outcomes in sildenafil treated HFpEF patients (Redfield et al. 2013). However, investigators reported that the plasma cGMP levels were not different between the study groups which might have contributed to the negative results.

In our study, vardenafil restored the activity of cGMP-PKG axis as indicated by increased plasma/cardiac cGMP concentrations and by the elevated p-VASP/VASP ratio. Through the improved cGMP signaling, vardenafil effectively reduced myocardial oxidative stress (as shown by reduced 3-NT staining of the myocardium and the decrease of catalase and thioredoxin-1) and subsequently reduced diabetes-associated DNA fragmentation and apoptosis (most probably via the inhibition of PARP1 cleavage). Besides, vardenafil treatment prevented the diabetes-related myocardial hypertrophy and fibrotic remodeling of the heart.

The protective properties of PDE5A inhibition might be attributed to its anti-oxidative effects (Dias-Junior et al. 2010) and to the restoration and enhancement of cGMP signaling (Radovits et al. 2009a) in the cardiomyocytes. Nevertheless, the above discussed regulatory cross-talk between the enhanced PKG signaling and the key members of cardiac remodeling like TGF-β signaling (Radovits et al. 2009a),

microvascular inflammation, endothelin-1, angiotensin II and aldosterone (Paulus et al. 2013) can be assumed in the background of the compound's anti-fibrotic effect. Our results are in correspondence with previous literature data that reported anti-hypertrophic and anti-fibrotic effects of PDE5A inhibition and enhanced cGMP signaling in an animal model of pathologic cardiac hypertrophy (Takimoto et al. 2005).
Regarding cardiac function in our type 2 DM model, we have shown that vardenafil treatment improved diastolic dysfunction both in vivo (decreased LV stiffness and improved Tau) and in vitro at the sarcomeric level (decreased cardiomyocyte $F_{passive}$) (see Section 11.1. Bibliography of the candidate's publications – Article I.).

7. Conclusions

Our present investigation confirmed that depending on its type, diabetes mellitus is associated with an impairment of cardiac function (mainly systolic dysfunction in type 1 while mainly diastolic dysfunction in type 2 DM). Moreover, different degree of nitro-oxidative stress, myocardial remodeling (fibrotic and hypertrophic) and apoptosis are present in the diabetic myocardium depending on the type of DM. Additionally, massive deterioration of the NO-sGC-cGMP-PKG signaling can be observed in the diabetic cardiomyocytes with the overexpression of the cGMP-degrading PDE5A enzyme, with lower intracellular levels of the second messenger cGMP and with dysfunctional PKG enzyme.

We found, however, that pharmacological modulation of the NO-sGC-cGMP pathway at different steps (sGC activation or PDE5A inhibition) has distinct cardioprotective effects in DM via the increase of intracellular cGMP and enhancement of PKG signaling. In the current studies we have shown that both the sGC activator cinaciguat and the PDE5A inhibitor vardenafil effectively raised intracellular/plasma cGMP levels and restored cGMP-PKG signaling in the myocardium without affecting blood glucose levels. These molecular changes were associated with attenuated cardiomyocyte hypertrophy, less severe fibrotic remodeling and markedly improved systolic and diastolic cardiac performance in our models. The underlying molecular effects of these beneficial properties might be a cross-talk with anti-oxidant, anti-hypertrophic and anti-fibrotic pathways in the diabetic myocardium.

Although many contributing factors have been identified in the progression of heart failure and in diabetic cardiomyopathy, in particular, we still lack drugs for optimal treatment of diabetic patients. Based on our results, a possible point of intervention might be to improve myocardial NO-sGC-cGMP-PKG signaling.

In conclusion, both sGC activation and PDE5A inhibiton were able to preserve myocardial function in diabetes mellitus. Thus, these compounds might provide a promising pharmacological treatment for patients suffering from diabetes-associated heart failure.

8. Summary

As a co-morbidity, DM is among the greatest contributors to the development of chronic HF. The dysfunctional metabolism in DM leads to the development of diabetic cardiomyopathy. Despite the knowledge we have gathered about the pathophysiological features (fibrotic, hypertrophic remodeling of the heart, nitro-oxidative stress, apoptosis and impairment of NO-sGC-cGMP-PKG pathway) of diabetic cardiomyopathy, the exact pathomechanism is still unknown.

Therefore, we aimed at investigating the pathophysiological differences of T1DM and T2DM related cardiomyopathy in different rat models. Thereafter, we have examined the possible cardioprotective features of stimulation of the cGMP-PKG pathway by different drugs including the sGC activator cinaciguat and the PDE5A inhibitor vardenafil.

We have shown in the first study that diabetic cardiomyopathy characterized by pathological remodeling of the heart for a different degree depending on the type of DM. T1DM was associated with more pronounced nitro-oxidative stress, more severe remodeling (fibrotic and hypertrophic) of the myocardium, more pronounced apoptosis and DNA injury that resulted in more severe cardiac dysfunction (systolic and diastolic dysfunction). In spite of that T2DM resulted in less severe nitro-oxidative stress, apoptosis and fibrosis while myocardial hypertrophy was comparable to T1DM and diastolic dysfunction (increased LV stiffness) developed with preserved systolic function.

We have shown for the first time that the sGC activator cinaciguat and the PDE5A inhibitor vardenafil exert cardioprotective effects in diabetic cardiomyopathy. Their potential beneficial effects include anti-oxidant, anti-apoptotic, anti-hypertrophic and anti-fibrotic properties. With the application of these compounds we were able to prevent the development of structural and molecular alterations in the diabetic myocardium and improve cardiac (including systolic and diastolic) function in both T1DM- and T2DM-associated cardiomyopathy.

Based on our results, sGC activation or PDE5A inhibition might be potential treatments alternatives for chronic heart failure in diabetic patients.

9. Összefoglalás

Diabétesz mellituszban a károsodott anyagcserefolyamatok eredményeként az ún. diabéteszes kardiomiopátia alakul ki. A diabéteszes kardiomiopátia patofiziológiájával kapcsolatban számos tény ismert (fibrotikus, hipertrofikus remodelláció, emelkedett nitro-oxidatív stressz, apoptózis és a NO-sGC-cGMP-PKG jelátvitel károsodása), ugyanakkor a betegség pontos patomechanizmusa még tisztázatlan.

Fentiek alapján jelen vizsgálatainkban célul tűztük ki mind az 1-es, mind pedig a 2-es típusú cukorbetegséghez társuló kardiomiopátia részletes patofiziológiai vizsgálatát állatmodelljeinkben. Továbbá vizsgáltuk a cGMP-PKG szignalizáció, sGC aktivátor illetve PDE5A inhibitor általi serkentésének lehetséges kardioprotektív hatásait patkánymodelljeinkben.

Kísérleteinkben igazoltuk, hogy a cukorbetegség típusától függően a szívizomzat remodellációja eltérő mértékű. T1DM-ben jelentősen emelkedett miokardiális nitro-oxidatív stresszt, a szív súlyos fokú fibrotikus, hipertrófiás átalakulását és fokozott apoptózis találtunk, mely jelentősebb kardiális (szisztolés és diasztolés) diszfunkcióval társult. Ezzel szemben T2DM esetén a nitro-oxidatív stressz, a fibrózis, az apoptózis és a DNS károsodás mértéke kevésbé volt kifejezett, míg a miokardium hipertrófiája hasonló mértékű volt T1DM-hez képest. Ehhez társultan megtartott szisztolés funkció mellett diasztolés diszfunkciót láttunk.

Munkánk során elsőként számoltunk be az sGC aktivátor cinaciguat és a PDE5A inhibitor vardenafil kardioprotektív hatásairól diabetészes kardiomiopátia modelljeinkben. A gyógyszerek potenciális előnyös hatásukat feltehetően antioxidáns, antiapoptotikus, antihipertrófiás ás antifibrotikus tulajdonságaiknak köszönhetik. A fenti szerek alkalmazásával mind a T1DM-hez, mind pedig a T2DM-hez társuló, a diabéteszes kardiomiopátiára jellemző strukturális és molekuláris elváltozások megelőzhetőek voltak. Ezek következményeként a szívizomzat szisztolés és diasztolés teljesítménye is számottevően javult a cukorbeteg állatokban.

Eredményeink alapján kijelenthetjük, hogy az sGC aktiváció és a PDE5A gátlás új terápiás alternatívák lehetnek a cukorbetegségben kialakuló krónikus szívelégtelenség kezelésében.

10. Bibliography

American Diabetes Association. (2016) 2. Classification and Diagnosis of Diabetes. Diabetes Care, 39 Suppl 1: S13-22.

American Diabetes Association. (2013) Economic costs of diabetes in the U.S. in 2012. Diabetes Care, 36(4): 1033-1046.

Bai P, Canto C. (2012) The role of PARP-1 and PARP-2 enzymes in metabolic regulation and disease. Cell Metab, 16(3): 290-295.

Begum N, Ragolia L. (2000) High glucose and insulin inhibit VSMC MKP-1 expression by blocking iNOS via p38 MAPK activation. Am J Physiol Cell Physiol, 278(1): C81-91.

Bernardo BC, Weeks KL, Pretorius L, McMullen JR. (2010) Molecular distinction between physiological and pathological cardiac hypertrophy: experimental findings and therapeutic strategies. Pharmacol Ther, 128(1): 191-227.

Beyer C, Zenzmaier C, Palumbo-Zerr K, Mancuso R, Distler A, Dees C, Zerr P, Huang J, Maier C, Pachowsky ML, Friebe A, Sandner P, Distler O, Schett G, Berger P, Distler JH. (2014) Stimulation of the soluble guanylate cyclase (sGC) inhibits fibrosis by blocking non-canonical TGFbeta signalling. Ann Rheum Dis, 74(7): 1408-1416.

Boudina S, Abel ED. (2007) Diabetic cardiomyopathy revisited. Circulation, 115(25): 3213-3223.

Boudina S, Abel ED. (2010) Diabetic cardiomyopathy, causes and effects. Rev Endocr Metab Disord, 11(1): 31-39.

Boudina S, Sena S, O'Neill BT, Tathireddy P, Young ME, Abel ED. (2005) Reduced mitochondrial oxidative capacity and increased mitochondrial uncoupling impair myocardial energetics in obesity. Circulation, 112(17): 2686-2695.

Bouloumie A, Bauersachs J, Linz W, Scholkens BA, Wiemer G, Fleming I, Busse R. (1997) Endothelial dysfunction coincides with an enhanced nitric oxide synthase expression and superoxide anion production. Hypertension, 30(4): 934-941.

Bugger H, Abel ED. (2014) Molecular mechanisms of diabetic cardiomyopathy. Diabetologia, 57(4): 660-671.

Burley DS, Ferdinandy P, Baxter GF. (2007) Cyclic GMP and protein kinase-G in myocardial ischaemia-reperfusion: opportunities and obstacles for survival signaling. Br J Pharmacol, 152(6): 855-869.

Cai L. (2006) Suppression of nitrative damage by metallothionein in diabetic heart contributes to the prevention of cardiomyopathy. Free Radic Biol Med, 41(6): 851-861.

Cai L, Kang YJ. (2003) Cell death and diabetic cardiomyopathy. Cardiovasc Toxicol, 3(3): 219-228.

Cai L, Li W, Wang G, Guo L, Jiang Y, Kang YJ. (2002) Hyperglycemia-induced apoptosis in mouse myocardium: mitochondrial cytochrome C-mediated caspase-3 activation pathway. Diabetes, 51(6): 1938-1948.

Chowdhry MF, Vohra HA, Galinanes M. (2007) Diabetes increases apoptosis and necrosis in both ischemic and nonischemic human myocardium: role of caspases and poly-adenosine diphosphate-ribose polymerase. J Thorac Cardiovasc Surg, 134(1): 124-131, 131 e121-123.

Cox EJ, Marsh SA. (2014) A systematic review of fetal genes as biomarkers of cardiac hypertrophy in rodent models of diabetes. PLoS One, 9(3): e92903.

Daniels A, Linz D, van Bilsen M, Rutten H, Sadowski T, Ruf S, Juretschke HP, Neumann-Haefelin C, Munts C, van der Vusse GJ, van Nieuwenhoven FA. (2012) Long-term severe diabetes only leads to mild cardiac diastolic dysfunction in Zucker diabetic fatty rats. Eur J Heart Fail, 14(2): 193-201.

Das A, Durrant D, Salloum FN, Xi L, Kukreja RC. (2015) PDE5 inhibitors as therapeutics for heart disease, diabetes and cancer. Pharmacol Ther, 147: 12-21.

Davidson KW, Burg M, Shimbo D. (2010) Endothelin-1 release and stimulation of the inflammatory cascade: is acute coronary syndrome triggered by watching spectator sports? J Am Coll Cardiol, 55(7): 643-644.

Desco MC, Asensi M, Marquez R, Martinez-Valls J, Vento M, Pallardo FV, Sastre J, Vina J. (2002) Xanthine oxidase is involved in free radical production in type 1 diabetes: protection by allopurinol. Diabetes, 51(4): 1118-1124.

Devereux RB, Roman MJ, Paranicas M, O'Grady MJ, Lee ET, Welty TK, Fabsitz RR, Robbins D, Rhoades ER, Howard BV. (2000) Impact of diabetes on cardiac structure and function: the strong heart study. Circulation, 101(19): 2271-2276.

Dias-Junior CA, Neto-Neves EM, Montenegro MF, Tanus-Santos JE. (2010) Hemodynamic effects of inducible nitric oxide synthase inhibition combined with sildenafil during acute pulmonary embolism. Nitric Oxide, 23(4): 284-288.

Eguchi K, Boden-Albala B, Jin Z, Rundek T, Sacco RL, Homma S, Di Tullio MR. (2008) Association between diabetes mellitus and left ventricular hypertrophy in a multiethnic population. Am J Cardiol, 101(12): 1787-1791.

Erdmann E, Semigran MJ, Nieminen MS, Gheorghiade M, Agrawal R, Mitrovic V, Mebazaa A. (2013) Cinaciguat, a soluble guanylate cyclase activator, unloads the heart

but also causes hypotension in acute decompensated heart failure. Eur Heart J, 34(1): 57-67.

Evgenov OV, Pacher P, Schmidt PM, Hasko G, Schmidt HH, Stasch JP. (2006) NO-independent stimulators and activators of soluble guanylate cyclase: discovery and therapeutic potential. Nat Rev Drug Discov, 5(9): 755-768.

Fabiato A, Fabiato F. (1979) Calculator programs for computing the composition of the solutions containing multiple metals and ligands used for experiments in skinned muscle cells. J Physiol (Paris), 75(5): 463-505.

Fang L, Radovits T, Szabo G, Mozes MM, Rosivall L, Kokeny G. (2013) Selective phosphodiesterase-5 (PDE-5) inhibitor vardenafil ameliorates renal damage in type 1 diabetic rats by restoring cyclic 3',5' guanosine monophosphate (cGMP) level in podocytes. Nephrol Dial Transplant, 28(7): 1751-1761.

Fang ZY, Schull-Meade R, Leano R, Mottram PM, Prins JB, Marwick TH. (2005) Screening for heart disease in diabetic subjects. Am Heart J, 149(2): 349-354.

Farhangkhoee H, Khan ZA, Kaur H, Xin X, Chen S, Chakrabarti S. (2006) Vascular endothelial dysfunction in diabetic cardiomyopathy: pathogenesis and potential treatment targets. Pharmacol Ther, 111(2): 384-399.

Fiedler B, Feil R, Hofmann F, Willenbockel C, Drexler H, Smolenski A, Lohmann SM, Wollert KC. (2006) cGMP-dependent protein kinase type I inhibits TAB1-p38 mitogen-activated protein kinase apoptosis signaling in cardiac myocytes. J Biol Chem, 281(43): 32831-32840.

Fiedler B, Lohmann SM, Smolenski A, Linnemuller S, Pieske B, Schroder F, Molkentin JD, Drexler H, Wollert KC. (2002) Inhibition of calcineurin-NFAT hypertrophy signaling by cGMP-dependent protein kinase type I in cardiac myocytes. Proc Natl Acad Sci U S A, 99(17): 11363-11368.

Fiordaliso F, Li B, Latini R, Sonnenblick EH, Anversa P, Leri A, Kajstura J. (2000) Myocyte death in streptozotocin-induced diabetes in rats in angiotensin II- dependent. Lab Invest, 80(4): 513-527.

Fontbonne A, Charles MA, Thibult N, Richard JL, Claude JR, Warnet JM, Rosselin GE, Eschwege E. (1991) Hyperinsulinaemia as a predictor of coronary heart disease mortality in a healthy population: the Paris Prospective Study, 15-year follow-up. Diabetologia, 34(5): 356-361.

Franssen C, Chen S, Unger A, Korkmaz HI, De Keulenaer GW, Tschope C, Leite-Moreira AF, Musters R, Niessen HW, Linke WA, Paulus WJ, Hamdani N. (2016a) Myocardial Microvascular Inflammatory Endothelial Activation in Heart Failure With Preserved Ejection Fraction. JACC Heart Fail, 4(4): 312-324.

Franssen C, Gonzalez Miqueo A. (2016b) The role of titin and extracellular matrix remodelling in heart failure with preserved ejection fraction. Neth Heart J, 24(4): 259-267.

Fredersdorf S, Thumann C, Ulucan C, Griese DP, Luchner A, Riegger GA, Kromer EP, Weil J. (2004) Myocardial hypertrophy and enhanced left ventricular contractility in Zucker diabetic fatty rats. Cardiovasc Pathol, 13(1): 11-19.

Frey R, Muck W, Unger S, Artmeier-Brandt U, Weimann G, Wensing G. (2008) Pharmacokinetics, pharmacodynamics, tolerability, and safety of the soluble guanylate cyclase activator cinaciguat (BAY 58-2667) in healthy male volunteers. J Clin Pharmacol, 48(12): 1400-1410.

Frustaci A, Kajstura J, Chimenti C, Jakoniuk I, Leri A, Maseri A, Nadal-Ginard B, Anversa P. (2000) Myocardial cell death in human diabetes. Circ Res, 87(12): 1123-1132.

Fulop N, Mason MM, Dutta K, Wang P, Davidoff AJ, Marchase RB, Chatham JC. (2007) Impact of Type 2 diabetes and aging on cardiomyocyte function and O-linked N-acetylglucosamine levels in the heart. Am J Physiol Cell Physiol, 292(4): C1370-1378.

Gao X, Xu Y, Xu B, Liu Y, Cai J, Liu HM, Lei S, Zhong YQ, Irwin MG, Xia Z. (2012) Allopurinol attenuates left ventricular dysfunction in rats with early stages of streptozotocin-induced diabetes. Diabetes Metab Res Rev, 28(5): 409-417.

Garcia Soriano F, Virag L, Jagtap P, Szabo E, Mabley JG, Liaudet L, Marton A, Hoyt DG, Murthy KG, Salzman AL, Southan GJ, Szabo C. (2001) Diabetic endothelial dysfunction: the role of poly(ADP-ribose) polymerase activation. Nat Med, 7(1): 108-113.

Gheorghiade M, Greene SJ, Filippatos G, Erdmann E, Ferrari R, Levy PD, Maggioni A, Nowack C, Mebazaa A, Investigators C, Coordinators. (2012) Cinaciguat, a soluble guanylate cyclase activator: results from the randomized, controlled, phase IIb COMPOSE programme in acute heart failure syndromes. Eur J Heart Fail, 14(9): 1056-1066.

Giacco F, Brownlee M. (2010) Oxidative stress and diabetic complications. Circ Res, 107(9): 1058-1070.

Giannetta E, Isidori AM, Galea N, Carbone I, Mandosi E, Vizza CD, Naro F, Morano S, Fedele F, Lenzi A. (2012) Chronic Inhibition of cGMP phosphodiesterase 5A improves diabetic cardiomyopathy: a randomized, controlled clinical trial using magnetic resonance imaging with myocardial tagging. Circulation, 125(19): 2323-2333.

Gonzalez A, Ravassa S, Beaumont J, Lopez B, Diez J. (2011) New targets to treat the structural remodeling of the myocardium. J Am Coll Cardiol, 58(18): 1833-1843.

Hamet P, Pang SC, Tremblay J. (1989) Atrial natriuretic factor-induced egression of cyclic guanosine 3':5'-monophosphate in cultured vascular smooth muscle and endothelial cells. J Biol Chem, 264(21): 12364-12369.

Hirschberg K, Radovits T, Loganathan S, Entz L, Beller CJ, Gross ML, Sandner P, Karck M, Szabo G. (2009) Selective phosphodiesterase-5 inhibition reduces neointimal hyperplasia in rat carotid arteries after surgical endarterectomy. J Thorac Cardiovasc Surg, 137(6): 1508-1514.

Hirschberg K, Tarcea V, Pali S, Barnucz E, Gwanmesia PN, Korkmaz S, Radovits T, Loganathan S, Merkely B, Karck M, Szabo G. (2013) Cinaciguat prevents neointima formation after arterial injury by decreasing vascular smooth muscle cell migration and proliferation. Int J Cardiol, 167(2): 470-477.

Hoeldtke RD, Bryner KD, McNeill DR, Hobbs GR, Baylis C. (2003) Peroxynitrite versus nitric oxide in early diabetes. Am J Hypertens, 16(9 Pt 1): 761-766.

Hopkins TA, Sugden MC, Holness MJ, Kozak R, Dyck JR, Lopaschuk GD. (2003) Control of cardiac pyruvate dehydrogenase activity in peroxisome proliferator-activated receptor-alpha transgenic mice. Am J Physiol Heart Circ Physiol, 285(1): H270-276.

Huynh K, Bernardo BC, McMullen JR, Ritchie RH. (2014) Diabetic cardiomyopathy: mechanisms and new treatment strategies targeting antioxidant signaling pathways. Pharmacol Ther, 142(3): 375-415.

Huynh K, Kiriazis H, Du XJ, Love JE, Gray SP, Jandeleit-Dahm KA, McMullen JR, Ritchie RH. (2013) Targeting the upregulation of reactive oxygen species subsequent to hyperglycemia prevents type 1 diabetic cardiomyopathy in mice. Free Radic Biol Med, 60: 307-317.

Irvine JC, Ganthavee V, Love JE, Alexander AE, Horowitz JD, Stasch JP, Kemp-Harper BK, Ritchie RH. (2012) The soluble guanylyl cyclase activator bay 58-2667 selectively limits cardiomyocyte hypertrophy. PLoS One, 7(11): e44481.

Joffe, II, Travers KE, Perreault-Micale CL, Hampton T, Katz SE, Morgan JP, Douglas PS. (1999) Abnormal cardiac function in the streptozotocin-induced non-insulin-dependent diabetic rat: noninvasive assessment with doppler echocardiography and contribution of the nitric oxide pathway. J Am Coll Cardiol, 34(7): 2111-2119.

Kajstura J, Fiordaliso F, Andreoli AM, Li B, Chimenti S, Medow MS, Limana F, Nadal-Ginard B, Leri A, Anversa P. (2001) IGF-1 overexpression inhibits the development of diabetic cardiomyopathy and angiotensin II-mediated oxidative stress. Diabetes, 50(6): 1414-1424.

Kiowski W, Sutsch G, Hunziker P, Muller P, Kim J, Oechslin E, Schmitt R, Jones R, Bertel O. (1995) Evidence for endothelin-1-mediated vasoconstriction in severe chronic heart failure. Lancet, 346(8977): 732-736.

Koitabashi N, Aiba T, Hesketh GG, Rowell J, Zhang M, Takimoto E, Tomaselli GF, Kass DA. (2010) Cyclic GMP/PKG-dependent inhibition of TRPC6 channel activity and expression negatively regulates cardiomyocyte NFAT activation Novel mechanism of cardiac stress modulation by PDE5 inhibition. J Mol Cell Cardiol, 48(4): 713-724.

Koka S, Aluri HS, Xi L, Lesnefsky EJ, Kukreja RC. (2014) Chronic inhibition of phosphodiesterase 5 with tadalafil attenuates mitochondrial dysfunction in type 2 diabetic hearts: potential role of NO/SIRT1/PGC-1alpha signaling. Am J Physiol Heart Circ Physiol, 306(11): H1558-1568.

Koka S, Das A, Salloum FN, Kukreja RC. (2013) Phosphodiesterase-5 inhibitor tadalafil attenuates oxidative stress and protects against myocardial ischemia/reperfusion injury in type 2 diabetic mice. Free Radic Biol Med, 60: 80-88.

Korkmaz-Icoz S, Al Said S, Radovits T, Li S, Brune M, Hegedus P, Atmanli A, Ruppert M, Brlecic P, Lehmann LH, Lahrmann B, Grabe N, Yoshikawa Y, Yasui H, Most P, Karck M, Szabo G. (2016) Oral treatment with a zinc complex of acetylsalicylic acid prevents diabetic cardiomyopathy in a rat model of type-2 diabetes: activation of the Akt pathway. Cardiovasc Diabetol, 15: 75.

Korkmaz-Icoz S, Radovits T, Szabo G. (2017) Targeting phosphodiesterase 5 as a therapeutic option against myocardial ischaemia/reperfusion injury and for treating heart failure. Br J Pharmacol.

Korkmaz S, Loganathan S, Mikles B, Radovits T, Barnucz E, Hirschberg K, Li S, Hegedus P, Pali S, Weymann A, Karck M, Szabo G. (2013) Nitric oxide- and heme-independent activation of soluble guanylate cyclase attenuates peroxynitrite-induced endothelial dysfunction in rat aorta. J Cardiovasc Pharmacol Ther, 18(1): 70-77.

Korkmaz S, Radovits T, Barnucz E, Hirschberg K, Neugebauer P, Loganathan S, Veres G, Pali S, Seidel B, Zollner S, Karck M, Szabo G. (2009) Pharmacological activation of soluble guanylate cyclase protects the heart against ischemic injury. Circulation, 120(8): 677-686.

Kovacs A, Alogna A, Post H, Hamdani N. (2016) Is enhancing cGMP-PKG signalling a promising therapeutic target for heart failure with preserved ejection fraction? Neth Heart J, 24(4): 268-274.

Kuhn M. (2003) Structure, regulation, and function of mammalian membrane guanylyl cyclase receptors, with a focus on guanylyl cyclase-A. Circ Res, 93(8): 700-709.

Kukreja RC, Ockaili R, Salloum F, Yin C, Hawkins J, Das A, Xi L. (2004) Cardioprotection with phosphodiesterase-5 inhibition--a novel preconditioning strategy. J Mol Cell Cardiol, 36(2): 165-173.

Kukreja RC, Salloum FN, Das A. (2012) Cyclic guanosine monophosphate signaling and phosphodiesterase-5 inhibitors in cardioprotection. J Am Coll Cardiol, 59(22): 1921-1927.

Kukreja RC, Salloum FN, Das A, Koka S, Ockaili RA, Xi L. (2011) Emerging new uses of phosphodiesterase-5 inhibitors in cardiovascular diseases. Exp Clin Cardiol, 16(4): e30-35.

Lainchbury JG, Burnett JC, Jr., Meyer D, Redfield MM. (2000) Effects of natriuretic peptides on load and myocardial function in normal and heart failure dogs. Am J Physiol Heart Circ Physiol, 278(1): H33-40.

Lapp H, Mitrovic V, Franz N, Heuer H, Buerke M, Wolfertz J, Mueck W, Unger S, Wensing G, Frey R. (2009) Cinaciguat (BAY 58-2667) improves cardiopulmonary hemodynamics in patients with acute decompensated heart failure. Circulation, 119(21): 2781-2788.

Lee DI, Vahebi S, Tocchetti CG, Barouch LA, Solaro RJ, Takimoto E, Kass DA. (2010) PDE5A suppression of acute beta-adrenergic activation requires modulation of myocyte beta-3 signaling coupled to PKG-mediated troponin I phosphorylation. Basic Res Cardiol, 105(3): 337-347.

Lee DI, Zhu G, Sasaki T, Cho GS, Hamdani N, Holewinski R, Jo SH, Danner T, Zhang M, Rainer PP, Bedja D, Kirk JA, Ranek MJ, Dostmann WR, Kwon C, Margulies KB, Van Eyk JE, Paulus WJ, Takimoto E, Kass DA. (2015) Phosphodiesterase 9A controls nitric-oxide-independent cGMP and hypertrophic heart disease. Nature, 519(7544): 472-476.

Lender D, Arauz-Pacheco C, Adams-Huet B, Raskin P. (1997) Essential hypertension is associated with decreased insulin clearance and insulin resistance. Hypertension, 29(1 Pt 1): 111-114.

Levy PD, Laribi S, Mebazaa A. (2014) Vasodilators in Acute Heart Failure: Review of the Latest Studies. Curr Emerg Hosp Med Rep, 2(2): 126-132.

Litwin SE, Raya TE, Anderson PG, Daugherty S, Goldman S. (1990) Abnormal cardiac function in the streptozotocin-diabetic rat. Changes in active and passive properties of the left ventricle. J Clin Invest, 86(2): 481-488.

Loganathan S, Radovits T, Hirschberg K, Korkmaz S, Barnucz E, Karck M, Szabo G. (2008) Effects of selective phosphodiesterase-5-inhibition on myocardial contractility and reperfusion injury after heart transplantation. Transplantation, 86(10): 1414-1418.

Loo DT. (2011) In situ detection of apoptosis by the TUNEL assay: an overview of techniques. Methods Mol Biol, 682: 3-13.

Lu Z, Xu X, Hu X, Lee S, Traverse JH, Zhu G, Fassett J, Tao Y, Zhang P, dos Remedios C, Pritzker M, Hall JL, Garry DJ, Chen Y. (2010) Oxidative stress regulates left ventricular PDE5 expression in the failing heart. Circulation, 121(13): 1474-1483.

Lukowski R, Krieg T, Rybalkin SD, Beavo J, Hofmann F. (2014) Turning on cGMP-dependent pathways to treat cardiac dysfunctions: boom, bust, and beyond. Trends Pharmacol Sci, 35(8): 404-413.

Maalouf RM, Eid AA, Gorin YC, Block K, Escobar GP, Bailey S, Abboud HE. (2012) Nox4-derived reactive oxygen species mediate cardiomyocyte injury in early type 1 diabetes. Am J Physiol Cell Physiol, 302(3): C597-604.

Marsh SA, Powell PC, Agarwal A, Dell'Italia LJ, Chatham JC. (2007) Cardiovascular dysfunction in Zucker obese and Zucker diabetic fatty rats: role of hydronephrosis. Am J Physiol Heart Circ Physiol, 293(1): H292-298.

McGavock JM, Victor RG, Unger RH, Szczepaniak LS, American College of P, the American Physiological S. (2006) Adiposity of the heart, revisited. Ann Intern Med, 144(7): 517-524.

Min W, Bin ZW, Quan ZB, Hui ZJ, Sheng FG. (2009) The signal transduction pathway of PKC/NF-kappa B/c-fos may be involved in the influence of high glucose on the cardiomyocytes of neonatal rats. Cardiovasc Diabetol, 8: 8.

Mizushige K, Yao L, Noma T, Kiyomoto H, Yu Y, Hosomi N, Ohmori K, Matsuo H. (2000) Alteration in left ventricular diastolic filling and accumulation of myocardial collagen at insulin-resistant prediabetic stage of a type II diabetic rat model. Circulation, 101(8): 899-907.

Moncada S, Palmer RM, Higgs EA. (1991) Nitric oxide: physiology, pathophysiology, and pharmacology. Pharmacol Rev, 43(2): 109-142.

Mosterd A, Hoes AW. (2007) Clinical epidemiology of heart failure. Heart, 93(9): 1137-1146.

Mourmoura E, Vial G, Laillet B, Rigaudiere JP, Hininger-Favier I, Dubouchaud H, Morio B, Demaison L. (2013) Preserved endothelium-dependent dilatation of the coronary microvasculature at the early phase of diabetes mellitus despite the increased oxidative stress and depressed cardiac mechanical function ex vivo. Cardiovasc Diabetol, 12: 49.

Murthy VK, Shipp JC. (1977) Accumulation of myocardial triglycerides ketotic diabetes; evidence for increased biosynthesis. Diabetes, 26(3): 222-229.

Nadruz W, Jr., Corat MA, Marin TM, Guimaraes Pereira GA, Franchini KG. (2005) Focal adhesion kinase mediates MEF2 and c-Jun activation by stretch: role in the activation of the cardiac hypertrophic genetic program. Cardiovasc Res, 68(1): 87-97.

Nagendran J, Archer SL, Soliman D, Gurtu V, Moudgil R, Haromy A, St Aubin C, Webster L, Rebeyka IM, Ross DB, Light PE, Dyck JR, Michelakis ED. (2007) Phosphodiesterase type 5 is highly expressed in the hypertrophied human right ventricle, and acute inhibition of phosphodiesterase type 5 improves contractility. Circulation, 116(3): 238-248.

Nemeth BT, Matyas C, Olah A, Lux A, Hidi L, Ruppert M, Kellermayer D, Kokeny G, Szabo G, Merkely B, Radovits T. (2016) Cinaciguat prevents the development of pathologic hypertrophy in a rat model of left ventricular pressure overload. Sci Rep, 6: 37166.

Oakes ND, Thalen P, Aasum E, Edgley A, Larsen T, Furler SM, Ljung B, Severson D. (2006) Cardiac metabolism in mice: tracer method developments and in vivo application revealing profound metabolic inflexibility in diabetes. Am J Physiol Endocrinol Metab, 290(5): E870-881.

Pacher P, Beckman JS, Liaudet L. (2007) Nitric oxide and peroxynitrite in health and disease. Physiol Rev, 87(1): 315-424.

Pacher P, Liaudet L, Soriano FG, Mabley JG, Szabo E, Szabo C. (2002) The role of poly(ADP-ribose) polymerase activation in the development of myocardial and endothelial dysfunction in diabetes. Diabetes, 51(2): 514-521.

Pacher P, Nagayama T, Mukhopadhyay P, Batkai S, Kass DA. (2008) Measurement of cardiac function using pressure-volume conductance catheter technique in mice and rats. Nat Protoc, 3(9): 1422-1434.

Pacher P, Szabo C. (2005) Role of poly(ADP-ribose) polymerase-1 activation in the pathogenesis of diabetic complications: endothelial dysfunction, as a common underlying theme. Antioxid Redox Signal, 7(11-12): 1568-1580.

Papp Z, Szabo A, Barends JP, Stienen GJ. (2002) The mechanism of the force enhancement by MgADP under simulated ischaemic conditions in rat cardiac myocytes. J Physiol, 543(Pt 1): 177-189.

Paulus WJ, Tschope C. (2013) A novel paradigm for heart failure with preserved ejection fraction: comorbidities drive myocardial dysfunction and remodeling through coronary microvascular endothelial inflammation. J Am Coll Cardiol, 62(4): 263-271.

Pearson JT, Jenkins MJ, Edgley AJ, Sonobe T, Joshi M, Waddingham MT, Fujii Y, Schwenke DO, Tsuchimochi H, Yoshimoto M, Umetani K, Kelly DJ, Shirai M. (2013) Acute Rho-kinase inhibition improves coronary dysfunction in vivo, in the early diabetic microcirculation. Cardiovasc Diabetol, 12: 111.

Poirier P, Bogaty P, Garneau C, Marois L, Dumesnil JG. (2001) Diastolic dysfunction in normotensive men with well-controlled type 2 diabetes: importance of maneuvers in echocardiographic screening for preclinical diabetic cardiomyopathy. Diabetes Care, 24(1): 5-10.

Pokreisz P, Vandenwijngaert S, Bito V, Van den Bergh A, Lenaerts I, Busch C, Marsboom G, Gheysens O, Vermeersch P, Biesmans L, Liu X, Gillijns H, Pellens M, Van Lommel A, Buys E, Schoonjans L, Vanhaecke J, Verbeken E, Sipido K, Herijgers P, Bloch KD, Janssens SP. (2009) Ventricular phosphodiesterase-5 expression is increased in patients with advanced heart failure and contributes to adverse ventricular remodeling after myocardial infarction in mice. Circulation, 119(3): 408-416.

Ponikowski P, Voors AA, Anker SD, Bueno H, Cleland JG, Coats AJ, Falk V, Gonzalez-Juanatey JR, Harjola VP, Jankowska EA, Jessup M, Linde C, Nihoyannopoulos P, Parissis JT, Pieske B, Riley JP, Rosano GM, Ruilope LM, Ruschitzka F, Rutten FH, van der Meer P, Authors/Task Force M, Document R. (2016) 2016 ESC Guidelines for the diagnosis and treatment of acute and chronic heart failure: The Task Force for the diagnosis and treatment of acute and chronic heart failure of the

European Society of Cardiology (ESC)Developed with the special contribution of the Heart Failure Association (HFA) of the ESC. Eur Heart J.

Privratsky JR, Wold LE, Sowers JR, Quinn MT, Ren J. (2003) AT1 blockade prevents glucose-induced cardiac dysfunction in ventricular myocytes: role of the AT1 receptor and NADPH oxidase. Hypertension, 42(2): 206-212.

Radovits T, Bomicke T, Kokeny G, Arif R, Loganathan S, Kecsan K, Korkmaz S, Barnucz E, Sandner P, Karck M, Szabo G. (2009a) The phosphodiesterase-5 inhibitor vardenafil improves cardiovascular dysfunction in experimental diabetes mellitus. Br J Pharmacol, 156(6): 909-919.

Radovits T, Korkmaz S, Loganathan S, Barnucz E, Bomicke T, Arif R, Karck M, Szabo G. (2009b) Comparative investigation of the left ventricular pressure-volume relationship in rat models of type 1 and type 2 diabetes mellitus. Am J Physiol Heart Circ Physiol, 297(1): H125-133.

Radovits T, Korkmaz S, Miesel-Groschel C, Seidel B, Stasch JP, Merkely B, Karck M, Szabo G. (2011) Pre-conditioning with the soluble guanylate cyclase activator Cinaciguat reduces ischaemia-reperfusion injury after cardiopulmonary bypass. Eur J Cardiothorac Surg, 39(2): 248-255.

Rajesh M, Batkai S, Kechrid M, Mukhopadhyay P, Lee WS, Horvath B, Holovac E, Cinar R, Liaudet L, Mackie K, Hasko G, Pacher P. (2012) Cannabinoid 1 receptor promotes cardiac dysfunction, oxidative stress, inflammation, and fibrosis in diabetic cardiomyopathy. Diabetes, 61(3): 716-727.

Rajesh M, Mukhopadhyay P, Batkai S, Mukhopadhyay B, Patel V, Hasko G, Szabo C, Mabley JG, Liaudet L, Pacher P. (2009) Xanthine oxidase inhibitor allopurinol attenuates the development of diabetic cardiomyopathy. J Cell Mol Med, 13(8B): 2330-2341.

Rajesh M, Mukhopadhyay P, Batkai S, Patel V, Saito K, Matsumoto S, Kashiwaya Y, Horvath B, Mukhopadhyay B, Becker L, Hasko G, Liaudet L, Wink DA, Veves A, Mechoulam R, Pacher P. (2010) Cannabidiol attenuates cardiac dysfunction, oxidative stress, fibrosis, and inflammatory and cell death signaling pathways in diabetic cardiomyopathy. J Am Coll Cardiol, 56(25): 2115-2125.

Ramirez E, Klett-Mingo M, Ares-Carrasco S, Picatoste B, Ferrarini A, Ruperez FJ, Caro-Vadillo A, Barbas C, Egido J, Tunon J, Lorenzo O. (2013) Eplerenone attenuated cardiac steatosis, apoptosis and diastolic dysfunction in experimental type-II diabetes. Cardiovasc Diabetol, 12: 172.

Redfield MM, Chen HH, Borlaug BA, Semigran MJ, Lee KL, Lewis G, LeWinter MM, Rouleau JL, Bull DA, Mann DL, Deswal A, Stevenson LW, Givertz MM, Ofili EO, O'Connor CM, Felker GM, Goldsmith SR, Bart BA, McNulty SE, Ibarra JC, Lin G, Oh JK, Patel MR, Kim RJ, Tracy RP, Velazquez EJ, Anstrom KJ, Hernandez AF, Mascette AM, Braunwald E, Trial R. (2013) Effect of phosphodiesterase-5 inhibition on exercise capacity and clinical status in heart failure with preserved ejection fraction: a randomized clinical trial. JAMA, 309(12): 1268-1277.

Rijzewijk LJ, van der Meer RW, Lamb HJ, de Jong HW, Lubberink M, Romijn JA, Bax JJ, de Roos A, Twisk JW, Heine RJ, Lammertsma AA, Smit JW, Diamant M. (2009) Altered myocardial substrate metabolism and decreased diastolic function in nonischemic human diabetic cardiomyopathy: studies with cardiac positron emission tomography and magnetic resonance imaging. J Am Coll Cardiol, 54(16): 1524-1532.

Roe ND, Thomas DP, Ren J. (2011) Inhibition of NADPH oxidase alleviates experimental diabetes-induced myocardial contractile dysfunction. Diabetes Obes Metab, 13(5): 465-473.

Ross SA, Tildesley HD, Ashkenas J. (2011) Barriers to effective insulin treatment: the persistence of poor glycemic control in type 2 diabetes. Curr Med Res Opin, 27 Suppl 3: 13-20.

Saenz de Tejada I, Angulo J, Cuevas P, Fernandez A, Moncada I, Allona A, Lledo E, Korschen HG, Niewohner U, Haning H, Pages E, Bischoff E. (2001) The phosphodiesterase inhibitory selectivity and the in vitro and in vivo potency of the new PDE5 inhibitor vardenafil. Int J Impot Res, 13(5): 282-290.

Salloum FN, Das A, Samidurai A, Hoke NN, Chau VQ, Ockaili RA, Stasch JP, Kukreja RC. (2012) Cinaciguat, a novel activator of soluble guanylate cyclase, protects against ischemia/reperfusion injury: role of hydrogen sulfide. Am J Physiol Heart Circ Physiol, 302(6): H1347-1354.

Schafer A, Fraccarollo D, Pfortsch S, Flierl U, Vogt C, Pfrang J, Kobsar A, Renne T, Eigenthaler M, Ertl G, Bauersachs J. (2008) Improvement of vascular function by acute and chronic treatment with the PDE-5 inhibitor sildenafil in experimental diabetes mellitus. Br J Pharmacol, 153(5): 886-893.

Schannwell CM, Schneppenheim M, Perings S, Plehn G, Strauer BE. (2002) Left ventricular diastolic dysfunction as an early manifestation of diabetic cardiomyopathy. Cardiology, 98(1-2): 33-39.

Semeniuk LM, Kryski AJ, Severson DL. (2002) Echocardiographic assessment of cardiac function in diabetic db/db and transgenic db/db-hGLUT4 mice. Am J Physiol Heart Circ Physiol, 283(3): H976-982.

Sharma V, McNeill JH. (2006) Diabetic cardiomyopathy: where are we 40 years later? Can J Cardiol, 22(4): 305-308.

Shen X, Zheng S, Metreveli NS, Epstein PN. (2006) Protection of cardiac mitochondria by overexpression of MnSOD reduces diabetic cardiomyopathy. Diabetes, 55(3): 798-805.

Shepherd DL, Nichols CE, Croston TL, McLaughlin SL, Petrone AB, Lewis SE, Thapa D, Long DM, Dick GM, Hollander JM. (2016) Early detection of cardiac dysfunction in the type 1 diabetic heart using speckle-tracking based strain imaging. J Mol Cell Cardiol, 90: 74-83.

Shimizu M, Umeda K, Sugihara N, Yoshio H, Ino H, Takeda R, Okada Y, Nakanishi I. (1993) Collagen remodelling in myocardia of patients with diabetes. J Clin Pathol, 46(1): 32-36.

Silva BR, Pernomian L, Bendhack LM. (2012) Contribution of oxidative stress to endothelial dysfunction in hypertension. Front Physiol, 3: 441.

Snoeckx LH, Cornelussen RN, Van Nieuwenhoven FA, Reneman RS, Van Der Vusse GJ. (2001) Heat shock proteins and cardiovascular pathophysiology. Physiol Rev, 81(4): 1461-1497.

Song D, Kuo KH, Yao R, Hutchings SR, Pang CC. (2008) Inducible nitric oxide synthase depresses cardiac contractile function in Zucker diabetic fatty rats. Eur J Pharmacol, 579(1-3): 253-259.

Soriano FG, Pacher P, Mabley J, Liaudet L, Szabo C. (2001) Rapid reversal of the diabetic endothelial dysfunction by pharmacological inhibition of poly(ADP-ribose) polymerase. Circ Res, 89(8): 684-691.

Stadler K. (2011) Peroxynitrite-driven mechanisms in diabetes and insulin resistance - the latest advances. Curr Med Chem, 18(2): 280-290.

Stanley WC, Lopaschuk GD, McCormack JG. (1997) Regulation of energy substrate metabolism in the diabetic heart. Cardiovasc Res, 34(1): 25-33.

Stasch JP, Pacher P, Evgenov OV. (2011) Soluble guanylate cyclase as an emerging therapeutic target in cardiopulmonary disease. Circulation, 123(20): 2263-2273.

Stasch JP, Schmidt PM, Nedvetsky PI, Nedvetskaya TY, H SA, Meurer S, Deile M, Taye A, Knorr A, Lapp H, Muller H, Turgay Y, Rothkegel C, Tersteegen A, Kemp-Harper B, Muller-Esterl W, Schmidt HH. (2006) Targeting the heme-oxidized nitric oxide receptor for selective vasodilatation of diseased blood vessels. J Clin Invest, 116(9): 2552-2561.

Szabo G, Radovits T, Veres G, Krieger N, Loganathan S, Sandner P, Karck M. (2009) Vardenafil protects against myocardial and endothelial injuries after cardiopulmonary bypass. Eur J Cardiothorac Surg, 36(4): 657-664.

Tabish SA. (2007) Is Diabetes Becoming the Biggest Epidemic of the Twenty-first Century? Int J Health Sci (Qassim), 1(2): V-VIII.

Takimoto E. (2012) Cyclic GMP-dependent signaling in cardiac myocytes. Circ J, 76(8): 1819-1825.

Takimoto E, Champion HC, Li M, Belardi D, Ren S, Rodriguez ER, Bedja D, Gabrielson KL, Wang Y, Kass DA. (2005) Chronic inhibition of cyclic GMP phosphodiesterase 5A prevents and reverses cardiac hypertrophy. Nat Med, 11(2): 214-222.

Takimoto E, Koitabashi N, Hsu S, Ketner EA, Zhang M, Nagayama T, Bedja D, Gabrielson KL, Blanton R, Siderovski DP, Mendelsohn ME, Kass DA. (2009) Regulator of G protein signaling 2 mediates cardiac compensation to pressure overload and antihypertrophic effects of PDE5 inhibition in mice. J Clin Invest, 119(2): 408-420.

Taye A, Abouzied MM, Mohafez OM. (2013) Tempol ameliorates cardiac fibrosis in streptozotocin-induced diabetic rats: role of oxidative stress in diabetic cardiomyopathy. Naunyn Schmiedebergs Arch Pharmacol, 386(12): 1071-1080.

Tokudome T, Horio T, Yoshihara F, Suga S, Kawano Y, Kohno M, Kangawa K. (2004) Direct effects of high glucose and insulin on protein synthesis in cultured cardiac myocytes and DNA and collagen synthesis in cardiac fibroblasts. Metabolism, 53(6): 710-715.

Tsai EJ, Kass DA. (2009) Cyclic GMP signaling in cardiovascular pathophysiology and therapeutics. Pharmacol Ther, 122(3): 216-238.

Turko IV, Li L, Aulak KS, Stuehr DJ, Chang JY, Murad F. (2003a) Protein tyrosine nitration in the mitochondria from diabetic mouse heart. Implications to dysfunctional mitochondria in diabetes. J Biol Chem, 278(36): 33972-33977.

Turko IV, Murad F. (2003b) Quantitative protein profiling in heart mitochondria from diabetic rats. J Biol Chem, 278(37): 35844-35849.

Van den Bergh A, Flameng W, Herijgers P. (2006) Type II diabetic mice exhibit contractile dysfunction but maintain cardiac output by favourable loading conditions. Eur J Heart Fail, 8(8): 777-783.

van Heerebeek L, Hamdani N, Falcao-Pires I, Leite-Moreira AF, Begieneman MP, Bronzwaer JG, van der Velden J, Stienen GJ, Laarman GJ, Somsen A, Verheugt FW, Niessen HW, Paulus WJ. (2012) Low myocardial protein kinase G activity in heart failure with preserved ejection fraction. Circulation, 126(7): 830-839.

van Heerebeek L, Hamdani N, Handoko ML, Falcao-Pires I, Musters RJ, Kupreishvili K, Ijsselmuiden AJ, Schalkwijk CG, Bronzwaer JG, Diamant M, Borbely A, van der Velden J, Stienen GJ, Laarman GJ, Niessen HW, Paulus WJ. (2008) Diastolic stiffness of the failing diabetic heart: importance of fibrosis, advanced glycation end products, and myocyte resting tension. Circulation, 117(1): 43-51.

Van Linthout S, Seeland U, Riad A, Eckhardt O, Hohl M, Dhayat N, Richter U, Fischer JW, Bohm M, Pauschinger M, Schultheiss HP, Tschope C. (2008) Reduced MMP-2

activity contributes to cardiac fibrosis in experimental diabetic cardiomyopathy. Basic Res Cardiol, 103(4): 319-327.

Varga ZV, Giricz Z, Liaudet L, Hasko G, Ferdinandy P, Pacher P. (2015) Interplay of oxidative, nitrosative/nitrative stress, inflammation, cell death and autophagy in diabetic cardiomyopathy. Biochim Biophys Acta, 1852(2): 232-242.

Varga ZV, Kupai K, Szucs G, Gaspar R, Paloczi J, Farago N, Zvara A, Puskas LG, Razga Z, Tiszlavicz L, Bencsik P, Gorbe A, Csonka C, Ferdinandy P, Csont T. (2013) MicroRNA-25-dependent up-regulation of NADPH oxidase 4 (NOX4) mediates hypercholesterolemia-induced oxidative/nitrative stress and subsequent dysfunction in the heart. J Mol Cell Cardiol, 62: 111-121.

Wang S, Mitu GM, Hirschberg R. (2008) Osmotic polyuria: an overlooked mechanism in diabetic nephropathy. Nephrol Dial Transplant, 23(7): 2167-2172.

Westermann D, Rutschow S, Jager S, Linderer A, Anker S, Riad A, Unger T, Schultheiss HP, Pauschinger M, Tschope C. (2007) Contributions of inflammation and cardiac matrix metalloproteinase activity to cardiac failure in diabetic cardiomyopathy: the role of angiotensin type 1 receptor antagonism. Diabetes, 56(3): 641-646.

Widyantoro B, Emoto N, Nakayama K, Anggrahini DW, Adiarto S, Iwasa N, Yagi K, Miyagawa K, Rikitake Y, Suzuki T, Kisanuki YY, Yanagisawa M, Hirata K. (2010) Endothelial cell-derived endothelin-1 promotes cardiac fibrosis in diabetic hearts through stimulation of endothelial-to-mesenchymal transition. Circulation, 121(22): 2407-2418.

Woodiwiss AJ, Libhaber CD, Majane OH, Libhaber E, Maseko M, Norton GR. (2008) Obesity promotes left ventricular concentric rather than eccentric geometric remodeling and hypertrophy independent of blood pressure. Am J Hypertens, 21(10): 1144-1151.

World Health Organization. (2016a). Diabetes country profiles 2016. Retrieved 01.08., 2016., from http://www.who.int/diabetes/country-profiles/hun_en.pdf?ua=1.

World Health Organization. (2016b). Global report on diabetes 2016. Retrieved 01.08., 2016., from http://www.who.int/diabetes/global-report/en/.

Xia Z, Kuo KH, Nagareddy PR, Wang F, Guo Z, Guo T, Jiang J, McNeill JH. (2007) N-acetylcysteine attenuates PKCbeta2 overexpression and myocardial hypertrophy in streptozotocin-induced diabetic rats. Cardiovasc Res, 73(4): 770-782.

Xu FP, Chen MS, Wang YZ, Yi Q, Lin SB, Chen AF, Luo JD. (2004) Leptin induces hypertrophy via endothelin-1-reactive oxygen species pathway in cultured neonatal rat cardiomyocytes. Circulation, 110(10): 1269-1275.

Yeshao W, Gu J, Peng X, Nairn AC, Nadler JL. (2005) Elevated glucose activates protein synthesis in cultured cardiac myocytes. Metabolism, 54(11): 1453-1460.

Yue P, Arai T, Terashima M, Sheikh AY, Cao F, Charo D, Hoyt G, Robbins RC, Ashley EA, Wu J, Yang PC, Tsao PS. (2007) Magnetic resonance imaging of progressive cardiomyopathic changes in the db/db mouse. Am J Physiol Heart Circ Physiol, 292(5): H2106-2118.

Zarain-Herzberg A, Garcia-Rivas G, Estrada-Aviles R. (2014) Regulation of SERCA pumps expression in diabetes. Cell Calcium, 56(5): 302-310.

Zhao CY, Greenstein JL, Winslow RL. (2016) Roles of phosphodiesterases in the regulation of the cardiac cyclic nucleotide cross-talk signaling network. J Mol Cell Cardiol, 91: 215-227.

Zimmet P, Alberti KG, Shaw J. (2001) Global and societal implications of the diabetes epidemic. Nature, 414(6865): 782-787.

Zou MH, Shi C, Cohen RA. (2002) Oxidation of the zinc-thiolate complex and uncoupling of endothelial nitric oxide synthase by peroxynitrite. J Clin Invest, 109(6): 817-826.

Zouein FA, de Castro Bras LE, da Costa DV, Lindsey ML, Kurdi M, Booz GW. (2013) Heart failure with preserved ejection fraction: emerging drug strategies. J Cardiovasc Pharmacol, 62(1): 13-21.

11. Bibliography of the candidate's publications

11.1. Publications related to the dissertation

I. Mátyás C, Németh BT, Oláh A, Török M, Ruppert M, Kellermayer D, Barta BA, Szabó G, Kökény G, Horváth EM, Beáta Bódi, Papp Z, Merkely B, Radovits T. (2017) Prevention of the development of heart failure with preserved ejection fraction (HFpEF) by the phosphodiesterase-5A inhibitor vardenafil in type-2 diabetic rats. Eur J Heart Fail, 19(3): 326-336.
IF: 6.968 (2016)

II. Mátyás C, Németh BT, Oláh A, Hidi L, Birtalan E, Kellermayer D, Ruppert M, Korkmaz-Icöz S, Kökény G, Horváth EM, Szabó G, Merkely B, Radovits T. (2015) The soluble guanylate cyclase activator cinaciguat prevents cardiac dysfunction in a rat model of type-1 diabetes mellitus. Cardiovasc Diabetol, 14: 145.
IF: 4.534

III. Radovits T, Korkmaz S, Mátyás C, Oláh A, Németh BT, Páli S, Hirschberg K, Zubarevich A, Gwanmesia PN, Li S, Loganathan S, Barnucz E, Merkely B, Szabó G. (2015) An altered pattern of myocardial histopathological and molecular changes underlies the different characteristics of type-1 and type-2 diabetic cardiac dysfunction. J Diabetes Res, 2015: 728741.
IF: 2.431

IV. Mátyás Cs, Barta BA, Németh BT, Oláh A, Hidi L, Birtalan E, Kellermayer D, Ruppert M, Korkmaz-Icöz S, Kökény G, Horváth EM, Szabó G, Merkely B, Radovits T. (2017) The soluble guanylate cyclase activator cinaciguat prevents cardiac dysfunction in a rat model of type-1 diabetes mellitus. Cardiol Hung, 47(1): 34-45.

V. Mátyás Cs, Sayour AA, Korkmaz-Icöz S, Oláh A, Németh BT, Páli Sz, Hirschberg K, Zubarevich A, Gwanmesia PN, Li S, Loganathan S, Barnucz E, Merkely B, Szabó G, Radovits T. (2017) An altered pattern of myocardial histopathological and molecular changes underlies the different characteristics of type-1 and type-2 diabetic cardiac dysfunction. Cardiol Hung, 47(2): 102-111.

11.2. Publications not related to the dissertation

I. Varga ZV, Matyas C, Erdelyi K, Cinar R, Nieri D, Chicca A, Nemeth BT, Paloczi J, Lajtos T, Corey L, Hasko G, Gao B, Kunos G, Gertsch J, Pacher P. (2017) β-Caryophyllene protects against alcoholic steatohepatitis by attenuating inflammation and metabolic dysregulation in mice. Br J Pharmacol, doi: 10.1111/bph.13722.
IF: 5.491 (2016)

II. Benke K, Sayour AA, Mátyás C, Ágg B, Németh BT, Oláh A, Ruppert M, Hartyánszky I, Szabolcs Z, Radovits T, Merkely B, Szabó G. (2017) Heterotopic Abdominal Rat Heart Transplantation as a Model to Investigate Volume Dependency of Myocardial Remodeling. Transplantation, 101(3): 498-505.
IF: 3.678 (2016)

III. Németh BT, Mátyás C, Oláh A, Lux Á, Hidi L, Ruppert M, Kellermayer D, Kökény G, Szabó G, Merkely B, Radovits T. (2016) Cinaciguat prevents the development of pathologic hypertrophy in a rat model of left ventricular pressure overload. Sci Rep, 6: 37166.
IF: 4.259

IV. Oláh A, Kellermayer D, Mátyás C, Németh BT, Lux Á, Szabó L, Török M, Ruppert M, Meltzer A, Sayour AA, Benke K, Hartyánszky I, Merkely B, Radovits T. (2017) Complete Reversion of Cardiac Functional Adaptation Induced by Exercise Training. Med Sci Sports Exerc, 49(3): 420-429.
IF: 4.141 (2016)

V. Koncsos G, Varga ZV, Baranyai T, Boengler K, Rohrbach S, Li L, Schluter KD, Schreckenberg R, Radovits T, Oláh A, Mátyás C, Lux Á, Al-Khrasani M, Komlódi T, Bukosza N, Máthé D, Deres L, Barteková M, Rajtík T, Adameová A, Szigeti K, Hamar P, Helyes Z, Tretter L, Pacher P, Merkely B, Giricz Z, Schulz R, Ferdinandy P. (2016) Diastolic dysfunction in prediabetic male rats: role of mitochondrial oxidative stress. Am J Physiol Heart Circ Physiol, 311(4): H927-943.
IF: 3.348

VI. Ruppert M, Korkmaz-Icöz S, Li S, Németh BT, Hegedüs P, Brlecic P, Mátyás C, Zorn M, Merkely B, Karck M, Radovits T, Szabó G. (2016) Myocardial reverse remodeling after pressure unloading is associated with maintained cardiac mechanoenergetics in a rat model of left ventricular hypertrophy. Am J Physiol Heart Circ Physiol, 311(3): H592-603.
IF: 3.348

VII. Matyas C, Varga ZV, Mukhopadhyay P, Paloczi J, Lajtos T, Erdelyi K, Nemeth BT, Nan M, Hasko G, Gao B, Pacher P. (2016) Chronic plus binge ethanol feeding induces myocardial oxidative stress, mitochondrial and cardiovascular dysfunction and steatosis. Am J Physiol Heart Circ Physiol, 310(11): H1658-1670.
IF: 3.348

VIII. Lee WS*, Erdelyi K*, Matyas C*, Mukhopadhyay P, Varga ZV, Liaudet L, Haskó G, Čiháková D, Mechoulam R, Pacher P. (2016) Cannabidiol limits Tcell-mediated chronic autoimmune myocarditis: implications to autoimmune disorders and organ transplantation. Mol Med, 22: 136-146.
IF: 3.457
*Equal contribution

IX. Oláh A, Németh BT, Mátyás C, Hidi L, Lux Á, Ruppert M, Kellermayer D, Sayour AA, Szabo L, Torok M, Meltzer A, Gellér L, Merkely B, Radovits T. (2016) Physiological and pathological left ventricular hypertrophy of comparable degree is associated with characteristic differences of in vivo hemodynamics. Am J Physiol Heart Circ Physiol, 310(5): H587-597.
IF: 3.348

X. Kovacs A, Oláh A, Lux Á, Mátyás C, Németh BT, Kellermayer D, Ruppert M, Torok M, Szabo L, Meltzer A, Assabiny A, Birtalan E, Merkely B, Radovits T. (2015) Strain and strain rate by speckle tracking echocardiography correlate with pressure-volume loop derived contractility indices in a rat model of athlete's heart. Am J Physiol Heart Circ Physiol, 308(7): H743-748.
IF: 3.324

XI. Oláh A, Németh BT, Mátyás C, Horváth EM, Hidi L, Birtalan E, Kellermayer D, Ruppert M, Merkely G, Szabó G, Merkely B, Radovits T. (2015) Cardiac effects of acute exhaustive exercise in a rat model. Int J Cardiol, 182: 258-266.
IF: 4.638

XII. Radovits T, Oláh A, Lux Á, Németh BT, Hidi L, Birtalan E, Kellermayer D, Mátyás C, Szabó G, Merkely B. (2013) Rat model of exercise-induced cardiac hypertrophy - hemodynamic characterization using left ventricular pressure-volume analysis. Am J Physiol Heart Circ Physiol, 305(1): H124-134.
IF: 4.012

XIII. Benke K, Sayour AA, Ágg B, Radovits T, Szilveszter B, Odler B, Németh BT, Pólos M, Oláh A, Mátyás C, Ruppert M, Hartyánszky I, Maurovich-Horvat P, Merkely B, Szabolcs Z. (2016) Gene polymorphisms as risk factors for predicting the cardiovascular manifestations in Marfan syndrome. Cardiol Hung, 46(2): 76-81.

XIV. Oláh A, Németh BT, Mátyás C, Horváth EM, Hidi L, Birtalan E, Kellermayer D, Ruppert M, Gellér L, Szabó G, Merkely B, Radovits T. (2016) Cardiac effects of acute exhaustive exercise in a rat model. Cardiol Hung, 46(1): 1-9.

XV. Oláh A, Lux Á, Németh BT, Hidi L, Birtalan E, Kellermayer D, Mátyás C, Ruppert M, Merkely G, Szabó G, Merkely B, Radovits T. (2013) Detailed hemodynamic characterization of athlete's heart – Left ventricular pressure-volume analysis. Cardiol Hung, 43(5): 224-232.

XVI. Radovits T, Mátyás C, Oláh A, Kökény G, Barnucz E, Szabó G, Merkely B. (2012) Effects of phosphodiesterase-5 inhibitor vardenafil on diabetic cardiovascular dysfunction. Cardiol Hung, 42(5): 272-279.

12. Acknowledgements

Firstly, I would like to express my sincere gratitude to my tutor Dr. Tamás Radovits for the continuous support of my PhD study and related research, for his patience, motivation, and immense knowledge. His guidance helped me in all the time of research and writing of this thesis.

Besides my tutor, I would like to thank Prof. Dr. Béla Merkely, and my thesis committee, for their insightful comments and encouragement, but also for the hard questions which incented me to widen my research from various perspectives. I would like to thank Dr. Violetta Kékesi and Dr. Judit Skopál for their continuous support and scientific advice.

My sincere thanks also goes to Prof. Dr. Pál Pacher and the members of his laboratory, who provided me an opportunity to join their team as a visiting fellow, and who gave me continuous support and advices regarding my projects and granted access to the laboratory.

I thank my fellow labmates from the Research Laboratory and from the Central Laboratory for the stimulating discussions and for all the fun we have had in the past years. Also I thank Prof. Dr. Zoltán Papp, Dr. Gábor Kökény, Dr. Eszter Mária Horváth and Dr. Ákos Lukáts for the opportunity to build a fruitful cooperation between our groups. In particular, I am grateful to Dr. Orsolya Láng and to Dr. László Kőhidai for enlightening me the first glance of research.

Finally, I must express my very profound gratitude to my family for providing me with unfailing support and continuous encouragement throughout my years of study and through the process of researching and writing this thesis. This accomplishment would not have been possible without them.